TRANSIENT COOKING RATES OF GROUND BEEF WITH INFRARED HEATING

Thesis for the Degree of Ph. D.
MICHIGAN STATE UNIVERSITY
Frank Donald Borsenik
1964

THESIS

12 y a State
University

TRANSIENT COOKING RATES OF GROUND BEEF WITH INFRARED HEATING

Ву

Frank Donald Borsenik

AN ABSTRACT OF A THESIS

Submitted to

Michigan State University
in partial fulfillment of the requirements
for the degree of

DOCTOR OF PHILOSOPHY

Department of Agricultural Engineering

ABSTRACT

TRANSIENT COOKING RATES OF GROUND BEEF WITH INFRARED HEATING

By Frank Donald Borsenik

The objectives of this study were to investigate

(1) the influence of infrared source temperatures, and (2) the effects of various infrared heat fluxes on the transient processing rates of ground beef. In addition, several related topics were examined. These were: (1) the effect of enclosed processing chamber reradiation on processing rates; (2) product volatile losses; and (3) product volume changes.

Ground beef was selected because it is fairly homogeneous and it normally represents the average composition of beef products. The average fat content of the product was 20%.

Three electric infrared heat sources were used to provide wave lengths from 1.233 to 3.164 microns, the quartz lamp, the quartz tube and the calrod unit. These heat sources were selected because of their flexibility in obtaining different heat source temperatures and various radiant energy fluxes.

Samples of ground beef, 3 inches wide, 6 inches long and one inch deep were used. The samples were placed in an

.

insulated container with a 3 inch by 6 inch surface exposed to the heat source. All samples were heated from approximately 45 to 170 F.

The processing rates of samples in an enclosed high emissivity volume were not significantly different from those in non-enclosed volumes. Samples were processed in non-enclosed chambers.

Five radiant heat source temperatures were used for processing, 4230.0, 3465.0, 2260.0, 1864.5 and 1648.7 R. A range of heat fluxes was used at each of the heat source temperatures. It was found that: (a) a linear relationship exists between surface heat flux and the average surface temperature; (b) a linear relationship exists between volatile loss and time at a given surface heat flux; (c) the rate of volatile loss can be represented by the Arrhenius equation, for first order chemical reactions; (d) a linear relationship exists for values of h(t - t;)/qs" vs. $\alpha \tau/s^2$ for various k/hs parameter values, within the following temperature ranges: above freezing to 122 F, 122 to 140 F, 140 to 157 F, 157 to 170 F; (e) a procedure is given to determine processing times; (f) decreasing the radiant heat source temperature from 4230 to 2260 R decreases processing times at the same heat flux, with a further reduction of heat source temperatures to 1648.7 R not essentially affecting the processing time; (g) the maximum total product losses occurred with a heat source temperature of 2260 R, the losses at other heat source

temperatures were not significantly different for the same heat flux; (h) the volume change was only significant between the 4230.0 and the 1648.7 R heat source temperatures.

From these results, it is recommended that a heat source temperature of 1864.5 R should be used for the radiant heat processing of fresh ground beef.

Approved Carl W. Hall

|5/64/

TRANSIENT COOKING RATES OF GROUND BEEF WITH INFRARED HEATING

Ву

Frank Donald Borsenik

A THESIS

Submitted to
Michigan State University
in partial fulfillment of the requirements
for the degree of

DOCTOR OF PHILOSOPHY

Department of Agricultural Engineering

ACKNOWLEDGEMENTS

The author expresses his sincere appreciation for the counsel, guidance, and interest of Dr. C. W. Hall, under whose supervision this work was accomplished.

He is also indebted to Dr. A. W. Farrall, Chairman of the Department of Agricultural Engineering, Michigan State University, for his support which made it possible to carry out the investigation. A special note of appreciation is expressed to Dr. S. E. Thompson and Dr. J. W. Thompson, Assistant Director and Director of the School of Hotel, Restaurant and Institutional Management, respectively, and to Henry Ogden Barbour, present Director of the School of Hotel, Restaurant and Institutional Management, Michigan State University, for their encouragement and financial aid during the course of the study.

Appreciation is expressed to Dr. J. L. Newcomer, former Director of the Food Service Research Industry

Center, Michigan State University, and to Dr. A. M. Dhanak,

Department of Mechanical Engineering, Michigan State

University, for their sympathetic understanding and helpful suggestions during the course of the study.

VITA

Frank Donald Borsenik

Oral Examination: May 6, 1964

Dissertation: Transient Cooking Rates for Ground Beef

with Infrared Heating

Outline of Studies:

Major Subject: Agricultural Engineering

Minor Subjects: Mechanical Engineering

Statistics

Biographical Items:

Born: October 19, 1933, Saginaw, Michigan

Undergraduate Studies:

Michigan State University, 1951-55

BSAE, 1955

Graduate Studies:

Michigan State University, 1955-58

MSAE, 1958

1958-1964

Experience:

1952-1955: part time engineering aid during under-

graduate studies for H. J. Heinz Co.,

Michigan and Indiana

1955-1956: Graduate assistantship, Department of

Agricultural Engineering, Michigan State

University.

1956-1957: Research Assistant, Department of Agricultural Engineering, Michigan State University.

1957-1964: Instructor, School of Hotel, Restaurant and Institutional Management, Michigan State University.

Membership in Organizations:

American Society of Agricultural Engineers

The Society of Sigma Xi (Scientific Honorary)

The Society for the Advancement of Food Service

Research

Sigma Pi Eta (National Hotel, Restaurant and Institutional Management Honorary)

TABLE OF CONTENTS

			Page
1.0	INTR	ODUCTION	1-1
2.0	REVI	EW OF LITERATURE	2-1
	2.1	The thermal properties of beef	2-2
		<pre>2.1.1 The specific heat of beef 2.1.2 Thermal conductivity of beef 2.1.3 Thermal diffusivity of beef 2.1.4 Latent heat factors in the</pre>	2-2 2-7 2-8
		2.1.5 The emissivity of beef	2-12
	2.2	The factors that affect beef processing The infrared and the conduction heating	2-16
	2.0	theories	2-19
		2.3.1 The infrared theory2.3.2 The conduction heating theory	2-19 2-26
	2.4	Electric infrared heat sources	2-30
3.0	EXPE	RIMENTAL APPARATUS	3-1
4.0	PROC	EDURE	4-1
	4.1 4.2	Electrical energy characteristics of the heat sources	4-1
	4.3	Physical measurements of the three heat sources Heat flux measurements Effect of surrounding walls and reradiation	4-1 4-2 4-3
	4.5	Transient processing rates of ground beef with infrared heating	4-6
5.0	RESU	LTS, CALCULATIONS AND DISCUSSION	5-1
	5.1	Calculation of the specific and latent heats of ground beef	5-1 5-3
	5.2	Calculation of geometrical angle factors Determination of the sample size for	5-3
		statistically equal heat fluxes on the sample surface	5-10

		Page
	5.4 Electrical energy characteristics of the three heat sources5.5 Calculation of the radiant heat outputs	5-16
	of the three heat sources	5-17
	5.5.1 Quartz lamp source 5.5.2 Calrod heat source 5.5.3 Quartz tube heat source	5-17 5-22 5-27
	5.6 Heat flux measurements5.7 Fitting of third degree polynominals to heat flux calculations for various distances between the sample surface	5-30
	and heat source units 5.8 Effect of surrounding walls and reradiation 5.9 Transient processing rates of ground beef with infrared heating	5-35 5-37 5-45
	<u>-</u>	
6.0	SUMMARY AND CONCLUSIONS	6-1
	6.1 Calculated and measured heat fluxes 6.2 The effect of environment wall re-	6-2
	radiation on processing time 6.3 The effects of heat source temperature	6-2
	and surface heat flux on processing times and weight losses 6.4 General recommendations	6-3 6-6
7.0	APPENDIX	7-1
8.0	EXAMPLE CALCULATIONS	8-1
9.0	REFERENCES	9_1

LIST OF TABLES

Table		Page
2.1	The composition of various meat cuts	2-4
4.1	Surface heat fluxes used in the processing of ground beef at different source temperatures	4-13
5.1.	Calculated specific heats of ground beef of average composition in various temperature ranges and the latent heats of fusion at the transition temperatures	5-3
5.2.	Geometrical angle factors between single unit heat sources and a parallel centered 18 sq in surface at different perpendicular distances	5-8
5.3.	Equivalent geometrical angle factors between single heat sources and a parallel centered surface with an equivalent surface area of one sq ft using an 18 sq in surface as a basis at different perpendicular distances	5-8
5.4.	Combined geometrical angle factors between a group of three similar heat sources and a parallel centered 18 sq in surface at different perpendicular distances	5-10
5.5.	Combined equivalent geometrical angle factors between a group of three similar heat sources and a parallel centered 18 sq in surface at different perpendicular distances	5-10
5.6.	Geometrical angle factors for various sample widths (c) and lengths (b) at a distance of four inches. The values in the table are F/dA (sq ft ⁻¹)	5-14
5.7.	Analysis of variance of F/dA of the various rows and columns of one quarter of a 5 in by 10 in surface reduced to elemental finite areas	5-16
5.8.	Comparison of manufacturers data and calculate watt inputs, based on volt and ampere averages, for the 1600 watt quartz lamp.	

Table		Page
5.9.	Comparison of manufacturers data and calculated watt inputs, based on volt and ampere averages, for the 1000 watt calrod unit	5-17
5.10.	Calculated heat balances of the quartz heat lamp at different voltages	5-21
5.11.	Comparison of calculated percent radiations from a 240 volt quartz lamp rated at 1600 watts at different voltages to the manufacturers data	5-22
5.12.	Calculated heat balances of the calrod unit at different voltages	5-26
5.13.	Comparison of calculated percent radiations from a 1000 watt, 240 volt calrod unit at different voltages to the manufacturers data	5-27
5.14.	Comparison of calculated radiant heat fluxes to measured radiant heat fluxes for different voltages and distances for one quartz lamp	5-31
5.15.	Comparison of calculated radiant heat fluxes to measured radiant heat fluxes for different voltages and distances for three quartz lamps	5-32
5.16.	Comparison of calculated radiant heat fluxes to measured radiant heat fluxes for different voltages and distances for one calrod unit	5-34
5.17.	Comparison of calculated radiant heat fluxes to measured radiant heat fluxes for different distances for a 120 volt, 550 watt quartz tube	5-35
5.18.	Results of orthogonal polynominal curve fitting to surface heat flux calculations for the equation: qs" = A+Bd+Cd ² +Dd ³ . Maximum deviations are also indicated	5-38
5.19.	Ground beef samples processed at 170 F at 946 Btu per sq ft-hr and λ of 1.194μ in an open room and in an enclosed volume	5-39
		シーンラ

Table		Page
5.20.	Analysis of variance of percent yields for enclosed volume vs. non-enclosed volume samples at 946 Btu per sq ft-hr and λ = 1.194 μ	5-40
5.21.	Analysis of variance of percent drippings for enclosed volume vs. non-enclosed volume samples at 946 Btu per sq ft-hr and λ = 1.194 μ	5-40
5.22.	Analysis of variance of percent volatile losses for enclosed volume vs. non-enclosed volume samples at 946 Btu per sq ft-hr and λ = 1.194 μ	5-40
5.23.	Analysis of variance of relative processing time (60 to 170 F) for enclosed volume vs. non-enclosed volume samples at 946 Btu per sq ft-hr and λ = 1.194 μ	5-41
5.24.	Polynominal constants for the fitting of time vs. temperature at the one in. depth for ground beef at 946 Btu per sq ft-hr and λ of 1.194 μ in an open room and in an enclosed volume. (Y=A+Bx+CX², Y is the temperature in F at the one inch sample depth and X is the time in minutes)	5-43
5.25.	Analysis of variance of (A) constants in the fitted polynominal equation of temperature vs. time at the one inch depth for ground beef at 946 Btu per sq ft-hr and at a λ of 1.194 μ in an open room and in an enclosed volume	5-44
5.26.	Analysis of variance of (B) constants in the fitted polynominal equation of temperature vs. time at the one inch depth for ground beef at 946 Btu per sq ft-hr and at a λ of 1.194 μ in an open room and in an enclosed volume	5-44
5.27.	Analysis of variance of (C) constants in the fitted polynominal equation of temperature vs. time at the one inch depth for ground beef at 946 Btu per sq ft-hr and at a λ of 1.194 μ in an open room and in an enclosed volume λ and λ at λ	5-44
	enclosed volume	7-44

Table		Page
5.28.	Convective, radiative and apparent coefficients of heat transfer from the surface of the sample to the room for various room temperatures and sample surface temperatures for each of the tests	5-52
5.29.	Correlation of temperature vs. time distribution patterns for various surface heat fluxes from a source temperature of 4230.0 R, λ = 1.233 μ . Y = A+BX represents the linear regression equation of $\alpha\tau/s^2$ (Y) vs. k/hs (X) at a constant $h(t_1-t_0)/qs$ ". R is the correlation of Y on X and the standard error is s_1	5-56
5.30.	Correlation of temperature vs. time distribution patterns for various surface heat fluxes from a source temperature of 3465.0 R, λ = 1.505 μ . Y = A+BX represents the linear regression equation of $\alpha\tau/s^2$ (Y) vs. k/hs (X) at a constant h(t ₁ -t ₀)/qs". R is the correlation of Y on X and the standard error is s ₁	5-57
5.31.	Correlation of temperature vs. time distribution patterns for various surface heat fluxes from a source temperature of 2260.0 R, λ = 2.308 μ . Y = A+BX represents the linear regression equation of $\alpha\tau/s^2$ (Y) vs. k/hs (X) at a constant $h(t_1-t_0)/qs$ ". R is the correlation of Y on X and the standard error is s ₁	5-58
5.32.	Correlation of temperature vs. time distribution patterns for various surface heat fluxes from a source temperature of 1864.5 R, λ = 2.797 μ . Y = A+BX represents the linear regression equation of $\alpha\tau/s^2$ (Y) vs. k/hs (X) at a constant $h(t_1-t_0)/qs$ ". R is the correlation of Y on X and the standard error is s_1	5-59
5.33.	Correlation of temperature vs. time distribution patterns for various surface heat fluxes from a source temperature of 1648.7 R, λ = 3.164 μ . Y = A+BX represents the linear regression equation of $\alpha\tau/s^2$ (Y) vs. k/hs (X) at a constant $h(t_1-t_0)/qs$ ". R is the correlation of Y on X and the standard error is s_1	5-60

Table		Page
5.34.	Percent volatile and dripping losses and volume change in length and width for ground beef processed at 170 F at various radiant heat temperatures and at different heat fluxes	5-73
5.35.	Analysis of variance of total processing losses for the different heat source temperatures	5-75
5.36.	Summary of "t" tests for comparing the percent total losses for each of the heat source temperatures	5-76
5.37.	Analysis of variance of percent volume change for the different heat source temperatures	5-77
5.38.	Summary of "t" tests for comparing the percent volume changes for each of the heat source temperatures	5-78
7.1.	Processing results of ground beef, processed to 170 F	7-1

LIST OF FIGURES

Figure		Page
2.1	Q, Btu/LB, and temperature relationships for 100% beef fat and beef with 20% fat	2-6
2.2	10 mm and one mm water absorption and wave length, microns, relationships; $E_{\lambda b}$ x $10^5/\sigma T^5$ and wavelength, microns, relationships for various black body surface temperatures (R)	2-6
2.3	Hottel's geometrical model for determining the geometrical angle factor between a differential surface and a parallel finite surface	2-25
2.4.	Surface element heat balance	2-25
4.1.	Heat source and pyrheliometer arrangement	4-4
4.2.	Product, copper container, insulated box and heat source arrangement	4-4
4.3	Experimental apparatus arrangement	4-10
5.1.	Relationships of a, b and c for determining the geometrical angle factor between a differential surface and a finite rectangular surface parallel to it	5-7
5.2.	Relationships of a, b, c for determining the geometrical angle factors from a heat source to a finite surface	5-7
5.3.	Relationships of c and a for determining the geometrical factors from a group of three heat sources to a finite surface (b relationships same as in Fig. 5.2)	5-7
5.4.	Relationships of c and b and distances for determining sample surface area	5-13
5.5.	(F/dA) values for surface elements from Fig. 5.4	5-13

Figure		Page
5.6.	Relationships of t (average product surface temperature) and qs" for ground beef	5-47
5.7.	Log $\left[\left(\frac{M_{o} - M}{M_{o}} \right) \tau^{-1} \right]$ and $(1/T_{s}) \times 10^{-3}$ relationships ground beef	5-47
5.8.	h(t ₁ - t ₀)/qs" and cτ/s ² relationships at various k/hs values for ground beef (C = 0.75) and a radiant heat source temperature of 4230.0 R. t ₁ (maximum) = 122 F	5-62
5.9	$h(t_1 - 122)/qs$ " and $\alpha\tau/s^2$ relationships at various k/hs values for ground beef (C = 0.80) and a radiant heat source at 4230.0 R. t_1 (maximum) = 140 F	5-62
5.10.	$h(t_1 - 140)/qs$ " and $\alpha \tau/s^2$ relationships at various k/hs values for ground beef (C = 0.74) and a radiant heat source at 4230.0 R. t_1 (maximum) = 157 F	5-62
5.11.	<pre>h(t₁ - 157)/qs" and ατ/s² relationships at various k/hs values for ground beef (C = 0.80) and a radiant heat source at 4230.0 R</pre>	5-62
5.12.	$h(t_1 - t_0)/qs$ " and $\alpha\tau/s^2$ relationships at various k/hs values for ground beef (C = 0.75) and a radiant heat source at 3465.0 R. t_1 (maximum) = 122 F	5-63
5.13.	$h(t_1 - 122)/qs$ " and $\alpha \tau/s^2$ relationships at various k/hs values for ground beef (C = 0.75) and a radiant heat source at 3465.0 R. t_1 (maximum) = 140 F	5-63
5.14.	$h(t_1 - 140)/qs$ " and $c\tau/s^2$ relationships at various k/hs values for ground beef (C = 0.74) and a radiant heat source at 3465.0 R. t_1 (maximum) = 157 F	5-63
5.15.	h(t ₁ - 157)/qs" and ατ/s ² relationships at various k/hs values for ground beef (C = 0.80) and a radiant heat source	5-63

Figure		Page
5.16.	$h(t_1 - t_0)/qs$ " and $\alpha\tau/s^2$ relationships at various k/hs values for ground beef (C = 0.75) and a radiant heat source at 2260.0 R. t_1 (maximum) = 122 F	5-64
5.17.	$h(t_1 - 122)/qs$ " and $\alpha\tau/s^2$ relationships at various k/hs values for ground beef (C = 0.80) and a radiant heat source at 2260.0 R. t_1 (maximum) = 140 F	5-64
5.18.	$h(t_1 - 140)/qs$ " and $\alpha\tau/s^2$ relationships at various k/hs values for ground beef (C = 0.74) and a radiant heat source at 2260.0 R. t_1 (maximum) = 157 F	5-64
5.19.	$h(t_1 - 157)/qs$ " and $\alpha\tau/s^2$ relationships at various k/hs values for ground beef (C = 0.80) and a radiant heat source at 2260.0 R	5-64
5.20.	$h(t_1 - t_0)/qs$ " and $\alpha\tau/s^2$ relationships at various k/hs values for ground beef (C = 0.75) and a radiant heat source at 1864.5 R. t_1 (maximum) = 122 F	5-65
5.21.	$h(t_1 - 122)/qs$ " and $\alpha \tau/s^2$ relationships at various k/hs values for ground beef (C = 0.80) and a radiant heat source at 1864.5 R. t_1 (maximum) = 140 F	5-65
5.22.	$h(t_1 - 140)/qs$ " and $\alpha \tau/s^2$ relationships at various k/hs values for ground beef (C = 0.74) and a radiant heat source at 1864.5 R. t_1 (maximum) = 157 F	5-65
5.23.	$h(t_1 - 157)/qs$ " and $\alpha\tau/s^2$ relationships at various k/hs values for ground beef (C = 0.80) and a radiant heat source at 1864.5 R	5-65
5.24.	$h(t_1 - t_0)/qs$ " and $\alpha\tau/s^2$ relationships at various k/hs values for ground beef (C = 0.75) and a radiant heat source at 1648.7 R. t_1 (maximum) = 122 F	5-66
5.25.	$h(t_1 - 122)/qs$ " and $\alpha r/s^2$ relationships at various k/hs values for ground beef (C = 0.80) and a radiant heat source at 1648.7 R. t_1 (maximum) = 140 F	5-66

Figure		Page
5.26.	$h(t_1 - 140)/qs$ " and $\alpha\tau/s^2$ relationships at various k/hs values for ground beef (C = 0.74) and a radiant heat source at 1648.7 R. t_1 (maximum) = 157 F	5-66
5.27.	<pre>h(t₁ - 157)/qs" and ατ/s² relationships at various k/hs values for ground beef (C = 0.80) and a radiant heat source at 1648.7 R</pre>	5-66
5.28.	$h(t_1 - 157)/qs$ " and $c\tau/s^2$ relationships at k/hs = 0.6 for ground beef (C = 0.80) at different radiant heat source temperatures, R	5-72
7.1.	Product (t _s - t _o) and time, min, relation- ships at different surface heat fluxes, Btu per sq ft-hr, and heat source temperatures, R. t _s , product surface temperature, F. t _o , initial product temperature, F	7-4
7.2.	Volatile loss, percent of initial product weight, and time, min, relationships at different surface heat fluxes, Btu per sq ft-hr, and heat source temperatures, R	7-4
7.3.	Product (t ₁ - t ₀) and time, min, relationships at different surface heat fluxes, Btu per sq ft-hr, and heat source temperatures, R. t ₁ , product temperature, l in depth, F; t ₀ , initial product temperature, F	7-5
7.4.	$h(t_1 - t_0)/qs$ " and $\alpha\tau/s^2$ relationships at four experimental k/hs values for ground beef (C = 0.75) and a radiant source at 3465.0 R. t_1 (maximum) =	7-5
	122 F	7-5

NOMENCLATURE

a. Simple Latin Letter Symbols

C	Out out the transfer of the tr	77 2 to
Symbol	Quantity	<u>Unit</u>
A	Area, surface and cross-sectional	s q ft
A	Element designation	• • • •
A	Element weight in a mixture	lb
Α	Orthogonal polynominal constant	• • • •
a	Distance between two radiating surfaces	in
B = b/a	Ratio of length (b) of a finite rectangle	
	surface to the distance (a) between the	
	rectangle surface and another radiating	
	surface	in
В	Element designation	• • • •
В	Element weight in a mixture	lb
В	Orthogonal polynominal constant	• • • •
b	Length of one side of a rectangle	in
С	Orthogonal polynominal constant	• • • •
С	Surface area of a rod extending from	
	a heat source	sq ft
C = c/a	Ratio of length (c) of a finite rectangle	
	surface to the distance (a) between the	
	rectangle surface and another radiating	
	surface	• • • •
С	Planck constant	cm per hr-sq ft
С	Planck constant	cm per R
С	Specific heat	Btu per lb-F
С	Length of one side of a rectangle surface	in
D	Perpendicular distance between two	
	radiating surfaces	in
D	Orthogonal polynominal constant	• • • • •

Symbol	Quantity	<u>Unit</u>
D	Element designation	• • • •
D	Element weight in a mixture	lb
đ	Perpendicular distance between two	
	radiating surfaces	in
đ	Diameter	ft
E	Emissive power factor	Btu
F	Geometrical angle factor	
F'	Equivalent angle factor	sq ft ⁻¹
G	Incident radiant energy on a surface	Btu
h	Coefficient of heat transfer	Btu per sq ft- hr F
k	Thermal conductivity	Btu per ft-hr F
L	Length	in
L	Latent heat of vaporization or con-	Btu per
	densation	lb
L	Characteristic surface length	ft
L = x/D	Ratio of the length (x) of a finite	
	rectangle surface to the distance (D)	
	between the rectangle surface and another	
	radiation surface	• • • •
$\Gamma = \lambda D$	Ratio of length (y) of a finite	
	rectangle surface to the distance (D)	
	between the rectangle surface and	
	another radiating surface	• • • •
m = (hC)	/kA) 1/2 A quantity composed of the	
	surface coefficient of heat transfer h,	
	the thermal conductivity k, the	
	circumference C, and the cross-	_1
	sectional area A	ft ⁻¹
M	Product weight	lb
p = (km)	-h)/(km+h) A quantity composed of the	
	thermal conductivity k, the surface	
	coefficient of heat transfer h, and the	
	quantity m	• • • •

Symbol	Quantity	Unit
Q	Heat capacity	Btu
q	Rate of heat flow	Btu per hr
qs"	Surface heat flux	Btu per s q ft-hr
R	Correlation coefficient	• • • •
r	Distance between the centers of two	
	radiating differential surfaces	in
S	Standard error estimate	• • • •
s	Depth	ft
T	Temperature in the absolute scale	R
t	Temperature in the international scale	F
T	Average temperature in the absolute scale	R
t	Average temperature in the international	
	scale	F
V	Volatile loss from product	gm
W	Condensing or vaporizing weight	lb per hr
W	Weight of a mixture of elements	lb
X	Time in the orthogonal polynominal	min
x	Length of a finite surface	in
x	Length of a differential volume	ft
Y	Temperature in the orthogonal polynominal	F
У	Width of a finite surface	in
У	Width of a differential volume	ft
z	Depth of a differential volume	ft
~	b. Simple Greek Letter Symbols	a £4. m.a.u
α	Thermal diffusivity	s q ft per hr
α	Radiation absorptivity	• • • •
€	Radiation emissivity	• • • •
θ	Temperature excess over a fixed	
	reference temperature	F
λ	Wave length of radiation	cm
ρ	Density	lb per cu ft
ρ	Radiation reflectivity	• • • •

Symbol	Quantity	<u>Unit</u>
σ	Stefan - Boltzman constant	Btu per hr-sq ft - F
τ	Time	hr
τ	Radiation transmissivity	• • • •
Ф	Angle of incidence = angular deviation	
	from normal direction	

1.0 INTRODUCTION

somewhat limited in food processing. The primary use of infrared radiation has been in the drying and dehydration of food products. Asselbergs, et al (8), Krupp (35) and Pollak (47) have reported on the radiant heat processing of various food products. They report two advantages of radiant heat processing over regular convection processing of similar products. These advantages are: fast heating response; generally shorter processing times. Krupp and Pollack attributed the faster processing times to the heat penetration effects of the electromagnetic waves. Asselbergs measured the heat penetration in apple tissue and found that heat penetration was dependent on the heat source temperature and the intensity of radiation.

The fundamental laws of radiant heat transmission require the following factors in order to evaluate heat transfer by radiation: (a) the temperature of the heat source; (b) the emissive properties of the source; (c) the surface area of the source of temperature; (d) the transmittance of the media between the source and the heated surface; (3) the reradiation properties of the media; (f) the geometrical arrangement of the source and receiver, sometimes called the geometrical angle factor; (g) the

absorptivity, reflectivity and transmitivity of the receiver;

(h) the emissivity of the receiver; (i) the surface temperature of the receiver; (j) the area of the receiver. Krupp and Pollak did not report information of this nature.

Asselbergs' work contained many of the above factors for some of the processed products, but it was incomplete for other products.

The thermal properties of the heat source can normally be found in the literature. DeWerth (19) presents a rather complete work on surface emissivities for non-food items. The other radiant heat transmission factors of the source and the media between the source and the product surface can normally be calculated from radiant heat theory. However, the radiant heat properties of food products are generally unavailable.

After the heat is absorbed by the surface, several factors influence the heating of the product at a given depth. Some of these factors are: (a) product environment temperature; (b) product surface heat convection; (c) product surface heat radiation loss, if applicable; (d) product surface moisture loss; (e) the thermal properties of the product, such as conductivity, specific heat and diffusivity; (f) product changes, such as chemical or biological; (g) internal heat generation or absorption; (h) product thickness; (j) convection of liquids within the product; and (k) time. A homogeneous product simplifies many of the above factors.

The surface heat losses or gains, other than radiation to the surface, can normally be calculated by the generally accepted equations for convection and radiation. However, the product surface temperature is generally not known, unless it is measured, as the surface temperature is dependent on the above listed parameters. The product moisture loss was found to be a linear function of time, at given high temperature environments by Lowe (37), McCance and Shipp (43). Jakob (33) handled the surface moisture loss by using an apparent coefficient of heat transfer.

The thermal properties of food products are normally difficult to find in the literature, and most of these data have been reported in the past ten years. This could indicate that the need for this information is becoming more apparent, as research is expanding for foods.

It has been generally recongized that chemical changes take place when a food is heat processed. The exact nature of these changes as well as the heat requirements to cause the changes are essential if food processing is to be completely analyzed.

If a food product can be considered basically homogeneous, various solutions of the Fourier conduction equation may have applications for limited boundary conditions. Heisler (26), Carslaw and Jaeger (13) have solved the Fourier equation for a radiation boundary condition with a surface heat loss to an environment. Heisler has also presented a graphical solution for the equation for various parameters.

Some authors have indicated that, for a moist product with surface moisture losses, the spectral absorption properties of water act as a limiting factor for radiant heat absorption. If this hypothesis is true, a critical examination of the critical region of moisture absorption should be performed. Also, equivalent radiation intensities should have similar effects on the heat processing of food products.

The above two hypotheses lead to the objectives of this study. The objectives are:

- 1. To investigate the influence of infrared source temperatures, within the critical spectral absorption wave lengths of water (one to three microns), on the transient processing rates of ground beef.
- 2. To investigate the influence of infrared heat fluxes on the transient processing rates of ground beef.

Ground beef was selected because it represents a fairly homogeneous meat-type moist food product.

2.0 REVIEW OF LITERATURE

The use of infrared radiation as a source of heat for food processing has been limited (8). Infrared energy has been used for the drying of macaroni (7), the blanching of celery and apples prior to freezing (9), and the peeling of apples (10). Asselbergs, et al (8) have blanched peas, asparagus, corn, beans, turnips, and carrots. They also prepared french fried potatoes and braised meat for beef stew.

The widest use of infrared radiation has been in drying and dehydration (6, 19, 25, 49, 54, 55, 58). It was thought that infrared radiation would offer many advantages over hot air drying because of the penetrating effect of the electromagnetic waves.

Shuman and Staley (55) points out that an evaluation of the uses of infrared should include fundamental studies on the types and properties of the heat sources and on the absorption and heat conducting characteristics of the product. Asselbergs, et al (8) revealed that such fundamental studies were lacking in a review of available literature.

Chase (15) has reported that the application of infrared heating to food processing is a matter of placing enough heat source elements into an oven to obtain acceptable processing times. He also reports that product color can

be changed by adjusting the heat source temperature.

In an attempt to correlate the various factors that affect the infrared or radiant heat processing of food and, in particular, ground beef, a review of literature on the subject will be covered in four general areas. These areas are: (a) the thermal properties of beef; (b) the factors that affect the processing or cooking of beef; (c) the basic infrared and the conductive heating theories; (d) the electric infrared heat sources.

2.1 The thermal properties of beef

The basic thermal properties of beef are: specific heat, conductivity, diffusivity, latent heat, emissivity and absorptivity.

2.1.1 The specific heat of beef

Sibel (52) first reported the specific heats of foodstuffs. He concluded that since most foods were composed of water and solids the specific heat would be between 0.2 and 1.00 Btu per 1b-F. The 0.2 value was used as the specific heat of the solid portion of the food and 1.00 was the specific heat of water. The water weight fraction added to the solid weight fraction multiplied by 0.2 gives the specific heat of the product. These figures were accepted until 1942, when Short, et al (53) measured the specific heat of various foodstuffs and found large deviations between their results and Siebel's. This was particularly

true in specific temperature ranges. Many authors (4, 5, 60) have listed the specific heat of food products but they did not define the temperature ranges.

Awberry and Griffiths (11) presented a graphical relationship between the percent water in meat and the specific heat of meat, for the temperature range of 18 to 48 C. They reported a specific heat of 0.375 Btu per 1b F at 0% water and 1.00 Btu per 1b F at 100% water, a linear relationship existed between the two points.

Mannhiem (39) also suggested that the specific heat of foodstuffs is directly related to the percent water in the product.

Daniels and Alberty (18) state that the specific heat of a product or a mixture of products is the weighted average proportion of the constituents which make up the product multiplied by the specific heat of each of the components. This concept has been generally accepted. If this concept is applied to food products and in particular meat, all that is required is the composition of meat and the specific heat of each of the elements that make up the meat.

Chatfield, et al (16) have reported the composition of various cuts of beef in terms of four basic constituents, realizing that each constituent is made up of similar subconstituents. The four basic constituents are: water, protein, fat and ash. The various cuts of beef and their percentages of each of the constituents are shown in Table 2.1.

Table 2	.l. The	composition	of	various	beef	cuts.
---------	---------	-------------	----	---------	------	-------

Beef cut	Protein, percent	Water, percent	Fat, percent	As h, percent
Chuck	18.6	65.0	16.0	0.9
Flank	19.9	61.0	18.0	0.9
Loin	16.7	57.0	25.0	0.8
Rib	17.4	59.0	23.0	0.8
Round	19.5	69.0	11.0	1.0
Rump	16.2	55.0	28.0	0.8

Schweigert and Payne (50) gave the average composition of beef, including chuck, flank, loin, rib, round and rump cuts. They reported the following:

Constituent	Percent
Protein	18.05
Water	61.00
Fats	20.17
Ash	00.78
	100.00

The American Meat Institute Foundation (3) reports that the specific heats of protein, water and ash are 0.44, 1.00 and 0.12 Btu per 1b-F, respectively. The Foundation also points out that fat is unstable in meat. Generally, triglycerides predominate in meat fats. The natural fats in beef are a mixture of triglycerides, monoglycerides and diglycerides, all of which are chemically quite homogeneous. The triglycerides will exist in two forms, the unstable α -form and the stable β -form. The α -form exists

in the solid state for the temperature range, freezing to 121.8 F. Its specific heat is 0.295 Btu per lb-F. The α -solid changes to α -liquid at 121.8 F, with each pound of fat absorbing 68.76 Btu at this temperature. The specific heat of the α -liquid is 0.527 Btu per lb-F. The α -liquid changes to β -solid at 139.1 F and releases 24.3 Btu per lb during the transition. The specific heat of the β -solid is 0.266 Btu per lb-F. The β -solid changes to β -liquid at 156.4 F and the fat absorbs 96.84 Btu per lb during the transition. The specific heat of β -liquid is 0.527 Btu per lb-F.

A graphical plot of fat heat content vs fat temperature is shown in Fig. 2.1.

If the above values of specific heat are used for protein, water, ash and fat in different temperature ranges, in the Daniels and Alberty specific heat equation the average specific heats should be fairly realistic. These values should also replace the values given in literature, which are not based on this or a similar method. The total heat content of beef, of average composition, is also shown in Fig. 2.1. The total heat content assumes that the specific heats of water, ash and protein are constant. However, in general the specific heat should vary with temperatures, as it does for water, but only single values have been reported for protein and ash.

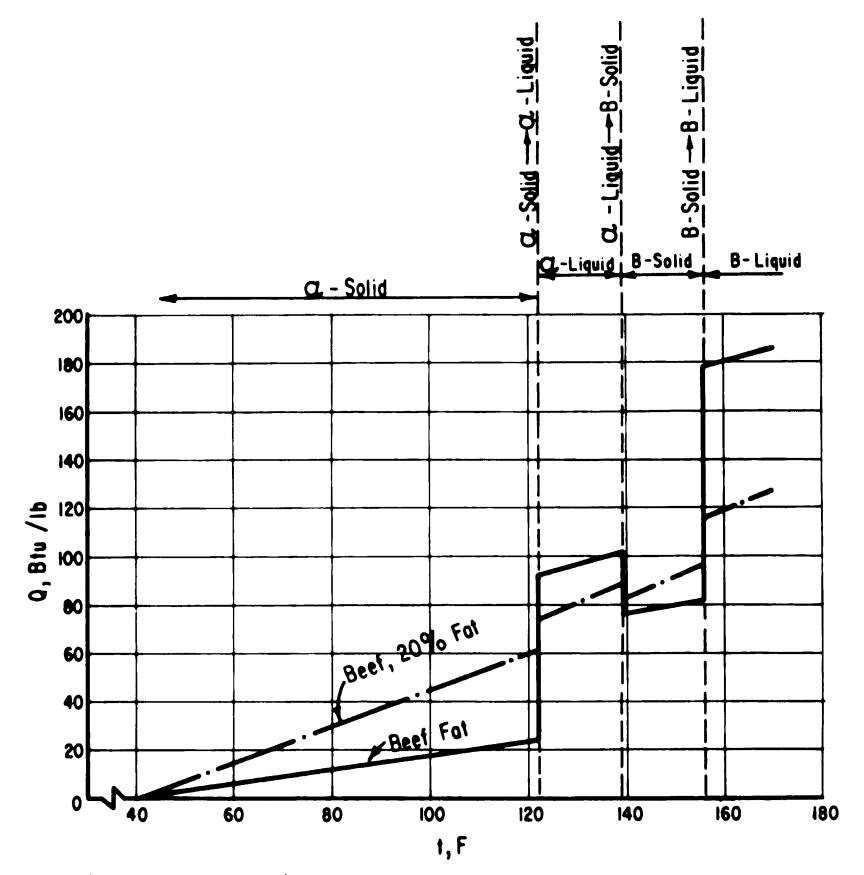


Fig. 2.1 Q, Btu/lb, and temperature relationships for 100% beef fat and beef with 20% fat.

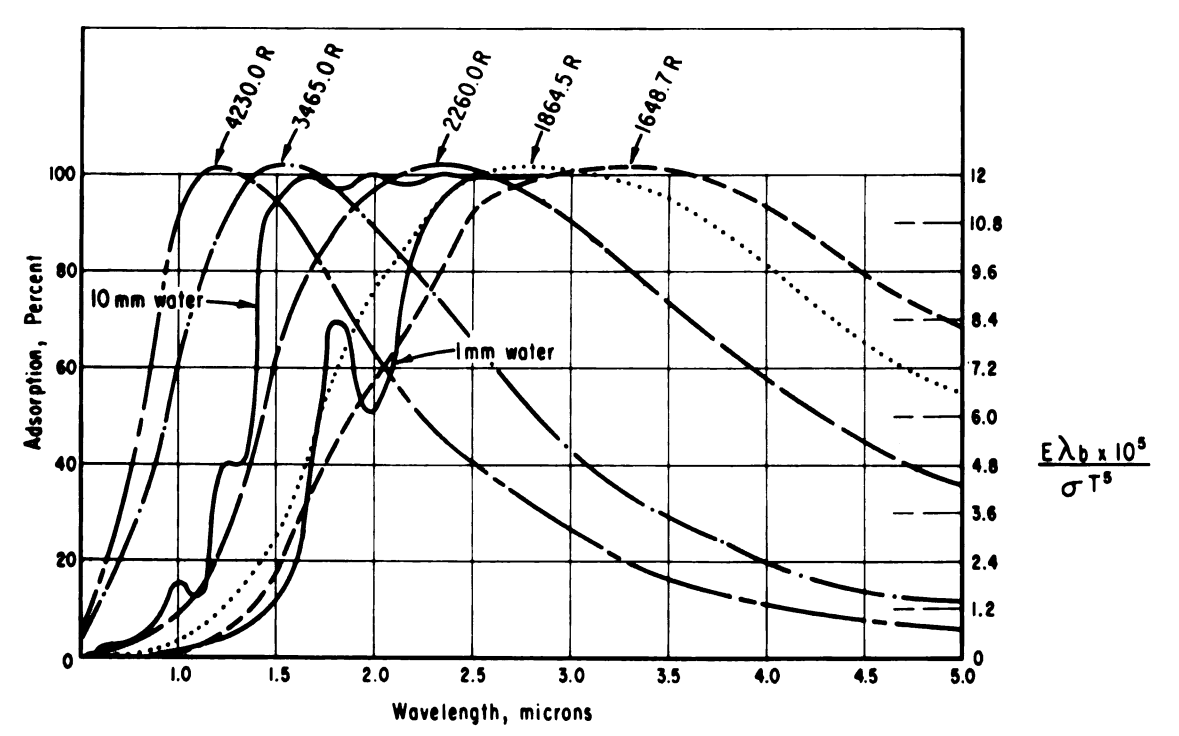


Fig. 2.2 10 mm. and one mm. water absorption and wave length, microns, relationships; $\mathbf{E}_{\lambda \mathbf{b}} \times 10^{5}/\sigma$ \mathbf{T}^{5} and wave length, microns, relationships for various blackbody source temperatures (R).

2.1.2 Thermal conductivity of beef

Information on the thermal conductivity of meats and related animal fats is very limited and often conflicting. Often the composition of the product is not specified and if the thermal conductivity has been experimentally determined, the temperature range for the determined value normally is not given. Because of the importance of freeze dried products in the past ten to fifteen years, most of the information is basically limited to temperatures below freezing.

Awberry and Griffiths (11) gave a thermal conductivity of beef of approximately 0.92 Btu-ft per sq ft-hr-F. However, they omitted the temperature or temperature range. They were primarily concerned with low temperatures. They also indicated that the thermal conductivity of horsemeat was 0.254 Btu-ft per sq ft-hr-F above its freezing temperature.

Tappel, et al (57) have reported the thermal conductivity of freeze dried meat as 1.3 Btu-ft per sq ft-hr-F for frozen meat at the beginning of drying to about 0.02 when the meat is dry. In "Advances of Food Research" (1) a similar value is used for the freeze dried product. In addition the following statement is made, "In general, little change would be expected in thermal conductivity from one meat sample to another, even with different kinds of meat." Again this statement does not indicate a

temperature range, or if the product is fresh, frozen or dried.

Cherneeva (17) reported that thermal conductivities of fat beef, lean beef and pork of moisture contents 74.5%, 78.5% and 78.8%, respectively, were identical at temperatures of 32 F and above. The thermal conductivity was 0.276 Btu-ft per sq ft-hr-F. Lentz (36) has also reported the same value for various meat products in the temperature range of 32 to 50 F. Lentz had measured the value in accordance with ASTM standards and also calculated the value using the Maxwell-Eucken formula. However, this formula assumes knowledge of the conductivities of fat free beef and beef fat. Lentz also reported that the thermal conductivities of meat products above freezing were about equal and about 10% below the established value for water. Sayles (48) recommended that the 0.276 Btu-ft per sq ft-hr-F value be used in the analysis of heat transfer in meat processing.

Cherneeva, Lentz and Sayles all agree on a thermal conductivity value, but they do not state what happens to the conductivity if or when moisture is lost from the surface of the product, a phenomenon that occurs in the processing of meat.

2.1.3 Thermal diffusivity of beef

The thermal diffusivity of beef has been given considerably more attention than the thermal conductivity.

Since diffusivity is dependent on thermal conductivity, specific heat and density, conflicting data appear in the literature.

Awberry and Griffiths (11) reported that the diffusivity of beef was about 0.0147 sq ft per hr in the temperature range of -40 to 80 C, for a density of approximately 73 lb per cu ft. Hurwicz and Tischer (29) reported in 1952 that the apparent diffusivities of solid pieces of shoulder clod beef, canner and cutter grades, were approximately 0.0067 and 0.0073 sq ft per hr at 225 and 255 F, respectively. Hurwicz and Tischer (30) also had found, in 1956, for solid pieces of beef rounds, that the apparent diffusivities were approximately 0.0163 and 0.0176 sq ft per hr for the temperature ranges, 225 to 261 F and 279 to 315 F, respectively. The diffusivities were significantly different in these two temperature ranges. They obtained the diffusivities from can processing heating and cooling curves. They failed to report the densities of the meats in both papers.

Evans (21) has reported that the diffusivity of most non-water constituents in food is lower than for water and would not be expected to vary greatly with temperature; therefore, the diffusivity of foods will be slightly less than those of water at similar temperatures, and will be expected to undergo a smaller variation with temperature, perhaps 5 to 20% less than for water.

Jackson (31) has classified food products depending on whether they exhibit conduction or convection heating curves and then subclassed by moisture content. Jackson states the following products will exhibit conduction heating curves throughout a canning process and will have thermal diffusivities close to that of water; these products include: solidly packed meat and marine products, such as corned beef, chicken loaf, minced clams, cod fish, sandwich spreads and spiced hams; meat and cereal mixtures, such as dog food and some meat loaf products. He also states that some products will exhibit convection heating curves but have thermal diffusivities considerably less than that for water, these include a few meat products with a low moisture and high fat or oil content.

olson and Schultz (45) have reported a diffusivity value of 0.005 sq ft per hr for spiced ham and that most meat products have a diffusivity similar to the spiced ham value. They also indicated that the 0.005 value is most frequently used in the canning industry for meats that exhibit conduction heating curves.

It is interesting to note that if the specific heat values as found by the Daniels and Alberty formula for the average composition of beef, and the recommended value of thermal conductivity are used with a boneless, basically homogeneous beef product, the result is a diffusivity close to that recommended by Olson and Schultz.

2.1.4 Latent heat factors in the processing of beef

Lowe (37) Lukianchuk (38), McCance and Shipp (43) all report that during processing of meat there is a loss of moisture and fat. Lowe, McCance and Shipp report that the volatile loss of a meat product consists of water vapor, while the dripping losses are primarily water and fats with small amounts of salts. McCance and Shipp first reported that the volatile loss of a beef product was a linear function of time. This was verified, at a later date, by Lowe. Lowe has also reported that higher final product temperatures result in a larger volatile loss. This latter statement would naturally follow if the previous remarks are correct, because a higher product temperature indicates a longer processing time, at equivalent processing rates.

If the volatile product loss is water and if the product surface temperature is known, the latent heat of vaporization can be found from steam tables.

In section 2.1.1, the latent heats of triglycerides were given for various $\alpha-$ and $\beta-$ transitions. These latent heats could then be applied to the fat changes within beef.

Lowe (37) also points out that protein denaturation probably occurs at 140 F, which is an endothermic process. The American Meat Institute Foundation (3) states that denaturation caused by thermal energy occurs at the same temperature. They suggest that thermal energy causes the rupture of intra- and interchain hydrogen bonds and this

results in the unfolding of certain protein chains, called peptide chains, and the reaction is an irreversible endothermic process. At about the same temperature, 140 F, α -form liquid fats change to β -form solid fats and energy is released in this process. This is probably why the product temperature rise is not accelerated during the exothermic latent heat process.

The American Meat Institute Foundation has indicated that there is not a statistically significant loss of amino acids under commercial methods of processing or cooking. The Institute indicates that the degree of fat dispersion is a function of product surface area and total fat mass and somewhat dependent on the degree of swelling, shrinkage or disintegration of the collangenous fibers in beef. Also, the elastin proteins in beef are not appreciably changed during processing.

2.1.5 The emissivity of beef

Absorption data of foodstuffs are almost nonexistent. However, Hall (25) has made the following general statements concerning products heated by infrared:

> 2.1.5.1 The absorptivity of non-conductors or insulators increases as the wave length of electromagnetic radiation in the infrared region is increased, that is, the temperature of the emitter is decreased.

- 2.1.5.2 Most hygroscopic materials have a low absorptivity in the range from 0.5 to 3 microns and a high absorptivity beyond 3 microns.
- 2.1.5.3 The maximum absorptivity of water occurs at 3, 6 and above 15 microns wave length.
- 2.1.5.4 Generally, as the temperature of a product increases the absorptivity decreases.
- 2.1.5.5 As the moisture content increases the absorptivity increases.

Infrared energy may be reflected, absorbed or transmitted through a body, both the absorpiton and trans-mittance are of primary importance in the processing of beef.

DeWerth (19) has reported that the surface color of a product has an effect on absorption, with lighter colored surfaces having lower absorption. He also found that the radiant heat source temperature had a critical effect on absorption. With high heat source temperatures, the surface color greatly influenced absorption rates, while low heat source temperatures reduced the differences in surface color effects. Hienton, et al (27) report that grey, green, brown and red colors have absorptions in the range, 0.65 to 0.75, while the lighter colors such as light green, yellow and white have absorptions in the range, 0.40 to 0.55. Hall (25) reported that the absorption of infrared energy by sand is a function of the percent of water in the sand, with higher water percentages

leading to higher absorptions.

Shuman (54) reported the absorption and wave length curve for orange juice solids, which indicated a maximum absorption at about 3.6 microns. He also stressed the importance of matching the wave length characteristics of the radiant heat source with the absorption properties of the product.

Schroeder (49) reported a linear correlation between initial moisture content and infrared drying rates, which were significant at the one percent level for four varieties of rice. Shuman (54) has reported that researchers have had disappointing results with infrared heating because of popular misconceptions about the energy and a lack of fundamental knowledge concerning the absorption of infrared energy.

Asselbergs, et al (8) reported on the heat penetration into apple tissue after five minutes exposure to three types of infrared radiators. These radiators were a quartz lamp, a quartz tube and a calrod, the electromagnetic wave lengths at maximum energy emission were 1.16, 2.35 and 2.65 microns, respectively. They found that by increasing the surface heat flux at each of the above wave lengths that the heat penetration increased. The heat penetration and surface heat flux relationship was basically linear in a given time period. Lastly, they reported that the infrared absorption characteristics of apple solids became important only during the advanced stages of dehydration.

However, they did not indicate how they defined these advanced stages of dehydration.

DeWerth (19) and Shuman (54) gave the spectral transmittance and absorption of various thicknesses of water. Some of these are reproduced in Fig. 2.2. Plotted in the same figure are various black body energy distributions at different source temperatures, these are plotted in accordance with Planck's law of energy distribution (46). From Fig. 2.2, it can be seen that lower source temperature radiations are almost totally absorbed by surface layers of water. Therefore, if a moist meat product has volatile losses during processing, this indicates that water is on or very close to the surface of the product and the absorption spectrum of such products could then be similar to that of water.

Sevick and Sunderland (51) reported in 1962 on the emissivity of beef. This is probably the first article to appear in literature on the measurement of emissivity of food products. Chase (14) and DeWerth (19) had assumed values close to that of water for their work. Sevick and Sunderland stated that the emissivity of lean beef muscle was 0.74 and 0.73 at 70 and 95 F, respectively. A linear relationship exists between these values. They also reported values of .780 and .775 for beef fat between the temperatures given above.

2.2 The factors that affect beef processing.

Lowe (37) states that when meat is processed or cooked the following changes may occur:

- 1. Color of meat
- 2. Weight
- Volume contraction
- 4. Fatty tissue
- 5. Structural proteins or connective tissue
- 6. Muscle fibers
- 7. Flavor

Most of these factors have already been discussed. However, her remarks on volume contraction are particularly interesting. She states the volume does not basically change until a temperature of 140 F is attained, then from 140 to 158 F, a high volume reduction occurs. The volume continues to decrease but at a much lower rate in the 158 to 248 F temperature range. In most cases the length and width are decreased but the product depth is increased. In all cases the reduction of volume is less than the total weight loss of the product. Lowe's statements are in general agreement with other researchers. For example, Meigs (44) found little volume change below 104 F, McCance and Shipp (43) indicated very small volume changes below 140 F. American Meat Institute Foundation (3) found that collagenous fibers, first swelled, then shrank, and finally disintegrated for well done beef (about 170 F). They also indicated that

shrinkage due to coagulation, or extensive protein denaturation is nearly complete at approximately 152 F.

Lowe (37) also suggests that the time required for processing or cooking is dependent on:

- 1. The method of processing
- 2. The processing temperature
- 3. The weight, surface area and maximum depth
- 4. The final product temperature
- 5. The composition of the meat
- 6. The degree of post mortem changes
- 7. The initial temperature of meat

Six of the seven above items normally appear in heat transfer equations for product temperature determination at a specific depth and time. Only the sixth item does not appear, although this factor is probably indirectly involved with product thermal properties, such as conductivity, specific heat, diffusivity and emissivity.

Product heat penetration rates, in minutes per degree temperature rise, or time-temperature curves are reported by Lowe (37), Towson (59) and Lukianchuk (38). An analysis of the heat penetration rate or curves indicated four definite rates or linear relationships within the temperature ranges given for the various α - or β -forms of fat in beef. The temperature ranges were: from the initial temperature, above freezing, to about 122 F; 122 to 140 F; 140 to 157 F; and above 157 F.

Chase (14) discussed surface heat flux effects on cake quality and found that 550 Btu per sq ft-hr was an optimal surface heat flux. He also stated that changes of 50 Btu per sq ft-hr from the optimal value of 550 reduced the quality of the cake. But, he did not take surface moisture evaporation into account in his calculations. If the latter factor had been determined, his surface heat flux rates would have probably increased. In addition, the energy requirement to cause the cake rising reaction was not considered. Therefore, the optimal value was probably higher than he indicated.

Pollak (47) has processed meat to a center temperature of 150 F, with a conventional convection type oven, with infrared radiation and with a microwave type cooker, utilizing the magnetron. He measured all product changes with each heat source and reported the results as percent heat source input and heat absorbed by the product ratio. He only indicated that the conventional oven temperature was set at 325 F and that the infrared device was placed three inches from the product. Electrical wattages of the elements, surface heat fluxes, product surface temperatures and other heat transfer information were not given.

Lowe (37) reported on the effects of various oven temperatures and final product temperatures on weight losses. Keating (34) reported similar information for forced convection processing of meat and other products. Chase (14) stated that when data are presented in the above manner,

heat transfer analysis is very difficult and in some cases impossible because of the lack of essential information. Chase is only one of the few authors, except for those concerned with canning processing, who attempted to analyze the mechanisms of heat transfer and correlate data on these results.

2.3 Infrared and the conduction heating theories

2.3.1 The infrared theory

The total radiant energy emitted per unit time per unit area is defined as the total emissive power and is often denoted by E (24). The amount of energy emitted by a body generally varies with wave length or frequency. The variation is often defined by the monochromatic emissive power E_{λ} , which is the amount of energy emitted in the spectral range λ to $d\lambda$ and is generally defined by $E_{\lambda}d\lambda$, so $E = \int_{-\infty}^{\infty} E_{\lambda}d\lambda$.

If radiant energy were incident upon a surface of finite thickness, the energy could be absorbed, reflected and transmitted. Total monochromatic absorptive, reflective and transmitive powers can be defined as above. From these, the absorptivity α , reflectivity ρ , and transmissivity τ , can be defined. The absorptivity (α) is defined as follows:

$$\alpha = \frac{1}{G} \int_{0}^{\infty} \alpha_{\lambda} G_{\lambda} d\lambda$$

Where G is the incident radiant energy, G_{λ} is the spectral distribution of G; α_{λ} is the fraction of the monochromatic incident energy absorbed and λ is the wave length. It would follow that $\alpha + \rho + \tau = 1$.

Kirchhoff established the following relationship: for radiation at the same wave length and temperature, the ratio of the emissive power to the absorptivity is the same for all bodies. The importance of Kirchhoff's law is indicated when one considers a black body. A black body is a body which absorbs all incident radiation ($\alpha = 1$). If a black body is a radiator no other body could radiate more heat than it. If $E_{\lambda b}$ is the monochromatic emissive power of a black body, then the monochromatic emissivity, ϵ_{λ} , of a non-black body is:

$$\epsilon_{\lambda} = E_{\lambda}/E_{\lambda b}$$

The total emissivity, ϵ , could then be defined as the absorptivity was defined above. If Kirchhoff's law is employed and if one of the bodies is a black body, the following relationship exists:

$$\alpha_{\lambda} = \epsilon_{\lambda}$$
, and $\alpha = \epsilon$

Kirchhoff's law specifies that these relationships exist at one temperature. If the behavior of a body can be approximated by considering $\alpha_{\lambda} = \epsilon_{\lambda} = \alpha = \epsilon$ for all wave lengths and temperatures, these bodies are called gray bodies.

Most radiation theory is developed on a black body basis or by assuming monochromatic properties. It is generalized from the monochromatic to the total spectral properties, and finally in some cases further generalized for gray bodies.

The Stefan-Boltzmann law relates the total emissive power of a black body to the absolute temperature of the same body, it is:

$$E_b = \sigma A_1 T^4$$

Where A_1 is the black body surface area of a finite depth (P), σ is the Stefan-Boltzmann constant (0.174 x 10⁻⁸ Btu per hr-sq ft - R⁴ (33)), and T is the absolute temperature, R.

Wein's displacement law states, if a wave of length λ_2 at T_2 is displaced from that of length λ_1 at T_1 , such that $\lambda_2 T_2 = \lambda_1 T_1$, the monochromatic emissive powers of these two wave lengths are directly proportional to the fifth power of the absolute temperatures. The relationship indicates that the maximum value of E_{λ}/T^5 occurs when $\lambda T = 5215.6$ micron - R. If the temperature of a black body source is known, the wave length of maximum energy emission can be solved for this value and is frequently used in literature (19, 25, 33, 48, 54).

Wein developed an equation for the spectral distribution of energy which was accurate for wave lengths up to two microns. Rayleigh and Jeans also developed an equation for the spectral distribution of energy, but it failed at low wave lengths. Planck (46) then proposed a law which fits experimental data, and was also consistent with the Stefan-Boltzmann law. Planck's law is as follows:

$$E_{\lambda b} = \frac{c_{1 \lambda}^{-5}}{e^{c_2/\lambda T} - 1}$$

This equation is particularly useful for plotting the spectral energy distributions of black bodies, gray bodies and other bodies with known monochromatic properties at given temperatures.

The radiant energy exchange between surfaces is dependent upon the emission, absorption and reflection characteristics, which were discussed above. It also involves the geometrical surface arrangements and the media between the surfaces. If air is the media between surfaces, it can generally be considered opaque (28). However, if it contains water vapor the absorption and emission of water vapor must be considered. If the saturation level and partial pressure of water vapor is low, the emission of energy from it is generally low and is often neglected in the radiant energy exchange between bodies (24, 28, 42, 48). A similar situation applies to carbon dioxide gas (24, 33). Only the case of diffuse radiation through a non-absorbing medium will be considered.

Jakob (33) gives a crude approximation for the net heat exchange by radiation between a completely convex

body which radiates diffusely to a completely concave enclosure at a lower temperature; it is:

q net =
$$\epsilon_1 \sigma A_1 (T_1^4 - T_2^4)$$
,

Where the subscripts 1 and 2 refer to the inner body and enclosure, respectively. Jakob also assumed that Lambert's law is valid and derived a general equation for diffuse radiation between two surfaces. He considered two differential surface elements, separated by a distance (r) at arbitrary angles to each other, the angle (Φ) was defined as the angle between (r) and the normal to the surface. The differential radiation from dA_1 to dA_2 would be:

$$dE_{(d_1)(d_2)} = \epsilon_1 \sigma T_1^4 \frac{\cos\phi_1 \cos\phi_2}{\pi r^2} dA_1 dA_2$$

$$= \epsilon_1 \sigma T_1^4 dA_1 \int_{A_2} \frac{\cos\phi_1 \cos\phi_2}{\pi r^2} dA_2$$

He then defined the geometrical angle factor $F_{(d_1)_2}$, as that fraction of the energy emitted from dA_1 which directly strikes the area A_2 ;

$$F_{(d_1)_2} = \int_{A_2} \frac{\cos d_1 \cos d_2}{\pi r^2}$$
.

A similar procedure is followed for $dE(d_2)(d_1)$;

$$dE_{(d_2)(d_1)} = \epsilon_2 \circ T_2^4 \frac{\cos\phi_1 \cos\phi_2}{\pi r^2} dA_1 dA_2$$

The energy exchange between dA_1 and dA_2 would be:

dq net =
$$dE_{(d_1)(d_2)} - dE_{(d_2)(d_1)}$$

= $\epsilon_1 \epsilon_2 \sigma(T_1^4 - T_2^4) \frac{\cos\phi_1 \cos\phi_2}{\pi r^2} dA_1 dA_2$

If F_{12} is the geometrical angle factor of A_1 versus A_2 , the geometrical angle factor is:

$$F_{12} = \frac{1}{A_1} \int_{A_1} \int_{A_2} \frac{\cos\phi_1 \cos\phi_2}{\pi r^2} dA_1 dA_2$$

so, q net = $\epsilon_1 \epsilon_2 F_{12} \circ A_1 (T_1^4 - T_2^4)$, if $F_{(d_1)_2}$ is constant over the surface A_1 .

Hottel (28) then applied the general geometrical angle factor equation to a specific situation. He found $F_{(d_1)_2}$ for a differential area radiating heat to a finite parallel surface area, Fig. 2.3 represents the geometry. For parallel surfaces: $\cos \phi_1 = \cos \phi_2$. The distance D is the perpendicular distance between surfaces, (r) is the distance drom dA_1 to dA_2 , x is the length of A_2 and y is the width of A_2 and A_2 and A_3 and A_4 and A_4 and A_5 and A_6 and A_6

$$F_{(d_1)_2} = \frac{1}{2^{\pi}} \left[\frac{L_2}{(L_2^2 + 1)^{1/2}} \sin^{-1} \frac{L_1}{(1 + L_2^2 + L_1^2)^{1/2}} + \frac{L_1}{(L_1^2 + 1)^{1/2}} \sin^{-1} \frac{L_2}{(L_2^2 + L_1^2 + 1)^{1/2}} \right].$$

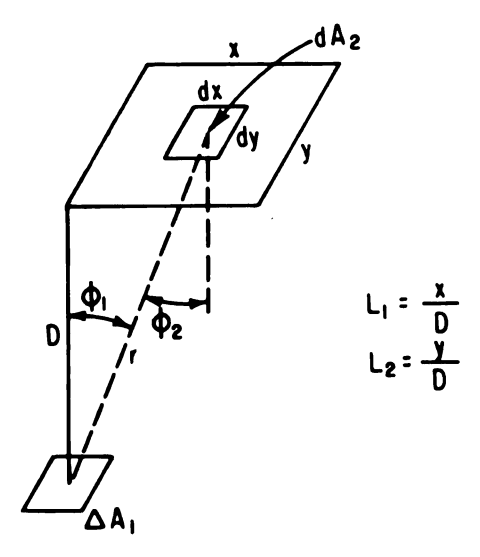


Fig. 2.3 Hottel's geometrical model for determining the geometrical angle factor between a differential surface and a parallel finite surface.

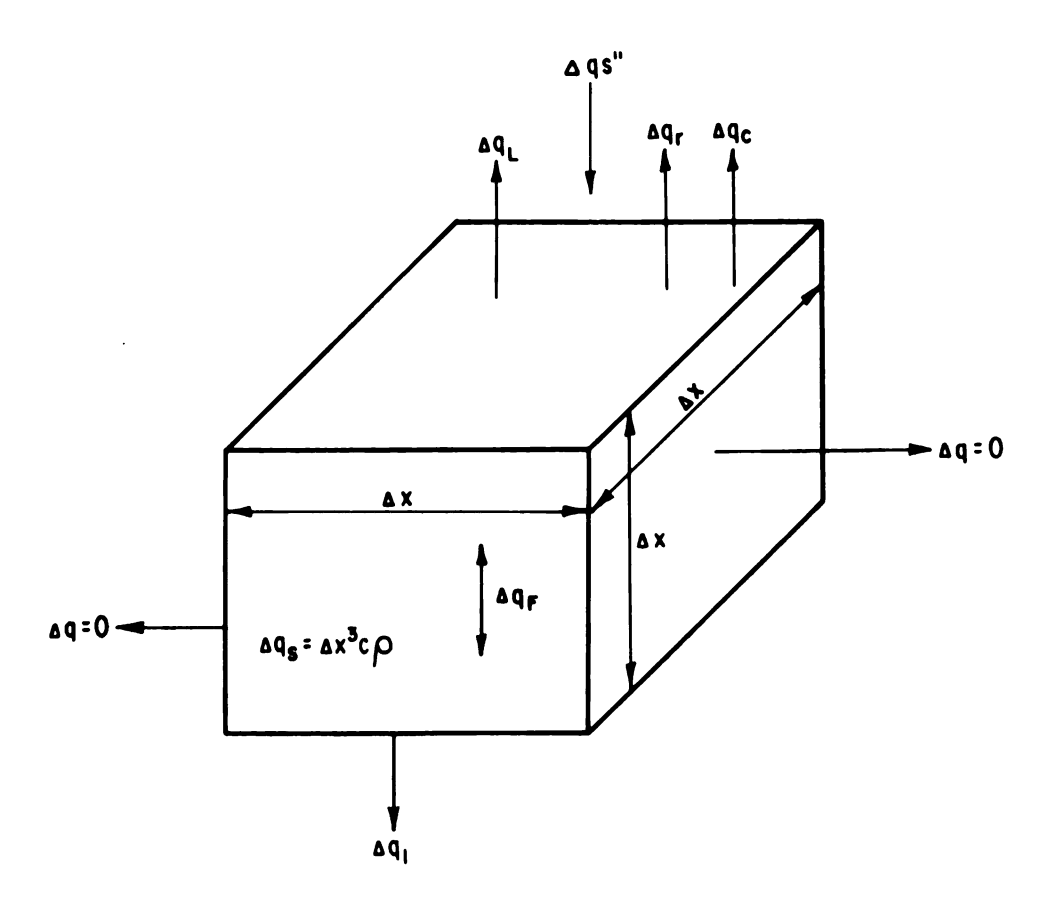


Fig. 2.4 Surface element heat balance.

McAdams (42) presented a graphical solution to the equation, as did Jakob. However, Jakob used different symbols, a, b, c, B and C for D, x, y, L_1 and L_2 , respectively.

Having determined the geometrical angle factors and knowing the surface emissivities, areas and temperatures, the radiant heat exchange between the surfaces can be determined. For the heated surface, subject to a high heat source temperature, with the heated surface being much lower in temperature, a constant surface heat flux (Btu per sq ft-hr) may be used according to Heisler (26).

2.3.2 The conduction heating theory

The Fourier differential equation of heat conduction without heat sources (23) is:

$$\frac{dt}{d\tau} = \alpha \left(\frac{d^2t}{dx^2} + \frac{d^2t}{dy^2} + \frac{d^2t}{dz^2} \right).$$

The equation assumes constant thermal properties of a homogeneous substance, also heat is not generated or absorbed by the body.

The equation can be simplified, and heat flow restricted to one direction if an infinitely wide surface area is used. Jakob (33) suggests that if an infinitely thick plate is used, its length and width may be finite if it is perfectly insulated around the edges, in which case the heat flow will be perpendicular to the surface.

Many solutions to the Fourier equation for different boundary conditions are given in the literature on

the subject (13, 26). However, before a solution can be determined for a particular problem, boundary conditions must be specified. To best indicate possible boundary conditions for processing meat, by high temperature radiant energy sources, a heat balance should be attempted for an element of the material. Fig. 2.4 represents a surface element of the product, with uni-directional heat flow. Aqs" represents the incident radiant heat on the surface, only $\triangle qs$ will be absorbed. $\triangle q$ is the radiant heat loss from the surface to the environment, if the temperature of the environment is lower than the surface temperature. $\Delta \mathbf{q}_{_{\mathbf{C}}}$ represents the surface convection heat loss to the environment, if the environment is again at a lower temperature. Δq_{τ} is a latent heat loss, or product volatile loss which can be represented in units of heat loss. Δq_1 is the heat transferred through the product. Δq_s is the heat stored within the product, this indicates a transient heat transfer problem, in contrast to a steady state problem. Finally, $\Delta \mathbf{q}_{_{\mathbf{F}}}$ is the heat absorbed or released in product changes. In the case of beef processed above 121.1 F this $\textbf{q}_{_{\mathbf{F}}}$ would represent the various changes of state for the α - and β -form fats. The α in the Fourier equation is thermal diffusivity, not to be confused with α -form fats within the meat product.

Heisler (26) solved the Fourier equation for a similar boundary condition, but he did not include the \mathbf{q}_{F} term above. His solution was for the induction heating of

metals, at given cycles per second and for given penetrations into the surface of the metal. He also assumed the product had a finite thickness and it was heated from both sides by similar surface heat fluxes. Jakob points out that a product that is perfectly insulated at some depth, can be considered a product of finite thickness, with a depth of one half of the finite thickness situation. Heisler's final solution is:

$$\frac{\text{t(m,X)-tb}}{\text{qs"/h}} = 1 - 2 \sum_{k=1}^{\infty} \frac{(\sin w_k)(\cos n w_k) \exp(-w_k^2 x)}{w_k + (\sin w_k)(\cos w_k)}$$

Where n indicates the relative position in the body; $X = (\alpha \tau)/L^2$, L is the depth, α is defined above, τ is time; qs" is the surface heat flux; h is the coefficient of surface heat loss; the initial product temperature, which is constant at $\tau = 0$; w_k is taken from : $nw = \cot w$, where w is an integer. He also gives an approximate solution for values of $X \le 0.2$. The solutions of these equations are given on his familiar Heisler charts, instead of θ_0/θ_1 he uses $1-h(\theta_0-\theta_1)/qs$ " as one of the parameters, the other parameters are unchanged for X > 0.2. On his chart for $X \leq 0.2$ the parameter $h(\theta - \theta_i)/qs$ " is used instead of 1 - $\theta/\theta_{\rm i}$. Except for the ${\bf q_F}$ heat term, this is a solution for the particular radiant heating problem. If $\boldsymbol{q}_{_{I\!\!P}}$ is considered at definite temperatures, which are known, perhaps charts similar to Heisler's could be plotted within various temperature ranges, with the $\mathbf{q}_{_{\mathbf{F}}}$ temperatures acting

as a parameter temperature for each temperature range. However, one of Heisler's boundary conditions should be checked if experimental data is to correspond with his solution. The particular boundary condition is that a final uniform product temperature is assumed to be qs"/h)F above the original product temperature.

The surface heat transfer coefficient depends on three types of heat transfer; they are radiation, convection and a latent heat of vaporization. The first two heat losses are easily handled by generally accepted heat transfer equations. Jakob (33) discusses the latent heat case, stating that if the weight of the vaporizing product is known (m), its latent heat of vaporization is known (L), then this can be equated to an apparent coefficient of heat transfer (h_L), the environment temperature (t_e) and the surface temperature (t_e), thus:

$$mL = h_L (t_s - t_e)$$

 $h_L = mL/(t_s - t_e)$.

The use of the apparent heat transfer coefficient is only valid if the rate of loss per unit of time is constant.

Carslaw and Jaeger (13) discuss the case of an infinitely wide plate of finite thickness, with a radiation boundary condition, and heat loss from the surface. They give, the solution for this surface temperature, temperature at the center and the average product temperature. Their solutions correspond to Heisler's.

2.4 Electric infrared heat sources

The three most common electric heat sources are quartz lamps, quartz tubes and calrods.

The quartz lamp consists of a coiled tungsten filament enclosed by a fused quartz envelope. The common electrical consumption of the lamp is 100 watts per linear inch of coiled filament length. At its rated voltage, the filament will operate at about 4500 R (12). The filament temperature is then reduced at voltages less than rated. The lamps can be made at almost an infinite number of lengths. At reduced voltages, the emissivity of tungsten is reduced (40) as well as the temperature, hence radiant heat cutputs are greatly reduced (12). In addition, the transmittance properties of fused quartz are also affected by different filament temperatures, generally the transmittance is decreased at lower temperatures (12). Fused quartz approaches a black body condition for a radiation of five microns and longer (12). The fused quartz then absorbs energy and reradiates heat at lower temperatures and at reduced intensities. The difference between the absorbed heat and the reradiated heat of the quartz envelope is either lost by convection to a lower temperature environment or conducted to the ends of the cylinder-type envelope, and the heat is lost by convection, radiation or conducted to the electrical terminal. At ordinary room air temperatures, the terminal may have an equilibrium temperature of about 200 F, under extremely high environment temperatures

the terminal may attain a temperature of 625 F, which is the maximum design terminal temperature (12).

The quartz tube consists of a coiled chromnickel filament, enclosed by a fused quartz envelope. The normal operating temperature of the filament is 2260 R at rated voltage. The chromnickel emissivity is a function of temperature, generally decreasing at lower temperatures (19). The general properties of fused quartz were given above and apply equally well for the quartz tube. The quartz tube end losses are similar to those indicated for the quartz lamp, except for a higher end or terminal temperature (12).

A 1600 watt, 240 volt quartz lamp has a 16 inch filament and an 18 inch fused quartz envelope. The 550 watt, 120 volt quartz tube has a 17 inch filament and an 18 inch fused quartz envelope. The quartz lamp and tube ends can be treated as short rods, transfering heat to an environment.

The calrod or radiant rod consists of an electrical resistance filament, which is covered by insulation, and the insulation is covered by a thin wall metal sheath. Heat is primarily transferred by conduction to the metal sheath which attains a temperature of about 1960 R under rated voltage and wattage. For example, a 240 volt, 1000 watt calrod will maintain a metal sheath temperature of about 1960 R when operated at ordinary room temperatures (19). This rod will be approximately 17.5 inches in length. The

actual length of the surface at the 1960 R must be determined or measured (12). The remaining surface, or the ends of the rod could then be treated as rods of medium or short length with a source temperature of 1960 R (at 240 volts).

Jakob (32) suggests the following equation for the heat loss of a not very long rod protruding from a heat source:

$$q_0 = (KhAC)^{1/2} \frac{1 - pe^{-m2L}}{1 + pe^{-m2L}} \theta_0$$

Where q_0 is the heat loss from the rod, K is the thermal conductivity, h is the surface heat transfer coefficient, A is conducting cross section area of the rod, C is the rod surface area, p is defined as (Km - h)/Km + h), m is defined as $(hC)/(KA)^{-1/2}$, L is the rod length, θ_0 is the temperature difference between the source and the environment. Jakob also suggests the following equation to determine the temperature distribution on the surface of the rod at various distances (x) from the source of heat:

$$\theta = \frac{\theta_0}{1 + pe^{-m2L}} (e^{-mx} + pe^{-m2L} e^{mx}),$$

Where θ is the temperature difference at the distance (x) and the environment, the other terms are defined above.

3.0 EXPERIMENTAL APPARATUS

- 3.1 Steel rule, accuracy $\pm 1/64$ inch
- 3.2 Vacuum tube voltmeter, accuracy + 5 volts AC
- 3.3 Ammeter, \pm 0.05 amperes AC
- 3.4 Brown Electronik Recording Potentiometer, accuracy

 + 1 F in the range of the experiments, + 4 F in the

 0 to 600 F range, both accuracies with iron constantan
 soldered thermocouples
- 3.5 Weighing scale, \pm 0.05 grams
- 3.6 Mercury in glass thermometer, accuracy ± 0.5 F
- 3.7 Variac transformer
- 3.8 Eppley radiation pyrheliometer, maximum transmittance of crystal 12 μ , heat flux range (unknown, but the instrument is primarily used for solar radiations)
- 3.9 Leeds-Northrup manual potentiometer with room temperature compensation setting, reading accuracy ±

 0.03 millivolts
- 3.10 Stop watch, accuracy + 0.005 minutes
- 3.11 Micrometer, accuracy + 0.001 inches
- 3.13 Insulated box, 8" (depth) X 6" (width) X 10" (length)
- 3.14 Relative weighing volatile loss scale, with vibrator, reading accuracy + 1 unit (the scale had a linear-unit

vs weight removal relationship)

3.15 Paper distance scale between heat source and sample
 surface, reading accuracy <u>+</u> 0.03 inches

4.0 PROCEDURE

4.1 Electrical energy characteristics of the heat sources

The electrical energy requirements of the three heat sources (quartz lamp, quartz tube and calrod) were measured by a voltmeter and ammeter. Voltage was controlled by a variac transformer. Three ampere measurements were made at each voltage increment of 20 volts for the quartz lamp and calrod, while only 120 volts were used for the quartz tube.

4.2 Physical measurements of the three heat sources

The diameters and lengths of the three heat sources were measured using a micrometer and measuring rule. Ten measurements were made of each of the diameters and lengths.

The filament diameters of both the quartz lamp and quartz tube were measured by a micrometer. The same instrument was used to measure the external shell diameter of the quartz lamp, quartz tube and calrod. Inside calipers were used to measure in interior diameter of the calrod steel shell. The filament measurements were made on only one lamp and tube, while at least three different units were used for external shell and length measurements.

4.3 Heat flux measurements

Heat flux measurements of the specific heat sources (quartz lamp, quartz tube and calrod) were made at different electrical voltages for the quartz lamp and calrod and for the normal operating voltage (120 volts) of the quartz tube. The heat flux measurements were also made at three distances from the heat source.

A variac transformer was used to regulate the voltage of the heat sources. The voltage was measured by a voltmeter. Heat flux measurements were made with a radiation pyrheliometer connected to a manually operated potentiometer. Voltage increments of 20 volts were used for the quartz lamp and calrod unit. To the quartz tube, 120 volts were applied. Heat fluxes were measured at six, nine and twelve inches from the center of the heat sources. One and three heat source unit fluxes were measured at the above voltages and distances for the quartz lamp. A one unit heat source was used for the calrod and quartz tube.

All heat flux measurements were made in a nonenclosed volume at normal room temperature. The wire leads
from the pyrheliometer to the potentiometer were shielded
from the heat source by highly reflective metal foil.
Room temperatures were measured by a mercury in glass
thermometer. A room temperature compensation was made
on the potentiometer. In all cases the exposure time of
the pyrheliometer was at least three minutes. A ten minute

minimum time period was used for the calrod to allow the heat source to approach its equilibrium temperature.

The pyrheliometer was placed perpendicular to the center of the heat source and similarly to the center-unit for the three unit source. The three units were parallel and were spaced one inch on centers. See Fig. 4.1.

4.4 Effect of surrounding walls and reradiation.

Six samples of ground beef from the same mass were cooked to determine the effect of reradiation from surrounding walls. The samples were one inch in depth, three inches wide and six inches long. The sample was placed in a copper container of the same size. The copper container was placed in an insulated container that provided at least two inches of insulation on the sides and bottom of the sample container. The top of the insulated container was flush with the top of the sample container, thus a three inch by six inch surface area was exposed (Fig. 4.2). The top of the insulated container was arranged parallel to a quartz lamp heat source. The sample container center was arranged perpendicular to the center of the heat source, with the six inch length parallel to the length of the heat source.

A constant lamp voltage (220 volts) and a constant distance from the center of the lamp source to the insulated container surface were maintained. This yielded a heat flux at the sample surface of 946 Btu per sq ft-hr at a

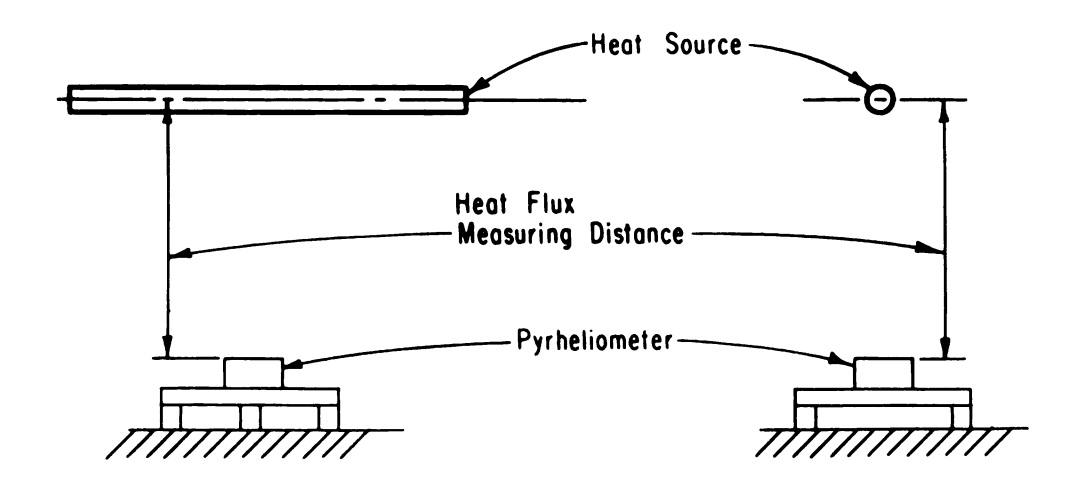


Fig. 4.1 Heat source and pyrheliometer arrangement.

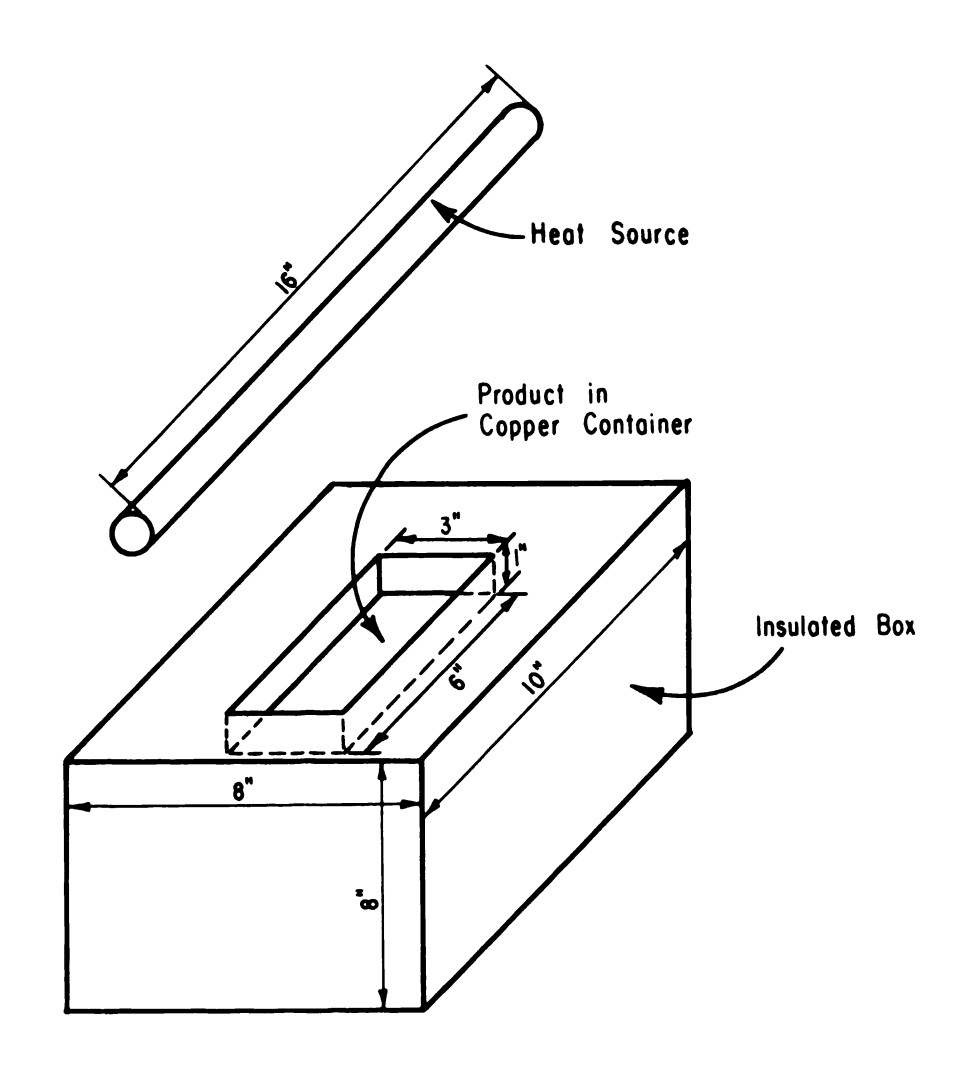


Fig. 4.2 Product, cooper container, insulated box and heat source arrangement.

maximum energy wave length of 1.194 μ . The samples were processed until the temperature at the one inch sample depth was 170 F. The following data were obtained: one inch sample depth and sample surface temperature at one minute intervals; the initial weight of the sample; the container weight; the final sample weight, including drippings; the dripping weight. The difference between the initial weight and final and dripping weights was determined as the volatile weight loss.

The three remaining samples were processed in a similar manner, except that the processing volume was totally enclosed. The enclosure was 36 inches by 48 inches by 48 inches. The insulated container and quartz lamp were located approximately in the center of the enclosure. The inside of the plywood enclosure was painted blackboard black. Various enclosure wall temperatures were measured and a shielded thermocouple was placed in the enclosure.

The sample surface temperature was measured by a thermocouple, which was soldered to a one inch square thin copper plate which was painted lamp black on the side exposed to the radiant heat source. The plate was fastened to the sample surface by fine wire staples driven into the sample. All thermocouple leads were shielded by highly polished metal foil. All thermocouple junctions were soldered.

4.5 Transient processing rates of ground beef with infrared heating

Samples of ground beef were processed at different surface heat fluxes and at different source temperatures.

The ground beef was purchased at one time from the same initial mass and packaged in one and three pound packages and frozen to 0 F on the same day it was ground. The beef* consisted of 160 pounds of lean beef and 40 pounds of beef fat. The frozen samples were removed from the freezer 24 hours before use and placed in a 35 F cooler, whereby defrosting could take place at a uniform rate for all samples. The samples were packaged in freezer paper (wax-coated on the side adjacent to the ground beef), to keep moisture losses to a minimum during storage and to prevent surface dehydration (freezer burn).

Five heat source temperatures were selected, namely: 4230.0 R, corresponding to the quartz lamp filament temperature, and operated under 200 volts AC; 3465.0 R, corresponding to the quartz lamp filament temperature, operated under 120 volts AC; 2260.0 R, corresponding to the quartz tube filament temperature, operated under 120 volts AC; 1864.5 R; corresponding to the calrod shell temperature, operating under 220 volts AC; 1648.7 R, corresponding to the calrod shell temperature, operating under 180 volts AC. These source temperatures would then be equivalent to the maximum energy emission from a black body at 1.233 µ

^{*}The beef, a mixture of choice grade cuts, was ground with first medium (5/16") and then fine (1/8") meat cutter blades.

1.505 μ ; 2.308 μ ; 2.797 μ and 3.164 μ , respectively, according to Wien's Displacement Law.* The above wave lengths cover the critical portion of the water absorption spectrum. DeWert (19).

Generally surface heat fluxes are not reported in the literature, only oven or autoclave temperatures. See Lowe (37), Lukianchuk (38), Chase (14) and others. However, Chase (14) had calculated surface heat fluxes from some of Lowe's earlier experiments and found some products of rather low moisture content had an optimum heat flux rate of about 550 Btu per sq ft-hr. Meats and especially ground beef have relatively high moisture contents, so a range of heat fluxes were used, starting with around 500 Btu per sq ft-hr to over 1000 Btu per sq. ft-hr, assuming the product was a black body. The heat fluxes are shown in Table 4.1.

A sample of ground beef was placed in a copper container 1 inch (depth) by 3 inches (width) by 6 inches (length). The copper container was then placed in an insulated box, which provided at least four inches of insulation on the bottom. The top surface, 3 inches by 6 inches, was left exposed and the ground beef sample was flush with the top of the insulated box. The heat source or sources were then placed parallel to the top surface

^{*}Black body radiation is a function of λT . The maximum of E_{λ}/T^5 occurs when λT = 5215.6 in R, where E_{λ} is the monochromatic emissive power. Giedt (24).

of the insulated box and the center of the heat source or heat sources were placed perpendicular to the center of the ground beef sample (1/2 width and 1/2 of the length). All samples were processed in an air conditioned room (80 F).

The distance between the heat source and the sample was varied to produce desired surface heat fluxes on the sample. Table 4.1 shows the relationships between surface heat fluxes and distances for the different sources, and source temperatures as well as the corresponding wave length, in microns (μ) , at which maximum energy emission occurs.

All ground beef samples were taken from the 35 F cooler and packed in the copper container, which had been previously weighed. The sample and copper container were then weighed. The weight of the ground beef samples ranged from 312 to 330 grams, excluding the copper container. The top surface of the ground beef was flush with the top of the copper container. Two soldered iron constantan thermocouples were placed on the bottom of the container, approximately three inches apart and approximately 2-1/2 inches from the ends and at one half of the width of the container, after the ground beef had been packed in place and weighed.

An iron constantan thermocouple had been soldered to one side of a one inch square copper plate, the other side of which was painted lamp black. The plate was centered on the ground beef surface and held in place by two staples

made of stiff fine wire. This plate was used to measure the surface temperature of the ground beef.

The copper container was placed in the insulated box, which was then placed on a weighing scale. The weighing scale was attached to a vibrator, which could be operated to minimize static scale error.

The thermocouple leads, which were attached to a Brown Electronik Recording Potentiometer, were shielded from the heat source or sources, by highly reflecting metal foil. Room air temperature was also measured by the potentiometer.

The heat source or sources were attached to a floating frame which could be adjusted to vary the distance between the heat source and the sample surface. As the product was being processed its weight was reduced by the volatile loss and periodically (every five or twenty minutes, depending on the heat flux) the difference between the initial weight of the sample, copper container and insulated box and the weight at that time was recorded and a distance adjustment was made to compensate for the decreased distance between sample surface and heat source. The maximum distance deviation was 0.03 inches in any one time increment.

Fig. 4.3 shows the arrangement of heat source, sample and weighing scale. The device for measuring the distance between the sample surface and the heat source is also shown in the figure.

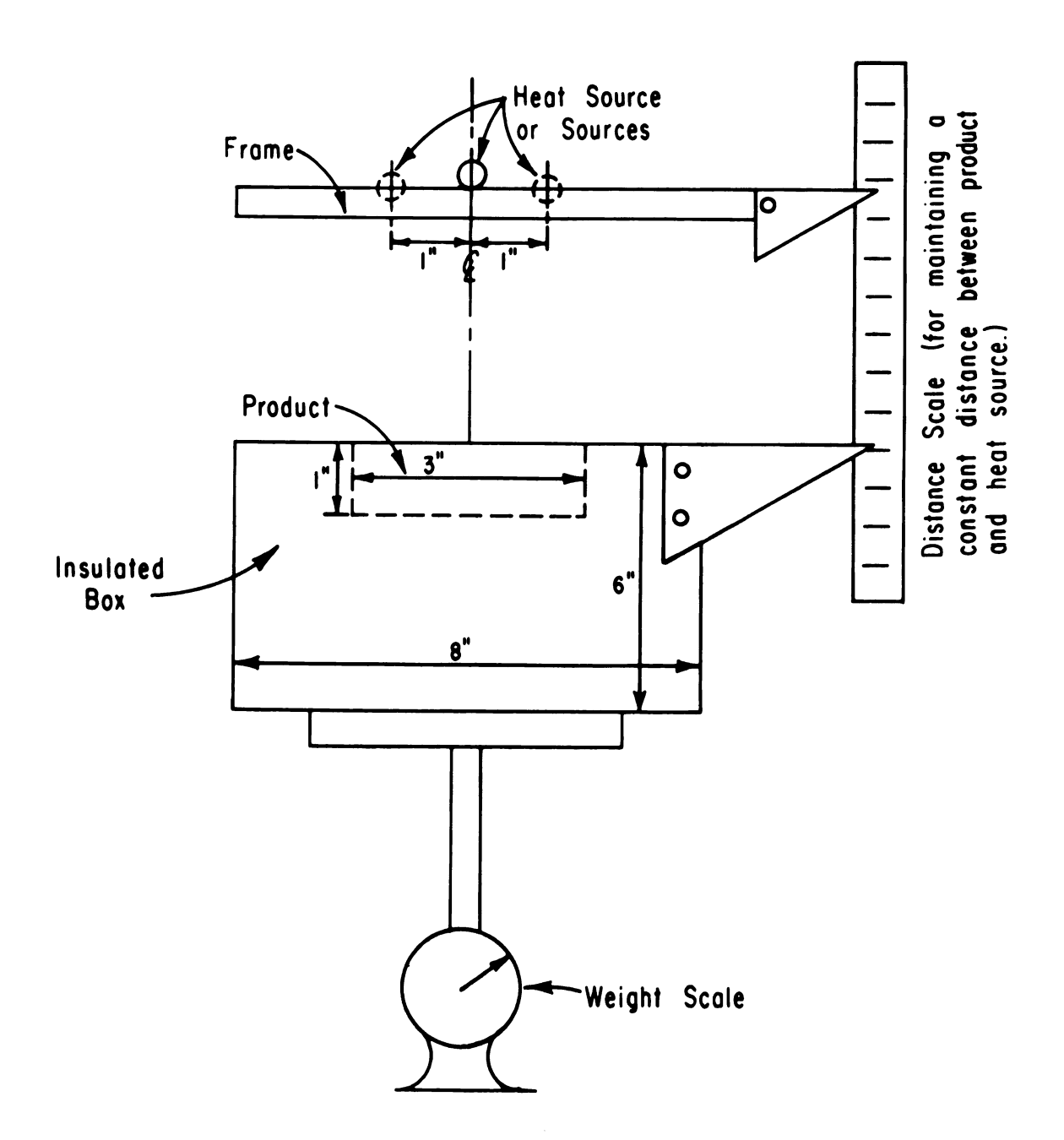


Fig. 4.3 Experimental apparatus arrangement.

All samples were processed until the temperature at the one inch sample depth was 170 F, the linear average of the two thermocouples at that depth.

The various sample temperatures were recorded every minute on the recording potentiometer.

The voltage, hence source temperature, was maintained by a manual variac transformer and a vacuum tube voltmeter. The amperes were measured by an AC ammeter. When three heat sources were used simultaneously, each heat source was regulated by individual variac transformers.

When the final processing temperature was attained the heat sources were shut off and the product was allowed to cool to at least 152 F, at the one inch depth, while the ground beef container was still in the insulated container. This cooling procedure is recommended by Lowe (37).

The thermocouples were removed from the ground beef after cooking, and the cooper container and the ground beef were weighed in grams. The difference between this weight and the initial copper container and ground beef weight was assumed to be the volatile weight loss of the product. The ground beef sample was then removed from the copper container and its width and length were measured. An attempt was made at measuring the depth of the product, but it was difficult to ascertain any change in height within $\pm 1/16$ inches, so depth changes were not indicated. The copper container, along with drippings, was weighed in grams. The difference between this weight and the initial

copper container was assumed to be the dripping weight.

The time-temperature relationships at the one inch depth and at the surface were recorded from the potentio-meter recording every five minutes, starting with the initial time at which the heating started (time zero) to the final processing temperature of 170 F at the one inch depth. The times at 122, 140 and 157 F were also recorded, if they did not occur at the five minute increments.

Summarizing, the following data were taken in each of the tests:

- 4.5.1 Copper container weight, grams
- 4.5.2 Ground beef weight, grams
- 4.5.3 Voltage of the heat sources
- 4.5.4 Amperes of the heat sources
- 4.5.5 Distances between heat sources and sample surface, inches
- 4.5.6 Time-temperature relationships, minutes
 - 4.5.6.1 Product surface, F
 - 4.5.6.2 One inch below the product surface, F
- 4.5.7 Time-relative sample weight loss relationship, per five and twenty minute time period, grams
- 4.5.8 Final sample weight, grams
- 4.5.9 Sample dripping weight loss, grams
- 4.5.10 Sample volatile weight loss, grams
- 4.5.11 Sample length and width changes, inches.

Table 4.1. Surface heat fluxes used in the processing of ground beef at different source temperatures.

	Quart	z Lamp			Quart	z Lamp			Quart	z Tube	
423	0.0 R;	$\lambda = 1.23$	3μ	346	5.0 R;	$\lambda = 1.50$	5µ	226	50.0 R;	$\lambda = 2.30$	8μ
Α	В	С	D	A	В	С	D	A	В	С	D
35	4.55	1124.01	1	10	5.14	1163.87	3	59	5.30	1151.82	3
34	4.73	1077.69	1	11	5.50	1077.48	3	63	5.60	1081.34	3
33	4.95	1024.06	1	12	5.81	1009.85	3	57	5.90	1016.45	3
32	5.20	967.05	1	13	6.19	934.40	3	58	6.25	947.25	3
1	5.50	903.57	1	36	6.38	899.23	3	69	6.55	893.41	3
2	5.81	843.72	1	14	6.56	868.11	3	60	6.90	836.52	3
3	6.19	777.33	1	15	7.01	797.34	3	62	7.30	778.42	3
4	6.49	729.93	1	16	7.61	716.54	3	66	7.75	721.09	3
5	6.75	692.37	1	37	8.00	671.65	3	61	8.25	666.42	3
6	7.13	643.27	1	17	8.33	637.57	3	68	8.70	624.24	3
7	7.69	580.94	1	18	9.19	562.60	3	65	9.30	576.10	3
8	8.06	545.35	1	38	9.95	507.88	3	67	10.00	528.96	3
9	9.00	472.90	1					64	10.75	484.86	3

A - test number

 $[\]ensuremath{\mathtt{B}}$ - distance between heat source and ground beef surface, inches

C - surface heat flux, Btu per sq ft-hr

D - number of source units used at the indicated distance to provide the indicated heat flux.

	Calr	od			Calrod		
	1864.5 R;	$\lambda = 2.797$		1	648.7 R;	$\lambda = 3.164$	
A	В	С	D	A	В	C	D
55	7.15	1029.76	3	39	4.00	1281.52	3
56	7.55	955.46	3	52	4.25	1203.40	3
29	3.20	916.62	1	47	4.45	1144.89	3
54	7.80	913.90	3	46	4.75	1063.17	3
28	3.43	862.77	1	45	5.05	988.37	3
53	8.15	860.29	3	42	5.30	931.20	3
27	3.65	813.66	1	44	5.65	857.93	3
26	3.90	761.61	1	40	6.00	792.69	3
25	4.15	712.07	1	41	6.45	718.77	3
19	4.50	650.08	1	43	6.90	655.43	3
20	4.80	601.10	1	49	7.40	595.28	3
21	5.06	561.91	1	51	7.90	544.16	3
22	5.44	510.22	1	50	8.55	487.96	3
23	5.61	489.10	1	48	9.25	436.25	3
24	6.18	426.28	1				
31	6.60	387.42	1				
30	7.10	348.24	1				

5.0 RESULTS, CALCULATIONS AND DISCUSSION

5.1 Calculation of the specific and latent heats of ground beef

The average composition of beef, including the following cuts: chuck, flank, loin, rib, round and rump, is given below:

Protein 18.05%

Water 61.00

Fats 20.17

Ash 00.78

Total 100.00%

The specific heats of protein, water and ash are 0.44, 1.00 and 0.12 Btu per lb F, respectively (3). The specific heats of the above three constituents vary slightly with temperature in the normal processing ranges.

Since triglycerides predominate in meat fats, although small amounts of mono- and diglycerides may be present, they are chemically quite homogeneous (3). The specific and latent heat properties of triglycerides have been analyzed in normal processing ranges. The triglycerides are known to exist in two forms, the α - and β -forms. The α -form is generally considered the unstable form and the β -form is recognized as a stable form of the fat. As the α -form changes states in processing, α -solid to α -liquid,

heat is absorbed and as the unstable α -form is changed to the stable β -form heat is released. Then the stable β -form changes from the solid to liquid state, again requiring heat. The specific and latent heats for the α - and β -forms and state changes were given in the review of literature.

As the specific heat of fat varies over a temperature range, its effects on the combined specific heat of meat should be considered. The average specific heat of meat, which consists of four definite substances of known specific heats is given by Daniels and Alberty (18). The equation follows the general form:

$$C = \frac{A}{W} \times C_A + \frac{B}{W} \times C_B + \frac{C}{W} \times C_C + \frac{C_D}{W} \times C_D + \dots$$

Where C is the average specific heat of the substance.

A, B, C, D, . . . are the weights of the various substances in the mixture.

 C_{A} , C_{B} , C_{C} , C_{D} , . . are the individual specific heats of substances A, B, C, D,

. . ., respectively.

W is the total weight of the mixture.

W = A + B + C + D + . . .

Now, for meat:

C = Percent Protein x C
(Protein) + Percent Water

x C (Water) + Percent Fat x C (Fat)

+ Percent Ash x C (Ash)

Table 5.1 shows the calculated specific heats of meat in specific temperature ranges and the latent heats of

fusion at the transition temperatures.

Table 5.1. Calculated specific heats of ground beef of average composition in various temperature ranges and the latent heats of fusion at the transition temperatures.

Temperature range, F	Specific heat (C)	Latent heat of fusion
32 121.8	0.75 (α-form)	
121.8		13.75 (α -solid to liquid)
121.8 139.1	0.80 (α-form)	
139.1		-4.86 (α - to β -form)
139.1 156.4	0.74 (β-form)	
156.4		19.37 (β -solid to liquid)
156.4 and over	0.80 (β-form)	

5.2 Calculation of geometrical angle factors

The general geometrical angle factor equation for determining the portion of the radiation emitted by a differential area dA_1 to a finite area A_2 is:

$$F_{(d_1)_2} = \int_{A_2} \frac{\cos^{\phi_1} \cos^{\phi_2}}{\pi r^2} dA_2$$

Where r is the distance between the areas dA_1 and dA_2 $\cos \phi_1$ is the angle measured from the normal to dA_1 to r $\cos \phi_2$ is the angle measured from the normal to dA_2 to r

 dA_2 is a differential area on the surface of $$\mathtt{A}_2$, to which r is measured
<math display="block">\mathtt{A}_2 \text{ is the total surface area receiving energy}$ from dA_1

If A_2 is parallel to dA_1 , $\cos\phi_1 = \cos\phi_2 = \cos\phi$, and if a, b and c are defined as in Fig. 5.1, and B = b/a and C = c/a, then:

$$F_{(d_1)_2} = \frac{1}{2\pi} \left[\frac{B}{(1+B^2)^{1/2}} \sin^{-1} \frac{C}{(1+B^2+C^2)^{1/2}} + \frac{C}{(1+C^2)^{1/2}} \sin^{-1} \frac{B}{(1+B^2+C^2)^{1/2}} \right]$$

Hence, the angle factor from the total surface $^{\rm A}_{\rm l}$ to $^{\rm A}_{\rm 2}$ is $^{\rm F}_{\rm 12}$ which is defined as:

$$F_{12} = \frac{1}{A_1} \int_{A_1} F_{(d_1)_2} dA_1$$

Jakob (33) further states that if A_1 is an arbitrary profile whose generatix is parallel in A_2 , dA_1 may be represented by its projected surface. A similar procedure was first called the "unit sphere method" by Herman and again suggested by Nusselt. If A_1 is a horizontal cylinder its projected area would then be LD, this then becomes the radiating surface area A_1 . If it is then broken into elemental areas, each elemental area is dA_1 . Also, if ΔL is the length of each area, the projected elemental area (dA_1) is ΔLD . This procedure was used to calculate

geometrical angle factors.

The heat source was divided into elemental lengths, one half of the source was studied, as the other half is symmetrical. The angle factors to one half of the parallel surface were determined from each of the elemental areas. See Fig. 5.2. The sample size was 3 inches (2c) x 6 inches (b) and the distances from the source to the sample were 3, 6, 9 and 12 inches (a).

From Fig. 5.2 it can be seen that areas dA_1 , dA_2 , dA_3 and dA_4 will emit energy to the surface. The distance for c will be constant (1-1/2") but b will vary dependent upon the elemental area, b could be 2, 4, 6, 8 or 10 inches, designated as areas 2, 4, 6, 8 and 10, respectively. Hence the following angle factors for the various c distances are calculated:

$$dA_1$$
 to c/2 surface : $F(d_1)_2 + F(d_1)_4$

$$dA_2$$
 to c/2 surface : $F(d_2)_6$

$$dA_3$$
 to c/2 surface: : $F(d_3)_8 - F(d_1)_2$

$$dA_4$$
 to c/2 surface : $F(d_4)_{10} - F(d_1)_4$

Hence the angle factor from one half of the source to a c/2 surface becomes:

$$\frac{1}{2}$$
 A₁ F₁₂ = (F(d₁)₆ + F(d₁)₈ + F(d₁)₁₀) dA₁
Where dA₁ = dA₂ = dA₃ = dA₄

Now, since only one half of the source was used and

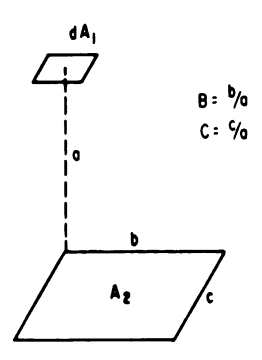


Fig. 5.1 Relationship of a, b, and c for determining the geometrical angle factor between a differential surface and a finite rectangular surface parallel to it.

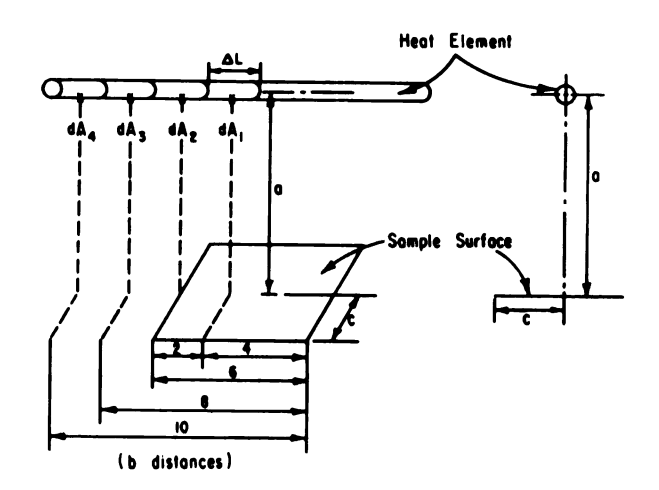


Fig. 5.2 Relationships of a, b, and c for determining the geometrical angle factors from a heat source to a finite surface.

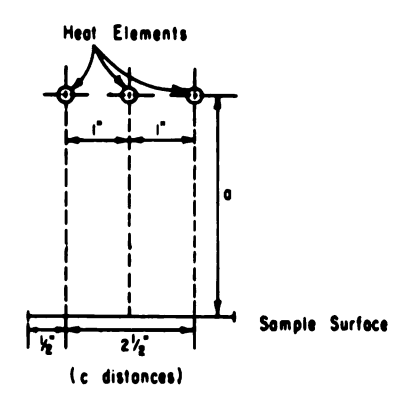


Fig. 5.3 Relationships of c and a for determining the geometrical angle factors from a group of three heat sources to a finite surface (b relationships are the same as in Fig. 5.2).

the other half is symmetrical and c/2 was used for the surface and the other half of the surface is symmetrical, the total angle factor becomes:

A₁ F₁₂ = 4(F(d₁)₆ + F(d₁)₈ + F(d₁)₁₀)dA₁ and, if: A₁ = L
$$\pi$$
D
$$dA_1 \text{ (projected surface area)} = \Delta LD$$
 then: F₁₂ = $\frac{\Delta L4}{L\pi}$ (F(d₁)₆ + F(d₁)₈ + F(d₁)₁₀), and for the quartz lamp, L = 16 inches and with 8 elemental lengths Δ L = 2 inches, so F₁₂ = $\frac{1}{2\pi}$ (F(d₁)₆ + F(d₁)₈ + F(d₁)₁₀).

Similar calculations were made for the quartz tube and the calrod unit. Table 5.2 is a summary of these calculations for 3, 6, 9 and 12 inches (a) distances.

The geometrical angle factors in Table 5.2 are for a surface of 18 square inches. Using these factors the radiant heat exchange between the source and the surface will be in Btu per sq ft-hr. The equivalent surface heat flux could then be calculated in Btu per sq ft-hr, using the 18 square inch surface as a basis. This calculation uses an equivalent angle factor, which is the ratio 144/18 multiplied by the angle factor from A₁ to the 18 square inch surface. These equivalent angle factors for the various (a) distances are shown in Table 5.3. If these equivalent angle factors are used in the following equation,* the

^{*} $qs'' = \epsilon_1 \epsilon_2 \sigma F_{12}^1 A_1 (T_1^4 - T_2^4)$

Where qs" is the surface heat flux (Btu per sq ft-hr). F_{12}^{1} is the equivalent geometrical angle factor. ϵ_1 , ϵ_2 , σ , A_1 , T_1^{4} , T_2^{4} have been previously defined.

computation will result directly in surface heat fluxes.

Table 5.2. Geometrical angle factors between single unit heat sources and a parallel centered 18 square inch surface at different perpendicular distances.

Perpendicular distance	Ge	ometrical an	gle factor
Between surfaces (inches)	Quartz lamp	Quartz tube	Calrod
3	0.051439	0.051795	0.059496
6	0.025652	0.025733	0.027395
9	0.014988	0.015407	0.015521
12	0.009742	0.009912	0.009680

Table 5.3. Equivalent geometrical angle factors between single heat sources and a parallel centered surface with an equivalent surface area of one square foot, using an 18 square inch surface as a basis at different perpendicular distances.

Perpendicular distance	Equivalent	geometrical	angle factor
Between surfaces (inches)	Quartz lamp	Quartz tube	Calrod
3	0.411511	0.414360	0.475968
6	0.205219	0.205864	0.219160
9	0.119903	0.123256	0.124168
12	0.077937	0.079296	0.077440

The geometrical angle factors were also calculated for the case in which three similar heat sources were used. For this case the sources were placed one inch on center and were parallel to each other. The sample surface was placed parallel to the three heat sources and its center

was perpendicular to the center of the center heat source. See Fig. 5.3. The angle factor from the center heat source to the sample surface would be the same as above, with the same (a) distances. The two remaining heat sources would have (c) distances of 1/2 inch and 2-1/2 inches, with b's similar to those above (2, 4, 6, 8, and 10 inches). The procedure for determining angle factors was similar to that above.

As each of the three sources are emitting equal amounts of energy a combined angle factor may be used with the area of a single heat source. The combined angle factor is the sum of the angle factors between the three heat sources and the sample surface, i.e., $(F_{12} \text{ (source 1)} + F_{12} \text{ (source 2)} + F_{12} \text{ (source 3)})$. The following equation expresses the radiant heat exchange between the three heat sources and the sample surface:

 $q = \epsilon_1 \epsilon_2 \sigma F_{12}$ (combined) $A_1 (T_1^4 - T_2^4)$ Where A_1 is the area of one heat source.

Table 5.4 shows the combined angle factors from the three heat sources to the 18 square inch surface area and Table 5.5 shows the equivalent combined angle factors from the three heat sources to a square foot surface area, using the 18 square inch surface area as a basis.

Table 5.4. Combined geometrical angle factors between a group of three similar heat sources and a parallel centered 18 square inch surface at different perpendicular distances.

Perpendicular distance	Combined	geometrical angle	factors
Between surfaces (inches)	3 Quartz lamps	3 Quartz tubes	3 Calrods
3	0.144151	0.145554	0.167783
6	0.074638	0.075892	0.080557
9	0.044402	0.045648	0.046151
12	0.028849	0.031769	0.022384

Table 5.5. Combined equivalent geometrical angle factors between a group of three similar heat sources and a parallel centered 18 square inch surface at different perpendicular distances.

Perpendicular distance	Combined	geometrical angle	factors
Between surfaces (inches)	3 Quartz lamps	3 Quartz tubes	3 Calrods
3	1.153205	1.164432	1.342264
6	0.597107	0.607136	0.644456
9	0.355217	0.365184	0.369208
12	0.230789	0.254152	0.179072

5.3 Determination of the sample size for statistically equal heat fluxes on the sample surface

Hottel (28) was the first to derive and publish a computational equation for the geometrical angle factor from a differential element to a parallel finite surface. McAdams (42) represented the equation graphically, using the same symbols as Hottel. Jakob (33) presented a

similar graphical solution but changed the symbols and increased the range of the graphical solution. Jakob's equation with symbol changes checks with Hottel's original equation and with McAdam's graphical solution, but Jakob's graphical solution gives lower geometrical angle factors than his equation and McAdams's graphical solution. This discrepancy appears as an incorrect labelling of one of the parameters (distance-width ratio). Following the procedure given by Jakob and the graphical solution of McAdams the maximum sample size was calculated.

The graphical solution to the geometrical angle factor equation depends on the parameters B (b/a) and C (c/a), where a is the distance between surfaces, b the length of the surface and c the width of the surface, measured from the center of the differential element. See Fig. 5.1. The geometrical angle factor equation gives the total angle factor to a finite surface, and as one approaches the heat source on a horizontal plane, that is reducing the C-parameter, the angle factor diminishes. This results in a higher relative surface heat flux (Btu per sq ft-hr) when the finite surface area is used as the area basis, i.e., if from a radiant heat exchange between two surfaces it was found that 100 Btu per hr is transmitted to a 14.4 sq in surface, the corresponding surface heat flux would be 1000 Btu per sq ft-hr, using the 14.4 sq in as a basis. However, not all differential surface elements are receiving exactly the same amount of heat per

hour, the above 1000 Btu per sq ft-hr is only an average for the entire surface. This averaging technique was used to determine geometrical angle factors for increment surface increases on a hypothetical sample surface.

The heat source, a single element parallel to the sample surface, was divided into eight equal element sizes, each two inches in length (corresponding to the 16 inch quartz lamp filament length). A hypothetical parallel surface was placed four inches from the heat source unit, parallel to it and the center of the hypothetical surface was placed perpendicular to the center of the heat source. An arbitrary sample width of five inches and length of ten inches was selected. The geometrical angle factors to fifteen surface elements on one quarter of the surface were determined, from the eight heat source elements. See Fig. 5.4.

Jakob (33) states the total geometrical angle factor to a finite area from a series of differential areas is the sum of the individual geometrical angle factors. Therefore, the angle factor to surface element 1 is:

$$F = \sum_{n=A}^{H} (F_n) dA$$

Where $F_A = F_7 - F_6$; b = 7 and 6 inches $F_B = F_5 - F_4$; b = 5 and 4 inches $F_C = F_3 - F_2$; b = 3 and 2 inches $F_D = F_1$; b = 1 inch $F_E = F_2 - F_1$; b = 2 inches and 1 inch

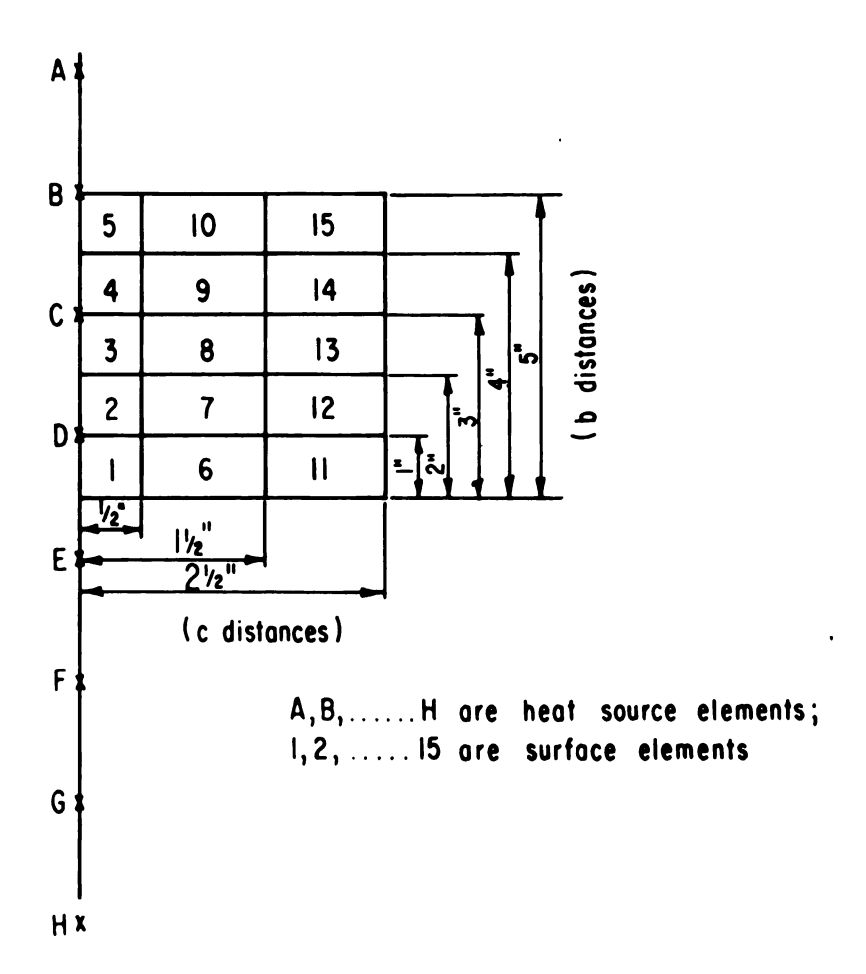


Fig. 5.4 Relationships of c and b distances for determining the sample surface area.

5/		10/		15/	
	0.056		0.051		0.048
ソ	0.058	و	0.053	4)	0.048
シ	0.060	8	0.054	13/	0.050
2)	0.060	ソ	0.055	12/	0.050
ソ	0.060	6 /	0.055	シ	0.052
	Α		В		С

Fig. 5.5 (F/dA) values for surface elements from Fig. 5.4.

 $F_F = F_4 - F_3 ; b = 4 \text{ and } 3 \text{ inches}$ $F_G = F_6 - F_5 ; b = 6 \text{ and } 5 \text{ inches}$ $F_H = F_8 - F_7 ; b = 8 \text{ and } 7 \text{ inches}$ Hence $F = F_8(dA) ; b = 8 \text{ inches, and } c = 1/2 \text{ inch,}$ a = 4 inches.

The geometrical angle factors to elements 6 and 11 would be similar, except that c would be 1-1/2 and 2-1/2 inches, respectively. This procedure was followed for all fifteen surface elements, i.e., the geometrical angle factors for surface elements 2, 7, 12 were ; $F = (F_9 + F_7 - F_8)dA$; for surface elements 3, 8, 13 were ; $F = (F_{10} + F_8 + F_6)dA$; for surface elements 4, 9, 14 were, $F = (F_{11} + F_9 + F_7 + F_5 - F_{10} - F_8 - F_6)dA$; and for surface elements 5, 10, 15 were, $F = (F_{12} + F_{10} + F_8 + F_6 + F_4 - F_{11} - F_9 - F_7 - F_5)dA$. These individual geometrical angle factor values were then taken from McAdam's graphical solution; they appear in Table 5.6.

Table 5.6. Geometrical angle factors for various sample widths (c) and lengths (b) at a distance of 4 inches. The values in the table are $F/dA(sq\ ft^{-1})$.

Length (b, inches)	W	idth (c, inches	;)
	0.5	1.5	2.5
4	0.025	0.070	0.110
5	.027	.075	.115
6	.028	.079	.120
7	.029	.082	.125
8	.030	.083	.130
9	.031	.084	.130
10	.032	.085	.130
11	.032	.086	.130
12	.032	.087	.130

The geometrical angle factors in Table 5.6 were then adjusted to a unit surface element area of one square inch for each of the elements, according to the averaging technique. For an elemental width of one half inch, the element has a corresponding surface area of one half square inch, hence dividing by one half square inch would give an angle factor or corresponding heat flux on a unit surface basis (Btu per sq in). This technique was used for c equal to 1.5 inches and 2.5 inches. Fig. 5.5 shows the results of this averaging technique with the F/dA factors indicated for each of the surface elements based on a unit surface element area of one square inch. Statistical differences of these results were tested by an analysis of variance technique. The elements corresponding to the c's of 1/2 inch, 1-1/2 and 2-1/2 inches are placed in columns A, B and C, respectively, while elements corresponding to b's of 1 inch, 2, 3, 4, and 5 inches are placed in rows 1, 2, 3, 4 and 5, respectively, as in Fig. 5.3. Table 5.7 shows the analysis of variance of the columns and rows of the sample surface.

The F-ratios for both columns and rows in Table 5.7 are insignificant at the 95% confidence level. It can then be concluded that the sample surface has an equal flux distribution over its entire surface when unit surfaces of one square inch each are compared in elemental rows and columns. Therefore, a 5 inch width by 10 inch length or lesser dimensioned sample may be used with a statistically

uniform surface heat flux. A three inch width and six inch length sample was for all tests.

Table 5.7. Analysis of variance of F/dA of the various rows and columns of one quarter of a 5 in by 10 in surface reduced to elemental finite areas (see Fig. 5.4).

Source of variance	Sum of squares	dF	Mean square	F-ratio
Rows	0.032	4	0.008	0.064*
Columns	0.2128	2	0.1064	0.849**
Residual	1.0032	8	0.1254	
Total	1.2480	14		

 $[*]F_{.95(4,8)} = 3.84$

5.4 Electrical energy characteristics of the heat sources

Tables 5.8 and 5.9 show the comparison between the manufacturers data and volt-ampere measurements of quartz lamps and calrod heat sources. Input watts are calculated, based on an average of three ampere readings at each of the voltages.

The rated watt input of the quartz tube was 550 watts and the calculated heat input, based on 120 volts and three ampere measurements, was also 550 watts.

The differences indicated in Tables 5.8 and 5.9 are probably the result of comparing a single unit to an average number of similar units produced by the manufacturer.

 $^{**}F_{.95(2,8)} = 4.46$

Table 5.8. Comparison of manufacturers data and calculated watt inputs, based on volts and ampere averages, for the 1600 watt quartz lamp.

Volts	Watts (manufacturer)	Watts (calculated)
220	1425	1474.0
200	1200	1270.0
180	1040	1076.4
160	865	904.0
140	688	732.2/
120	560	573.6
100	416	433.0
80	288	305.6

Table 5.9. Comparison of manufacturers data and calculated watt inputs, based on volt and ampere averages, for the 1000 watt calrod unit.

Volts	Watts (manufacturer)	Watts (calculated)
220	830	847.0
200	680	693.4
180	560	554.9
160	460	434.7
140	340	333.6
120	245	246.0
100	173	175.0

5.5 Calculation of the radiant heat outputs of three heat sources

5.5.1 Quartz lamp source

The calculation of the radiant heat output of the quartz lamp at different voltages is based on the following basic assumptions: (a) the electrical energy input to the lamp is converted to heat; (b) heat is lost by convection and radiation to a 80 F room with surfaces at the same

temperature as the room; (c) the room surfaces have an emissivity of unity; (d) the lamp is a gray body with emissivity equal to absorptivity. Other assumptions will be indicated below.

5.5.1.1 The radiation from the tungsten lamp filament is:

$$q_{r1} = \epsilon_1 A_1 \sigma (T_1^4 - T_R^4)$$
Where $\epsilon_1 = 0.023 + 7.6 \times 10^{-5} (t_1)$, emissivity of the filament. Marks Handbook (40) states that the emissivity of tungsten is 0.032 and 0.35 at 80 F and 6000 F, respectively, and that linear interpolation is possible between these temperatures; with t_1 the filament temperature in F.

A₁ is the filament surface area, the length and diameter of the filament were 16 and 0.065 inches, respectively. If the filament is assumed to be a rod, its surface area is 0.0227 ft².

$$\sigma = 0.174 \times 10^{-8}$$

 T_1 is the filament temperature, R

 $\mathbf{T}_{\mathbf{R}}$ is the room temperature, 540 R

The filament temperatures were taken from the tungsten color temperature data supplied by the manufacturer.

5.5.1.2 The heat radiated to the room from the filament is: $q = q_{r1}\tau$, where τ is the transmittance of

quartz subject to various source temperatures. Fostoria Pressed Steel Corporation (12) states the following relationships between τ and source temperature (t):

<u> </u>	t, F
0.495	1200
0.530	1300
0.633	1800
0.715	2240
0.780	2680
0.820	3140
0.845	3580
0.860	4030

Linear interpolation is permissible between the temperature increments given above. Marks Handbook (40) and Jakob (32) state that ϵ of fused quartz at room temperature is 200 F. Assuming that linear interpolation is permissible between 200 and 1200 F, the following relationship will be true for this range:

$$\epsilon = 0.935 - 4.3 \times 10^{-2} \text{ (t-200)}$$

5.5.1.3 The radiation from the quartz shell is:

$$q_{r2} = \epsilon_2 A_2 \sigma (T_2^4 - T_R^4)$$

Where to is taken from above

 A_{γ} is the shell surface area, and assuming the 18 inch length of the shell is at a constant temperature. The shell diameter is 0.375 inches, therefore A2 is equal to 0.147 sq ft $\sigma = 0.174 \times 10^{-8}$

$$\sigma = 0.174 \times 10^{-6}$$

T₂ is the shell temperature, R

 T_{R} is the room temperature, 540 R

5.5.1.4 The convection from the quartz shell to the room is:

$$q_{c2} = hA_2 (t_2 - t_R)$$

Where $h = \frac{0.24}{D_2^{1/4}} (t_2 - t_R)^{1/4}$ as stated by Jakob (32) and and Giedt (24), for N_{GR} . $N_{PR} = 10^4$ to 10^8 at the average surface film temperature, the maximum and minimum N_{GR} . N_{PR} products were 2.69 x 10^4 and 2.59 x 10^4 , based on the manufacturers ratings at different filament voltages.

 $A_2 = 0.147 \text{ sq ft}$

t₂ = shell surface temperature, F

 $t_R = room temperature, 80 F$

or by substituting the computational equation of h into q_{c_2} $q_{c_2} = \frac{0.24xA_2}{D_2^{1/4}} \quad (t_2 - t_R)^{5/4}$

5.5.1.5. The heat balance of the quartz shell is:

the heat absorbed by the quartz shell is equal

to the heat input to the filament, as calcu
lated from the measured wattage input, minus

the heat radiated from the filament to the

room, or heat transmitted by the quartz shell,

or

q(absorbed by the quartz shell) = $q_{r2} + q_{c2}$ = $\epsilon_2 A_2 \sigma (T_2^4 - T_R^4) + \frac{0.24 x A_2}{D_2^{1/4}} (t_2 - t_R)^{5/4}$ The quartz surface temperature was computed by using an iteration technique, forcing q_{r2} and q_{c2} to equal the heat absorbed by the quartz shell, a \pm 2% limit was used in the iteration process. Therefore, the heat absorbed by the quartz shell was equal q_{r2} plus q_{c2} plus Δ , where Δ was within 2% of the heat absorbed by the quartz shell.

Table 5.10 shows the results of the computations and the last column of the table is the computed percent radiation at different voltages based on the radiation at 240 volts.

Table 5.10. Calculated heat balances of the quartz heat lamp at different voltages.

Volts	q input	q _{rl}	q _{r2}	q _{c2}	Δ	q _{rl} +q _{r2}	Percent q
240	5461	4620	497	348	4	5117	100.0
220	5032	3929	676	431	4	4605	90.1
200	4336	3334	610	398	6	3944	77.2
180	3675	2659	610	398	8	3269	63.9
160	3086	2080	610	398	2	2690	52.6
140	2500	1626	517	357	0	2143	41.9
120	1958	1156	470	335	3	1626	31.8
100	1478	801	378	291	8	1179	23.1
80	1043	494	301	252	4	795	15.5

Table 5.11 shows the comparison between the calculated radiation based on wattage measurements and the radiation percentages at different voltages based on 240 volts as supplied by the manufacturer.

In all cases the calculated radiations were higher than the radiation percentages supplied by the manufacturer. However, the manufacturers data is an average for many

Table 5.11. Comparison of calculated percent radiations from a 240 volt quartz lamp rated at 1600 watts at different voltages to the manufacturers data.

Volts	Percent q _r (manufacturer)	Percent q _r calculated	Percent difference*
240	100.0	100.0	0
220	87.0	90.1	3.57
200	73.0	77.2	5.75
180	61.0	63.9	4.54
160	50.0	52.6	5.20
140	40.0	41.9	4.76
120	30.5	31.8	4.26
100	21.5	23.1	4.27
80	14.0	15.5	10.70

*Percent difference =

$$\begin{pmatrix} \frac{\text{Percent } q_r \text{ calculated - Percent } q_r \text{ manufacturer}}{\text{Percent } q_r \text{ manufacturer}} \end{pmatrix} 100\%$$

quartz lamps, while the calculated radiation is dependent on the measured wattage inputs to the filament. The calculated radiation also assumes an 80 F environment temperature, whereas the environment temperature used by the manufacturer is unknown. Due to windings of the filament an electrical inductance probably occurs so that the 100% electrical conversion to heat is not an exact assumption. The calculated radiation is used as a basis to determine surface heat fluxes.

5.5.2 Calrod heat source

The calculation of the radiant heat output of the calrod at different voltages is based on the following

basic assumptions: (a) all of the electrical energy input to the unit is converted to heat; (b) heat is lost by radiation and convection to an 80 F room with surfaces at the same temperature; (c) the room surfaces have an emissivity of unity; (d) the unit is a gray body. Other assumptions will be indicated below.

5.5.2.1 The radiation from the unit is:

$$q_{r1} = \epsilon_1 A_1 \sigma (T_1^4 - T_R^4)$$

Where ϵ_1 = 0.79, Marks Handbook (40) and DeWerth (19) A_1 is the radiating surface area of the calrod at T_1 , the diameter of the calrod unit was measured and found to be 0.43 inches, the length of the surface at T_1 was determined as 13 inches, as this was the length that appeared as a cherry red color when the unit was operated at 220 volts, so A_1 = 0.122 sq ft

 $\sigma = 0.174 \times 10^{-8}$

 $\mathbf{T}_{\mathbf{R}}$ is the room temperature, 540 R

 T_1 is the surface temperature as supplied by the manufacturer, R

5.5.2.2 The convection heat loss from the unit is:

$$q_{c1} = hA_1 (t_1 - t_R)$$

Where $h = \frac{0.24}{D^{1/4}} (t_1 - t_r)^{1/4}$, for $N_{GR} \cdot N_{PR} = 10^4$ to 10^8

at an average surface film temperature, the maximum and minimum $N_{GR} \cdot N_{PR}$ products were 6.17 x 10⁴ and 3.64 x 10⁴ at 100 and 240 volts, respectively, based on the manufacturers unit surface temperatures at these voltages.

 $t_{R}^{}$ is the room temperature, F

5.5.2.3 The end heat losses of the calrod unit

Heat may be lost by convection and radiation by the ends of the unit.

For the convection heat loss, Jakob (32) states the following equation may be used for a not very long rod protruding from a heat source:

$$q_C = (khAC)^{1/2} \frac{1 - pe^{-m2L}}{1 + pe^{-m2L}} (t_1 - t_R)$$

Where k is the thermoconductivity of the rod, k=26

h is the convective film coefficient, for this

case it is assumed to be equal to the h

computed above for the convective heat loss

to the environment.

A is the cross-section area of the conducting rod, it is further assumed that only the steel shell portion of the rod will conduct

heat, the inner diameter is 0.375 inches and the outer diameter is 0.43 inches for the steel shell.

C is the outer surface area of the rod, the diameter is 0.43 inches and the length is 2.25 inches.

$$p = \frac{km - h}{km + h}, k \text{ and } h \text{ are defined above}$$

$$m = \left(\frac{hc}{kA}\right)^{1/2}, h, C, k \text{ and } A \text{ are defined above}$$

L = length of the rod, 2.25 inches

t₁ = source temperature, temperature of the 13
 inch length of calrod as supplied by the
 manufacturer

 $t_{R} = room temperature, 80 F$

The total convection heat loss is $2q_{\mathbb{C}}$ as there are two ends. To determine the radiation end losses, the average rod temperature was used:

$$t_{average} = t_R + \frac{q_C}{hAc}$$

Where t_R is the room temperature, 80 F

 $\mathbf{q}_{\mathbf{C}}$ is computed from above, convection heat loss

h is computed from above

C is the surface area of the rod

then, $q_r = \epsilon_1 C \sigma (T_{average}^4 - T_R^4)$, where ϵ_1 , C, σ , $T_{average}$ and T_R are defined above and q_{r2} the radiative heat loss of one of the ends, so the total radiative heat loss for

both ends is

$$q_{r2} = 2q_r$$
.

Table 5.12 shows the results of the above computation. The Δ column indicates the difference between q_{total} heat losses and the measured wattage inputs. The last column is the percent heat input based on the 240 volt, wattage input, which may be compared to the manufacturer's watt input of the calrod and the measured wattage input in Table 5.9.

Table 5.12 Calculated heat balances of the calrod unit at different voltages.

Volts	q _{rl}	q _{c1}	q _{r2}	q _{c2}	q total calculated	q input	Δ	Percent q input
240	2480	585	228	124	3417	3413	4	100.0
220	2030	538	194	115	2877	2891	14	84.3
200	1550	477	160	103	2290	2367	77	67.0
180	1230	428	132	93	1883	1894	11	55.2
160	888	362	100	80	1430	1484	54	41.9
140	622	309	80	69	1080	1139	59	31.7
120	432	258	58	58	805	840	34	23.7
100	271	199	42	46	558	597	41	16.4

Table 5.13 shows the comparisons between the calculated radiation and the radiation percentages at different voltages based on 240 volts as supplied by the manufacturer. The last column of the table shows the percent difference based on manufacturers data.

In all cases the calculated radiations were higher than the radiation percentages supplied by the manufacturer. The calculated radiations assume an 80 F environment temperature, whereas the environment temperature used by the

manufacturer is unknown. Also the assumptions made by the manufacturer regarding the emissivity of the surface are unknown. Lastly, these calculated radiations will correspond to the measured heat fluxes with a higher correlation than those supplied by the manufacturer. See Table 5.16. These calculated radiations are used as a basis to determine surface heat fluxes.

Table 5.13. Comparisons of calculated percent radiation from 1000 watt, 240 volt calrod unit at different voltages to the manufacturers data.

Volts	Percent q radiation (manufacturer)	Percent q radiation (calculated)	Percent difference
240	100.0	100.0	0
220	78.0	82.1	5.26
200	59.0	63 .2	7.12
180	45.0	50.3	11.20
160	31.0	36.5	17.72
140	20.5	26.0	26.85
120	13.0	18.1	39.10
100	7.3	11.6	59.0

^{*}Percent difference =

5.5.3 Quartz tube heat source

The calculated heat balance at 120 volts for the quartz tube is dependent upon the following basic assumptions:

(a) all the electrical energy input to the unit is converted to heat; (b) heat is lost by convection and radiation to an 80 F room with surfaces at the same temperature; (c) the room surfaces have an emissivity of unity; (d) the unit is

a gray body. Other assumptions will be indicated below.

5.5.3.1 The radiation from the filament is: $q_r = \epsilon_1 A_1 \sigma (T_1^4 - T_R^4)$

Where ϵ_1 = 0.753, the emissivity of the chromnickel filament, DeWerth (19) and Marks Handbook (40) state the emissivity is 0.76 and 0.64 at 1894 F and 125 F, respectively, and that linear interpolation is permissable between these temperatures. At 120 volts and 550 watts the filament has a 1800 F rating, as stated by the manufacturer (12).

A₁ = 0.05081 sq ft, the diameter of the filament
 is 0.137 inches and its length is 17
 inches, it is assumed that the coiled
 type filament is a rod of the same diameter
 and length.

 $\sigma = 0.174 \times 10^{-8}$

 T_1 = 2260 R, the filament temperature, the filament is rated at 1800 F

 $T_R = 540$ R, the room temperature, 80 F

5.5.3.2 The heat transmitted by the fused quartz shell is:

 $q_{rl} = \tau q_r$

Where τ = 0.633, the transmittance of fused quartz, subject to a radiation at 1800 F, Fostoria Pressed Steel Corporation (12).

5.5.3.3 The radiation from the quartz shell is:

$$q_{r2} = \epsilon_2 A_2 \sigma (T_1^4 - T_R^4)$$

Where $\epsilon_2 = 0.935 - 0.043 \times 10^{-2}$ (t-200), relationship derived from above (quartz lamp)

A₂ = 0.1477 sq ft, where the shell diameter is
 0.375 inches and the shell length is 18
 inches, it is assumed the entire shell
 is at a constant temperature.

$$\sigma = 0.174 \times 10^{-8}$$

 ${\bf T}_2$ is the shell temperature, ${\bf R}$

 $T_{R} = 540 R$, room temperature

5.5.3.4 The convection heat loss from the quartz shell is:

 $q_{C2} = hA_2 (t_2 - t_R)$ Where $h = \frac{0.24}{D^{1/4}} (t_2 - t_R)^{1/4}$, for $N_{GR} \cdot N_{PR} = 10^4$ to 10^8 at the average surface film temperature, the $N_{GR} \cdot N_{PR}$ product was 3.44 x 10^4 , based on the manufacturers rating at 120 volts, the diameter of shell is 0.375 inches, t_2 and t_R are given above

 $A_2 = 0.1477 \text{ sq ft, given above}$ t₂ and t_B are given above

5.5.3.5 The heat balance on the quartz shell is:

The heat absorbed by the quartz shell is equal to the heat input to the filament, as calculated from the

measured watt input, minus the heat radiated from the filament to the room, or heat transmitted by the fused quartz shell.

q (absorbed by the quartz shell) =
$$q_{r2} + q_{c2}$$

= $\epsilon_2 A_2 \sigma (T_2^4 - T_R^4) + \frac{0.24 A_2}{D_2^{1/4}} (t_2 - t_R)^{5/4}$

The quartz surface temperature was computed by using an iteration technique, forcing q_{r2} and q_{c2} to equal q absorbed by the quartz shell, a \pm 1% limit was used. Therefore, the heat absorbed by the quartz shell was q_{r2} plus Δ , where Δ was within \pm 1% of the heat absorbed by the quartz shell. The results were: q_r (filament) = 1096 Btu per hr; q_{r2} (shell) = 448 Btu per hr; q_{c2} = 327 Btu per hr; Δ = 6 Btu per hr.

These calculations, or q (radiation) = 1544 Btu per hr, were used as a basis to determine heat fluxes at various distances.

5.6 Heat flux measurements

5.6.1 Quartz lamp comparisons between measured and calculated heat fluxes are shown in Tables 5.14 and 5.15 for different distances and voltages. The percent differences are also shown. Table 5.14 is for one lamp and Table 5.15 is for three lamps.

The results in Tables 5.14 and 5.15 indicate the influence of distance or geometrical angle factor on the measured heat fluxes. As the pyrheliometer is moved further from the heat source the measured heat fluxes approach the

Comparison of calculated radiant heat fluxes to measured radiant heat fluxes for different voltages and distances for one quartz lamp. Table 5.14.

6 in. Distance	ance		ni 6	in. Distance		12 in.	Distance	Ф
q meas.	q cal.	Percent diff.*	q meas.	q cal.	Percent diff.*	d meas.	q cal.	Percent diff.*
802.53	945.03	-15.1	527.93	552.15	-4.38	359.55	358.90	0.18
691.72	809.38	-14.5	451.55	472.90	-4.53	307.03	307.38	-0.11
570.70	98.029	-14.9	371.65	391.96	-5.18	254.98	254.78	0.08
465.65	552.04	-15.8	305.15	322.54	-5.39	207.15	209.65	-0.72
374.00	439.78	-14.9	240.52	256.95	-6.39	166.03	167.02	-0.59
282.35	333.69	-15.4	181.77	194.96	-6.77	124.20	126.73	2-3
197.75	241.95	-18.3	128.43	141.37	-9.15	88.13	91.89	-4.09
124.20	163.15	-23.9	77.90	95.32	-18.32	54.87	61.96	-11.42

*Percent difference = $\begin{pmatrix} q & \text{meas.- q cal.} \\ q & \text{cal.} \end{pmatrix}$ 100%

Comparison of calculated radiant heat fluxes and measured radiant heat fluxes for different voltages and distances for three quartz lamps. Table 5.15.

† 2000 2000
rercent diff.* q meas. q cal
1025.78 1062.78
-8.25 876.55 910.23
-7.60 733.55 754.45
-8.59 597.72 620.82
-7.98 473.17 494.58
-8.19 361.08 375.26
-9.74 255.80 272.10
-16.70 160.15 183.48

*Percent difference = $\begin{pmatrix} q & meas.-q & cal. \\ q & cal. \end{pmatrix}$ 100%

calculated heat fluxes. The Eppley pyroheliometer is primarily used for measuring solar radiation fluxes, which do not approach the higher heat fluxes above. In addition the crystal on the pyroheliometer does not transmit beyond a 12 micron wave length, so with low lamp surface temperatures only a fraction of this energy is received by the thermopile. The angle factor influence is also indicated in the above tables. As the pyroheliometer is moved a greater distance from the heating source the angle factor is decreased, approaching the angle factor used in solar radiation measurements.

- 5.6.2 Calrod comparisons between measured and calculated heat fluxes are shown in Table 5.16 for different distances and voltages. The percent differences are also shown.
- 5.6.3 Quartz tube comparisons between measured and calculated heat fluxes are shown in Table 5.17 for different distances at a constant voltage of 120 volts. The percent differences are also shown.

The interpretation of these and the calrod results is similar to that given for the quartz lamp.

Comparison of calculated radiant heat fluxes to measured radiant heat fluxes for different voltages and distances for one calrod unit. Table 5.16.

6	6 in. Distance	ance	O'	9 in. Distance	ance		12 in.	12 in. Distance	
Volts	q meas.	q cal.	Percent diff.*	q meas.	q cal.	Percent diff*	q meas.	q cal.	Percent diff.*
220	403.03	444.89	-9.35	247.14	252.06	-1.95	164.11	157.20	4.39
200	318.43	339.70	-6.26	194.26	192.46	0.94	122.59	120.03	2.13
180	238.53	269.57	-11.51	147.26	152.73	-3.58	94.79	95.25	-0.48
160	168.81	194.61	-12.73	101.05	110.26	-8.35	65.41	68.77	-4.88
140	115.54	136.32	-15.24	68.94	77.32	-10.72	45.44	48.17	-5.66
120	74.03	94.68	-21.85	43.09	53.64	-19.65	28.59	33.45	-14.52
100	41.91	59.39	-29.45	26.24	33.65	-22.00	16.06	20.99	-23.50

*Percent difference = $\begin{pmatrix} q \text{ meas.-q cal.} \\ q \text{ cal.} \end{pmatrix}$ 100%

Table 5.17. Comparison of calculated radiant heat fluxes to measured radiant heat fluxes for different distances for a 120 volt, 550 watt quartz tube.

		Distance	
	6 inches	9 inche s	12 inches
q measured	296.89	173.90	112.01
q calculated	317.85	190.31	122.43
Percent difference*	-3.69	-9.45	-9.31

*Percent difference =
$$\left(\frac{\text{q meas.- q cal.}}{\text{q cal.}}\right)$$
 100%

5.7 Fitting of third degree polynominals to heat flux calculations for various distances between the sample surface and heat source units

Third degree orthogonal polynominals were fitted to the calculated surface heat fluxes. Five heat source temperatures were selected, namely, 4230.0, 3465.0, 2260.0, 1864.5 and 1648.7 R, to determine the effect of source temperature on the rate of processing. By using the previous calculated radiant heat outputs of the three heat sources at their respective voltages to give the above temperatures and by using the appropriate equivalent geometrical angle factors at various distances, it is possible to calculate surface heat fluxes at given distances.

The following equation could be used:

$$qs'' = q_r \times F_{12}^{1}$$

Where qs" is the surface heat flux, Btu per sq ft-hr ${\bf q}_{\bf r}$ is the total radiant heat output of the source, Btu per hr

 F_{12}^{-1} is the equivalent angle factor for a particular distance, sq ft⁻¹

This technique is shown because it gives an accurate heat flux from a source to a surface when angle factors have been calculated for several distances and it is desired to determine heat fluxes at increment intermediate distances, without going through the complete geometry of the system each time the distance between source and sample is changed. Also, if a definite heat flux is desired, the polynominal could be solved for the appropriate distance between surfaces, if the rest of the geometry of the system remains the same.

A third degree polynominal was fitted to the calculated heat fluxes for 3, 6, 9 and 12 inches. This polynominal is to be used only for distances between 3 and 12 inches from the heat source and only for a 3 inch by 6 inch sample surface. If the range, 3 inches to 12 inches, is to be increased, it is recommended that several more geometrical shape factors be calculated to cover all distances in the new range and a new polynominal be fitted. The degree of the polynominal is only limited by the desired correlation and the number of increment angle factors used.* The orthogonal polynominal fitting technique is given by Snedecor (56).

The general form of the third degree polynominal is: $qs'' = A + Bd + Cd^2 + Dd^3$

^{*}The maximum polynominal degree is (n-1) where n is number of orthogonal angle factors.

Where qs" is the surface heat flux, Btu per sq ft-hr
A, B, C and D are the polynomial constants
d is the perpendicular distance, inches.

The results of the orthogonal polynominal fitting are given in Table 5.18. The table also includes, the correlation coefficient and the maximum deviation of qs" from actual calculations. It was interesting to note that the maximum deviations always occurred at the greatest distance from the heat source.

These orthgonal polynominals could then be used to calculate surface heat fluxes at any distance between 3 and 12 inches.

5.8 Effect of surrounding walls and reradiation

The data showing the effect of reradiation from surrounding enclosure walls and the data without these walls are in Table 5.19.

The maximum enclosure surface temperature at the end of the processing was 128 F and the minimum temperature was 120 F. The maximum internal air temperature of the enclosure was 97 F while the minimum was 90 F. The actual effects of the enclosure can be shown by the following analysis of variance tables.

Results of orthogonal polynominal curve fitting to surface heat flux calculations for the equation: $qs'' = A + Bd + Cd^2 + Dd^3$. Maximum deviations are also indicated. Table 5.18.

Heat	No. of heat		Polynominal constants	constants		Correl. max.	max.
Temp. R	Source units	A	В	ບ	D	Coeff.	Dev. (△ qs")
4230.0	ı	3219.9400	9988.969-	60.5278	-1.8900	0.9999	0.01
3465.0	е	3609,9950	-752.2810	63.9178	-1.9743	0.9999	90.0
2260.0	ю	3647,4493	-750.1824	62.6983	-1.8865	0.9999	0.07
1864.5	1	2046.5447	-478.8873	43.8616	-1.4229	0.9999	0.01
	ĸ	5684.0522	-1319.6428	123.7591	-4.2281	0.9999	0.03
1648.7	т	3444.0304	-799.5919	74.9884	-2.5619	0.9999	0.03

Ground beef samples processed to 170 F at 946 Btu per sq ft-hr and λ^* of 1.19 μ in an open room and in an enclosed volume. 5.19. Table

		Open Room		Enc	Enclosed Volume	lume
Sample	٦	2	Э	4	5	9
Initial weight (gm)	316.70	320.00	320.70	321.20	321.40	321.15
Final weight (gm)	219.90	226.80	220.90	237.10	244.35	237.20
Percent yield**	69.44	70.88	68.88	73.82	76.03	73.86
Dripping weight (gm)	72.00	00.99	74.70	60.65	47.20	59.70
Percent drippings	22.73	20.63	23.29	18.88	14.69	18.59
Volatile loss (gm)	24.80	27.20	25.10	23.45	29.85	24.25
Percent volatile loss	7.83	8.49	7.83	7.30	9.28	7.55
Initial temperature (F)	45	20	54	49	44	50
Total time to 170 F (min)	92	80	71	77	80	79
Relative time (60 to 170 F) (min.)	99	73	99	89	71	72
Room temperature (F)	85	83	68	82	78	77

* Under black body conditions the maximum energy emission would occur at this wave length.

** Percent yield is equal to the final weight of the product, excluding drippings, divided by the initial weight of the product.

Table 5.20. Analysis of variance of percent yields for enclosed volume vs. non-enclosed volume samples at 946 Btu per sq ft-hr and λ = 1.194 $\mu.$

Source of variance	Sum of squares	đf	Mean square	F ratio*
Means	35.09	1	35.09	26.19
Within	5.34	4	1.34	
Total	40.42	5		

*F.95 (1,4) = 7.71

Table 5.21. Analysis of variance of percent yields for enclosed volume vs. non-enclosed volume samples at 946 Btu per sq ft-hr and λ = 1.194 μ .

Scurce of variance	Sum of squares	đf	Mean square	F ratio*
Means	34.99	1	34.99	9.41
Within	14.88	4	3.72	
Total	49.87	5		

*F.95 (1,4) = 7.71

Table 5.22. Analysis of variance of percent volatile losses for enclosed volume vs. non-enclosed volume samples at 946 Btu per sq ft-hr and λ = 1.194 μ .

Source of variance	Sum of squares	đf	Mean square	F ratio*
Means	0.80	1	0.80	1.21
Within	2.62	4	0.66	
Total	3.42	5		

*F.95 (1,4) = 7.71

Table 5.23. Analysis of variance of relative processing time (60 to 170 F) for enclosed volume vs. non-enclosed volume samples at 946 Btu per sq ft-hr and λ = 1.194 μ .

Source of variance	Sum of squares	df	Mean square	F ratio*
Mean	0.61	1	0.61	0.48
Within	5.13	4	1.28	
Total	5.74	5		

*F.95 (1,4) = 7.71

From the above tables it is apparent that: (a) there is a difference in percent yield, with the enclosed volumed samples having a significantly higher yield; (b) there is a difference in percent drippings, with the non-enclosed volume samples having a significantly higher dripping weight; (c) the enclosure has no significant effect on volume loss; (d) the enclosure has no significant effect on relative processing time.

The effect of the enclosure on heat transfer and processing time is not significant at a heat flux of 946 Btu per sq ft-hr at a λ of 1.194 μ . The apparent factor in this test was the volatile loss which contributes a latent heat loss factor or an apparent h. The apparent h was not significant while holding the other heat transfer factors (λ , qs, t_R, t_i, area and final temperature) essentially constant. The relative processing time should not have shown a change, unless the reradiation of the

surrounding walls would increase heat transfer. This was not significant.

Due to the low wall surface temperature in the enclosed volume, the volatile loss of the product increased the water vapor pressure of the enclosed air and as the transmission of water vapor above 5 μ is insignificant, any reradiated heat would be absorbed by the water vapor. This would also be true for the non-enclosed volume. However, this would not be true for highly reflective surface enclosures.

As a result, all subsequent tests were conducted in non-enclosed volumes (except for the physical size of the room) and all highly reflective surfaces which could influence the radiative angle factor were shielded with a high emissivity surface.

Higher yields have also been reported by Keating (34) with a forced convection enclosure (oven) containing a free liquid surface. The higher percentage yield is a result of a lower dripping weight. It could then be hypothesized that dripping weight is a function of at least four factors: (a) the product; (b) produce moisture content; (c) surface temperature or surface heat flux; (d) vapor pressure of the environment. The latter two factors would then be critical in this experiment. With an essentially constant heat flux, the moisture diffusion would be at some specified rate, also with a constant surface vapor pressure the moisture diffusion would be at another rate.

With the enclosed volume the surface vapor pressure should be higher than with the non-enclosed volume, which could reduce moisture diffusion and result in a lower dripping weight and hence higher product yield.

A second degree orthogonal polynominal was fitted to the actual data (relative times for 60 to 170 F) for each of the six tests* and the corresponding constants were analyzed by the analysis of variance technique. The polynominal constants and corresponding correlation coefficients are shown in Table 5.24.

Table 5.24. Polynominal constants for the fitting of time vs. temperature at the one inch depth for ground beef at 946 Btu per sq ft-hr and a λ of 1.194 μ in an open room and in an enclosed volume. (Y = A + BX + CX², Y is the temperature in F at the one inch sample depth and X is the time in minutes.)

			 	
Sample	A	B	С	Correlation coefficient(R)
Open room				
1	56.76	2.6914	-0.0152	0.9990
2	58.19	2.3510	-0.0115	0.9995
3	56.07	2.5773	-0.0131	0.9944
Enclosed v	olume			
4	57.00	2.4631	-0.0121	0.9935
5	57.53	2.3052	-0.0099	0.9993
6	57.61	2.3694	-0.0113	0.9996

*The fitting of a third degree polynominal was not significant at the 99% level as measured by an F test ratio on the remaining sum of squares.

Table 5.25. Analysis of variance of (A) constants in the fitted polynominal equation of temperature vs. time at a one inch depth for ground beef at 946 Btu per sq ft-hr and at a λ of 1.194 μ in an open room and in an enclosed volume.

Source of variance	Sum of squares	đf	Mean square	F ratio*
Means	0.21	1	0.21	0.328
Within	2.56	4	0.64	
Total	2.77	5		

^{*}F.95 (1,4) = 7.71

Table 5.26. Analysis of variance of (B) constants in the fitted polynominal equation of temperature vs. time at a one inch depth for ground beef at 946 Btu per sq ft-hr and at a λ of 1.194 μ in an open room and in an enclosed volume.

Sources of Variance	Sum of squares	đf	Mean square	F ratio*
Means	0.0387	1	0.0387	1.877
Within	0.0827	4	0.0206	
Total	0.1114	5		

^{*}F.95 (1,4) = 7.71

Table 5.27. Analysis of variance of (C) constants in the fitted polynominal equation of temperature vs. time at a one inch depth for ground beef at 946 Btu per sq ft-hr and at a λ of 1.194 μ in an open room and in an enclosed volume.

Source of variance	Sum of squares	đ£	Mean squares	F ratio*
Means	704.31x10-8	1	704.31x10-8	3.01
Within	936.67x10-8	4	234.17x10 ⁻⁸	
Total	1640.98x10-8	5		

^{*}F.95 (1,4) = 7.71

Tables 5.25, 5.26 and 5.27 show that there is not a significant difference in the fitted polynominal constants of the open room vs. enclosed volume environments. Therefore, there is not a significant difference in temperatures at the one inch depth vs. time relationship. This was also indicated in Table 5.23 in terms of total processing time. This indicates that there is no appreciable reradiation from the walls of the enclosure and that the absorption of energy by water vapor is insignificant.

5.9 Transient processing rates of ground beef with infrared heating.

Samples of ground beef (one inch depth, three inches width, six inches length) were processed at different surface heat fluxes generated by five different source temperatures. The following results were obtained:

- 5.9.1 Initial ground beef weights
- 5.9.2 Dripping losses
- 5.9.3 Volatile losses
- 5.9.4 Surface time-temperature relationships
- 5.9.5 Time-temperature relationships at the one inch sample depths
- 5.9.6 Time volatile weight losses
- 5.9.7 Sample length and width changes

Table 7.1, in the appendix, shows the initial ground beef sample weights, dripping losses, volatile losses, sample length and width changes and total processing times

between the initial product temperature and 170 F.

Fig. 7.1, in the appendix, shows typical surface temperature-time relationships for several tests at different source temperatures. The average surface temperature was calculated for all tests by taking the sample surface temperatures in five minute increments starting with the initial surface temperature and ending with the final surface temperature, these average product surface temperatures were then plotted against the surface heat flux. See Fig. 5.6 The following linear equation was obtained:

 $t_s = 139.60 + 0.04251 qs$ ",

with: R = 0.9218 and $S_1 = 4.12$,

Where t_s is the average surface temperature, F
qs" is the surface heat flux, Btu per sq ft-hr
R is the linear correlation coefficient

S₁ is the standard error estimate

The above relation was obtained so the average percent volatile loss rate could be obtained. The conversion of water to water vapor should be a first order chemical reaction, if it is first order the familiar empirical equation proposed by Arrhenius should follow (18).

According to the empirical equation a straight line would be obtained when the logarithm of the rate constant, in this case, the percent volatile loss per unit of time is plotted against the reciprocal of the absolute temperature.

Fig. 5.7 shows the result of such a plot. The following

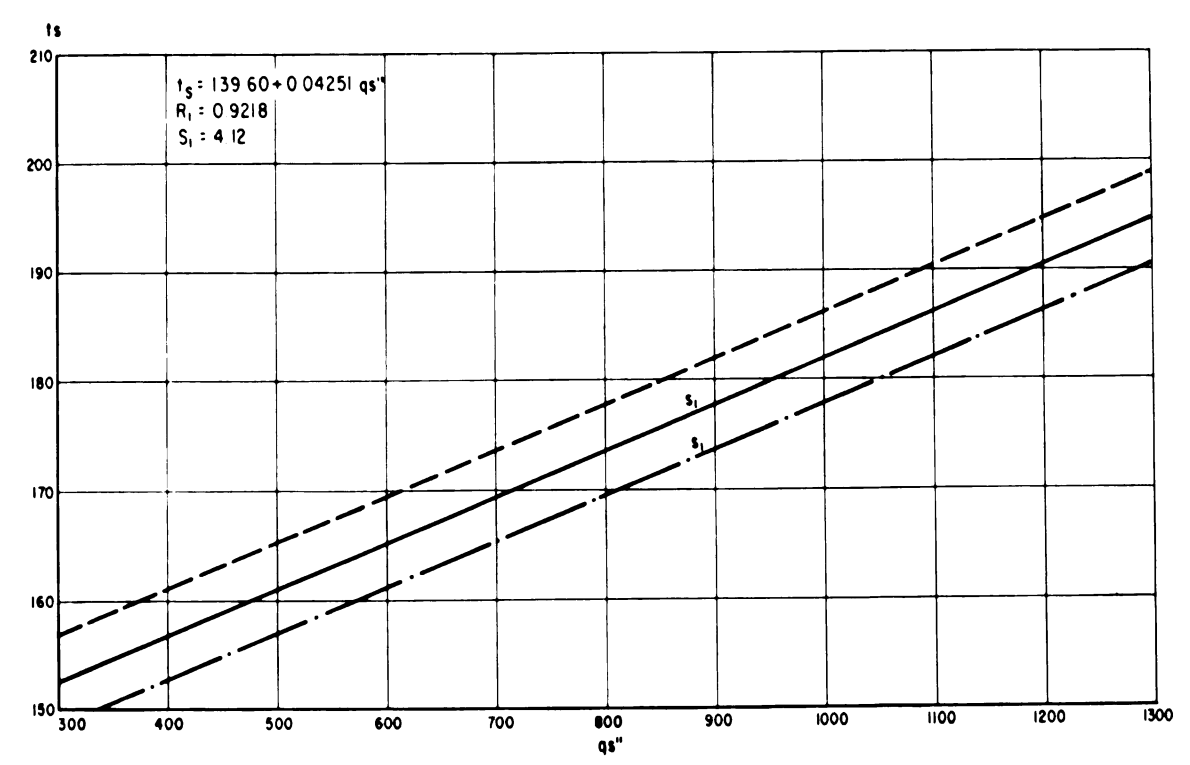
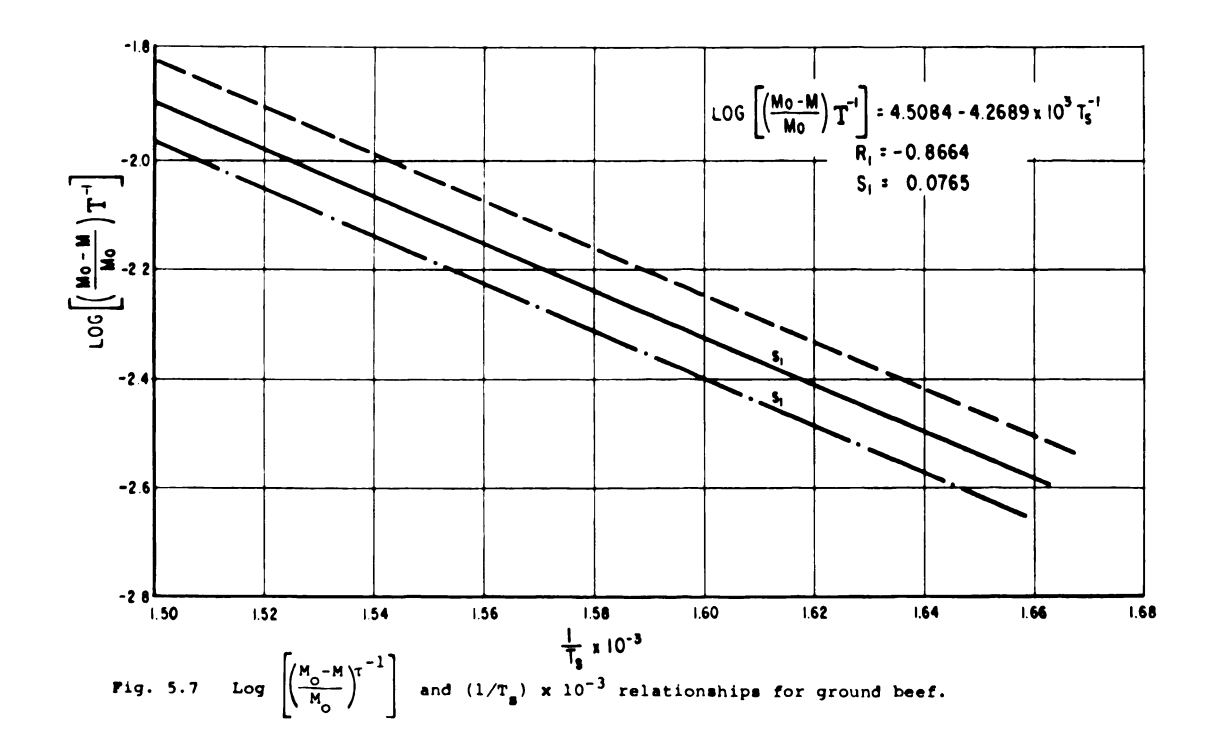


Fig. 5.6 Relationships of $t_{\rm g}$ (average product surface temperature) and qs" for ground beef.



linear equation was obtained:

$$LOG\left[\frac{M_{o}-M}{M_{o}}\right]^{\tau-1} = 4.5084 - 4.2689 \times 10^{3} T_{s}^{-1},$$

with: R = 0.8664 and $S_1 = 0.0765$,

Where M_{Ω} is the initial weight of the product

M is the final weight of the product including dripping losses

is the total processing time, hours

T is average surface temperature, R.

It can be noted from the above expression that

$$\left(\frac{M_{O}-M}{M_{O}}\right)\tau^{-1}$$
 is the volatile loss per hour or the reaction

rate of converting water to water vapor.

Fig. 7.2, in the appendix, shows several typical time-volatile loss relationships, from these it can be noted that a linear relationship very closely approximates the rate of volatile loss for a particular surface heat flux and source temperature. This apparent linear relationship will be used next.

McCance and Shipp (43) have reported that water and weight losses from lean beef processed at a constant temperature are linear with respect to time.

Heisler (26), Carslaw and Jaeger (13) have developed time-temperature relationships that in part depend upon the surface heat loss when a substance is heated at the surface by radiation. If the surface is in an environment at a temperature different than its surface, the surface may gain or lose heat to its environment. Equations have been developed for surface heat losses by convection and radiation. Giedt (24) and Jakob (32) give the following equation for the convection heat transfer coefficient for a horizontal surface being heated or cooled and facing upward: $h_{\rm C} = 0.25 \, (t_{\rm S} - t_{\rm e})^{1/3}, \, {\rm for} \, N_{\rm GR} \cdot N_{\rm PR} > 10^8 \, {\rm or} \, 10^9, \, {\rm all} \, N_{\rm GR} \cdot N_{\rm PR}$

 $h_{\rm C} = 0.25 \; (t_{\rm s} - t_{\rm e})^{1/3}$, for $N_{\rm GR} \cdot N_{\rm PR} > 10^8$ or 10^9 , all $N_{\rm GR} \cdot N_{\rm PR}$ products were greater than 10^9 , with an average of 8.2 x 10^9 for the experimental data.

Where h_{C} is the convection heat transfer coefficient, Btu per sq ft-hr F

 t_s is the surface temperature, F

 t_e is the environment temperature, t_s > t_e in this case, the surface is losing heat to the environment, F

L is the characteristic surface length, ft

Mark's Handbook (40) gives the following equation
to determine the equivalent radiative coefficient:

$$h_{r} = 0.00692 \in \left(\frac{T_{Av}}{100}\right)^{3}$$

Where hr is the radiative heat transfer coefficient,

Btu per sq ft-hr F

 ϵ is the emissivity of the radiation surface $T_{\mbox{Av}}$ is the average temperature of the surface and its environment, R

Jakob (33) also states that an apparent coefficient of heat transfer may be used for the heat of condensation.

This apparent coefficient of heat transfer is given by the following equation:

$$q_L = WL = h_L (t_s - t_e),$$

Where \boldsymbol{q}_{L} is the total latent heat gain, Btu per hr

W is the weight of the condensed product, lbs per hr

L is the latent heat of condensation, Btu per lb

 $\mathbf{h}_{\mathbf{L}}$ is the apparent coefficient of heat transfer,

Btu per sq ft-hr F

t is the surface temperature, F

t is the environment temperature, F

The linear relationship obtained above, see Fig. 5.6, can now be used to determine an apparent coefficient of heat transfer, h_L . As the volatile losses from food products consist of water vapor (3, 37) the latent heat of vaporization may be taken from steam tables. The apparent coefficient of heat transfer may be defined by the following equation:

$$h_{L} = \frac{Percent \ V \ M_{o} \ L}{(t_{s} - t_{e})\tau}$$

Where $h_{\mathbf{L}}$ is the apparent coefficient of heat transfer, in Btu per sq ft-hr F

V is the volatile loss, percent

 M_{\odot} is the initial sample weight, lb

L is the latent heat of vaporization of water at a temperature t_s, in Btu per lb

t, is the average surface temperature, F

t is the environment temperature, F

τ is the processing time, from the initial product temperature to 170 F, hours.

The combination of h_c , h_r and h_L represents the coefficient of heat transfer from the sample surface in Btu per $\mathbf{s}q$ ft-hr \mathbf{F} , then \mathbf{h} is the sum of the three coefficients. The \mathbf{h}_c and \mathbf{h}_L coefficients may be combined because the velocity of the surface volatile loss is approximately 1.1 x 10^{-5} ft per sec as compared to a velocity of approximately 1 ft per sec at a 0.5 ft distance above the surface for free convection of air, based on average surface conditions. This \mathbf{h} should then satisfy the requirement of equation developed by Heisler. These results, \mathbf{h}_c , \mathbf{h}_r and \mathbf{h}_L , are given in Table 5.28 as well as the average surface temperature for each of the tests.

This sum of coefficients was then used in the K/hs parameter, for the plotting of the data. The other two parameters are:

 $\alpha \tau / s^2$ and

 $h(t_1 - t_0)/qs$ ",

Where α is the thermal diffusivity, $\alpha = \frac{k}{pc}$; where k is the themal conductivity, Btu ft per sq ft-hr F; p is the density, lb per cu ft; c is the specific heat, But per lb F.

- τ is the time, hours
- s is the depth at which the temperature is measured, ft
- h is the sum of the coefficients of heat transfer, equal to $h_c + h_r + h_L$, in Btu per sq ft-hr F t is the temperature at a depth s, F

Table 5.28. The convective, radiative and apparent coefficients of heat transfer from the surface of the sample to the room for various room temperatures and sample surface temperatures for each of the tests.

Test No.	λ	ts	t _e	h _C	h _r	h _L	hc+hr+hL
35 34 33 32 1 2 3 4 5 6 7 8	1.233	182 179 183 175 178 166 163 171 177 169 171 163	80 80 79 79 78 78 77 78 80 78 79 79	1.21 1.22 1.20 1.21 1.17 1.16 1.19 1.21 1.18 1.19 1.16	1.03 1.03 1.03 1.03 1.00 0.99 1.02 1.03 1.00 1.02 1.00 0.99	3.85 4.00 3.37 3.39 4.24 2.93 3.70 3.37 3.18 2.92 3.02 2.53 2.38	6.09 6.24 5.62 5.62 6.48 5.10 5.85 5.58 5.41 5.10 5.23 4.69 4.51
10 11 12 13 36	1.505	198 190 185 182 181	79 79 80 79 80	1.26 1.24 1.22 1.21 1.21	1.05 1.03 1.03 1.03	5.94 4.51 5.04 4.11 3.59	8.25 6.78 7.29 6.35 5.83
14 15 16 37 17 18 38		176 170 163 169 170 169	80 81 81 80 79 80	1.20 1.17 1.15 1.17 1.18 1.17	1.03 1.03 1.00 1.02 1.02 1.02 0.99	3.98 3.92 4.41 3.23 3.25 3.02 2.39	6.21 6.12 6.56 5.42 5.45 5.21 4.52
59 63 57 58 69 60 62 66 61 68 65 67 64	2.308	186 188 185 182 179 173 167 168 162 165 156	79 78 78 78 79 79 79 79 79	1.23 1.23 1.22 1.21 1.19 1.19 1.17 1.16 1.16 1.13	1.03 1.03 1.03 1.03 1.03 1.03 1.00 1.00	4.94 3.81 4.16 3.92 4.54 3.78 3.82 3.91 3.06 3.28 3.03 2.49 2.29	7.20 6.17 6.42 6.17 6.78 6.00 6.10 6.08 5.23 5.44 5.19 4.60 4.40

Table 5.28.--Continued.

Test No.	λ	ts	^t e	h _C	h _r	h _L	hc+hr+hL
55 56 29 54	2.797	182 178 177 182	83 80 77 80	1.21 1.21 1.21 1.21	1.03 1.03 1.03 1.03	5.56 4.66 3.64 4.36	7.80 6.90 5.88 6.60
28 53 27 26 25 19 20 21 22 23 24 31 30		173 180 178 172 167 171 166 165 159 161 157	79 78 78 78 78 79 79 78 78 78	1.19 1.21 1.21 1.19 1.17 1.17 1.17 1.17 1.14 1.16 1.14	1.03 1.03 1.02 1.00 1.02 1.00 1.00 0.99 0.99 0.98	3.81 3.82 3.73 3.42 3.29 3.00 3.20 3.12 3.03 2.99 2.19 2.15 2.12	6.03 6.06 5.97 5.63 5.46 5.21 5.37 5.29 5.20 5.12 4.34 4.28 4.23
39 52 47 46 45 42 44 40 41 43 49 51 50 48	3.164	205 186 184 183 183 174 173 170 171 161 163 158	79 78 78 79 79 78 79 79 78 79 79	1.28 1.23 1.23 1.22 1.22 1.22 1.20 1.19 1.18 1.19 1.16 1.16 1.14	1.07 1.03 1.03 1.03 1.03 1.03 1.03 1.02 1.02 0.99 1.00 0.99	5.64 6.40 4.77 4.59 4.36 4.03 3.90 3.80 3.16 3.16 3.21 3.24 2.47 2.42	7.99 8.66 7.03 6.85 6.61 6.28 6.13 6.02 5.80 5.37 5.36 5.40 4.60 4.52

 t_{o} is the initial product temperature, F qs" is the surface heat flux, in Btu per sq ft-hr The thermal diffusivity was assumed to be constant within a given temperature range. The values of specific heat were given in Table 5.1. As latent heats are involved in the changing of fat from solid to liquid in both the α -

and β - forms and from the α - to β -state, at specific temperatures, one graphical presentation of the data covering the entire processing range could not be used. Four plots are used for each of the five source temperatures at different heat fluxes. The first plot covers the range from the initial product temperature to 122 F, the temperature at which α -solid fat changes to α -liquid fat (actually 121.8 F). The second plot covers the range from 122 to 140 F, the latter temperature is the temperature at which α -liquid fat changes to β -solid fat (actually 139.1 F). The third plot includes the spread from 140 to 157 F, the latter temperature is the temperature at which β -solid fat changes to β -liquid fat (actually 156.4 F). The final graph presents the temperatures above 157 F, where the β -fat remains in the liquid state for normal processing product tempera-Several of these plots for different source temperatures and heat fluxes are shown in Fig. 7.3 in the appendix.

The above initial temperatures for the four plots change for each graph, dependent on the latent heat temperature of the fat in the product. The following parameters are then used for each of the changes of state of the fat:

- 5.9.8 First plot: $h(t_1 t_0)/qs$ ", the terms are defined above
- 5.9.9 Second plot: $h(t_1-122)/qs$ ", the 122 F temperature is the temperature at which α -solid fat changes to α -liquid fat

- 5.9.10 Third plot: $h(t_1 140)/qs$ ", the 140 F temperature is the temperature at which α -liquid fat changes to β -solid fat
- 5.9.11 Fourth plot: $h(t_1 157)/qs$ ", the 157 F temperature is the temperature at which β -solid fat changes to β -liquid fat

Heisler (26) has also shown his graphical solutions for $\alpha\tau/s^2$ values less than 0.2 on linear Cartensian coordinates. Within certain limits of $\alpha\tau/s^2$ the plotting of Heisler graphical solutions are very nearly linear, with a high linear correlation. Therefore, straight lines were drawn through the various plots of $h(t_1 - t_0)/qs$ " vs $\alpha\tau/s^2$ for each of the k/hs parameters for the various source temperatures. See again Fig. 7.3 in the appendix. Fig. 7.4, in the appendix, shows an example of the plotted experimental data for various k/hs values, with a radiation source temperature of 3465.0 R.

These data were then correlated by holding the $h(t_1 - t_0)/qs$ " parameter constant at three different values and finding a linear regression line for the remaining two parameters, k/hs and $\alpha\tau/s^2$. This represents a transformation of axis. The linear regression transformation was carried out for each of the five source temperatures, at each of the four temperature ranges and at each of three constant $h(t_1 - t_0)/qs$ " values. These correlations are shown in Tables 5.29, 5.30, 5.31, 5.32 and 5.33.

Table 5.29. Correlation of temperature vs time distribution patterns for various surface heat fluxes from a source temperature of 4230.0 R, λ of 1.233 μ . Y = A + BX represents the linear regression equation of $\alpha\tau/s^2(Y)$ vs. k/hs(X) at a constant h(t₁ - t₀)/qs". R is the correlation of Y on X and the standard error is s₁.

•					
h(t ₁ -t _o)/qs"	t,F	A	В	R*	s ₁
0.30	< 122	0.1988	0.2479	0.5560	0.0281
0.40		0.2281	0.3769	0.6082	0.0334
0.50		0.2527	0.5119	0.6736	0.0383
	122 < t	o < 140			
0.08	_	-0.0798	0.3242	0.9796	0.0246
0.10		-0.1044	0.4154	0.9046	0.0133
0.12		-0.1302	0.5101	0.8919	0.0176
	140 \leq t	<u> </u>			
0.06	_	-0.3552	0.8528	0.8483	0.0362
0.09		-0.6130	1.4311	0.8301	0.0654
0.12		-0.8792	2.0232	0.8263	0.0933
	157 <u></u> t	0			
0.06		-0.2909	0.7507	0.9103	0.0232
0.08		-0.3804	0.9875	0.9161	0.0294
0.10		-0.4752	1.2315	0.9109	0.0379

^{*}R.95 (N=13) = 0.476, if $R \neq 0$

Table 5.30. Correlation of temperature vs time distribution patterns for various surface heat fluxes from a source temperature of 3465.0 R, λ of 1.505 μ . Y = A + BX represents the linear regression equation of $\alpha\tau/s^2(Y)$ vs k/hs(X) at a constant h(t₁ - t₀)/qs". R is the correlation of Y on X and the standard error is s₁.

h(t ₁ -t _o)/qs"	t,F	A	B	R*	s_l
	< 122				
0.30		0.1439	0.2620	0.5806	0.0321
0.40		0.1463	0.4222	0.7351	0.0362
0.50		0.1400	0.5830	0.8245	0.0372
	122 <u></u> t _o	< 140			
0.08		-0.0551	0.2692	0.8360	0.0164
0.10		-0.0811	0.3485	0.8635	0.0189
0.12		-0.0984	0.4159	0.9634	0.0115
	140 <u></u> t _o	< 157			
0.06		-0.1975	0.5460	0.8647	0.0295
0.09		-0.3241	0.8901	0.9233	0.0344
0.12		-0.4492	1.2314	0.9302	0.0452
	157 <u><</u>	to			
0.06		-0.2499	0.6658	0.9424	0.0219
0.08		-0.2977	0.8333	0.9418	0.0276
0.10		-0.3461	1.0055	0.9344	0.0356

^{*}R.95 (N=12) = 0.497, if $R \neq 0$

Table 5.31. Correlation of temperature vs time distribution patterns for various surface heat fluxes from a source temperature of 2260.0 R, λ of 2.308 μ . Y = A + BX represents the linear regression equation of $\alpha\tau/s^2$ (Y) vs k/hs(X) at a constant h(t₁ - t₀)/qs". R is the correlation of Y on X and the standard error is s₁.

$h(t_1-t_0)/qs$ "	t,F	A	В	R*	s_l
	< 122				
0.30		0.1153	0.2737	0.8253	0.0170
0.40		0.0887	0.4695	0.9024	0.0201
0.50		0.0574	0.6718	0.8763	0.0331
	122 <u> </u> t _o	< 140			
0.08		-0.0568	0.2358	0.9601	0.0061
0.10		-0.0891	0.3313	0.6424	0.0326
0.12		-0.1308	0.4411	0.9822	0.0075
	140 <u></u> t _o	< 157			
0.06		-0.2330	0.5724	0.9319	0.0199
0.09		-0.3872	0.9382	0.9623	0.0230
0.12		-0.5024	1.2318	0.9753	0.0250
	157 \leq t_0				
0.06		-0.259	0.6351	0.9496	0.0159
0.08		-0.2964	0.7558	0.9791	0.0140
0.10		-0.3837	0.9684	0.9728	0.0225

*R.95 (N=13) = 0.476, if $R \neq 0$

Table 5.32. Correlation of temperature vs time distribution patterns for various surface heat fluxes from a source temperature of 1864.5 R, λ of 2.797 μ . Y = A + BX represents the linear regression equation of $\alpha\tau/s^2$ (Y) vs k/hs (X) at a constant h(t₁ - t₀)/qs". R is the correlation of Y on X and the standard error is s₁.

h(t ₁ -t _o)/qs"	t,F	A	В	R*	s_1
	< 122				
0.30		0.1911	0.1588	0.5178	0.0275
0.40		0.2260	0.2476	0.5885	0.0356
0.50		0.2305	0.3893	0.7503	0.0359
	122 \leq t_o	< 140			
0.08		-0.0287	0.1978	0.9173	0.0088
0.10		-0.0464	0.2712	0.9976	0.0019
0.12		-0.0676	0.3501	0.9880	0.0057
	140 <u></u> t _o	< 157			
0.06		-0.2508	0.6209	0.8821	0.0348
0.09		-0.4528	1.0948	0.9057	0.0537
0.12		-0.6304	1.5203	0.9378	0.0590
	157 <u></u> t _o				
0.06		-0.2486	0.6386	0.9101	0.0304
0.08		-0.3364	0.8663	0.9171	0.0394
0.10		-0.4290	1.1000	0.9186	0.0496

*R.95 (N=17) = 0.412, if $R \neq 0$

Table 5.33. Correlation of temperature vs time distribution patterns for various surface heat fluxes from a source temperature of 1648.7 R, λ = 3164 μ . Y = A + BX represents the linear regression equation of $\alpha\tau/s^2$ (Y) vs k/hs (X) at a constant h(t₁ - t₀)/qs". R is the correlation of Y on X and the standard error is s₁.

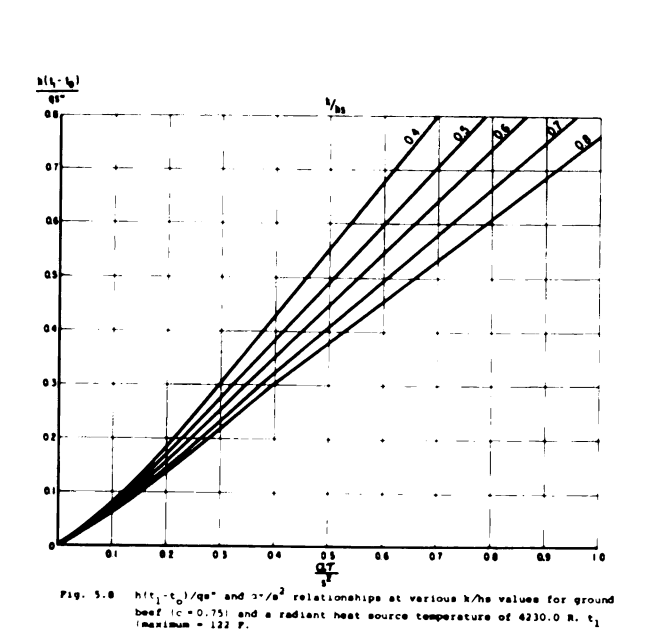
h(t ₁ -t ₀)/qs"	t,F	A	В	R*	s ₁
	< 122				
0.30		0.1379	0.2426	0.7264	0.0247
0.40		0.1515	0.3780	0.8271	0.0276
0.50		0.1677	0.4960	0.8108	0.0385
	122 < t _o	< 140			
0.08	_	-0.0289	0.1937	0.9386	0.0076
0.10		-0.0461	0.2622	0.9686	0.0072
0.12		-0.0644	0.3328	0.9696	0.0090
	140 <u></u> t _o	< 157			
0.06		-0.1248	0.3946	0.8954	0.0220
0.09		-0.2099	0.6515	0.9156	0.0307
0.12		-0.2919	0.9047	0.9288	0.0388
	157 < t _o				
0.06		-0.1261	0.4041	0.9569	0.0131
0.08		-0.1630	0.5314	0.9608	0.0164
0.10		-0.2121	0.6824	0.9507	0.0240

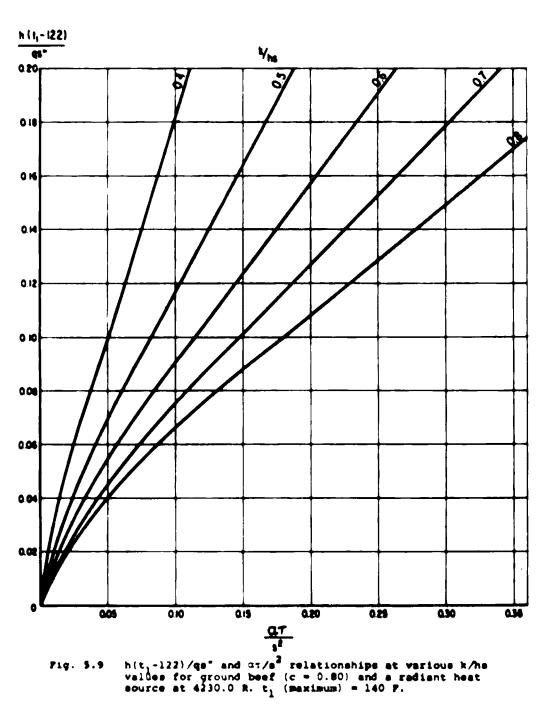
^{*}R.95 (N=14) = 0.458, if $R \neq 0$

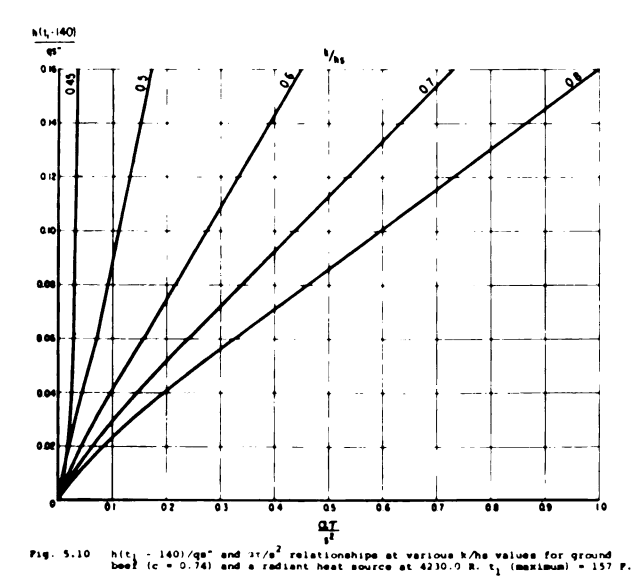
The results of the previous five tables, Tables 5.29, 5.30, 5.31, 5.32 and 5.33 are plotted in Fig. 5.8 through 5.27.

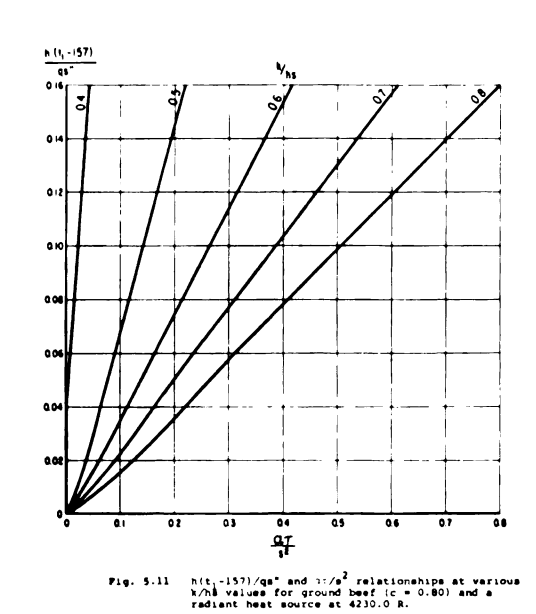
At this point it may be desirable to summarize the steps involved in computing the time (τ) required to reach a temperature at a depth (s) or given a time (τ) the steps involved to determine the temperature at some depth (s). The steps are:

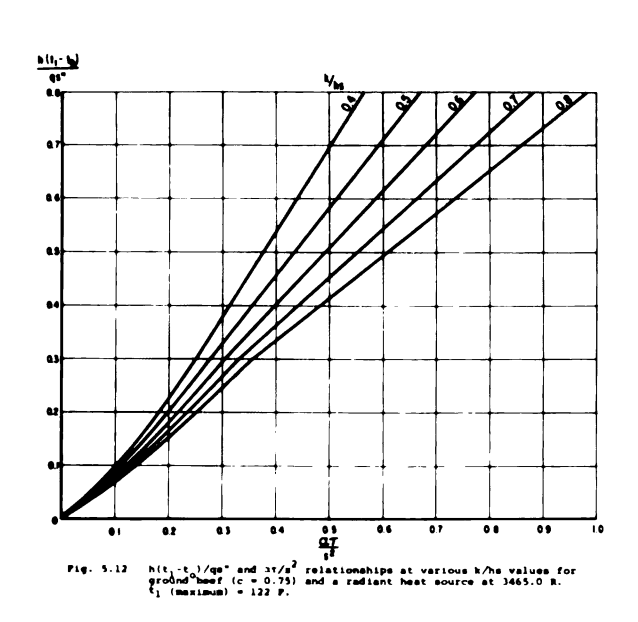
- 5.9.12 <u>Given</u> a heat flux, Btu per sq ft-hr, the average surface temperature of the product can be found from Fig. 5.6, F.
- 5.9.13 Knowing the average surface temperature, the volatile rate loss can be found in Fig. 5.7 in percent of the initial product weight per hour, hence pounds per hour.
- 5.9.14 Knowing the average surface temperature and the volatile loss in pounds per hour, the convective, radiative and apparent coefficients of heat transfer can be computed and the combined h can be found.
- 5.9.15 <u>Having</u> selected a product with known thermal properties and latent heat changes, and having selected a source temperature, either one or several of the Figs. 5.8 through 5.27 could be used to determine the time or times to reach a specific temperature or specific temperatures can be determined.

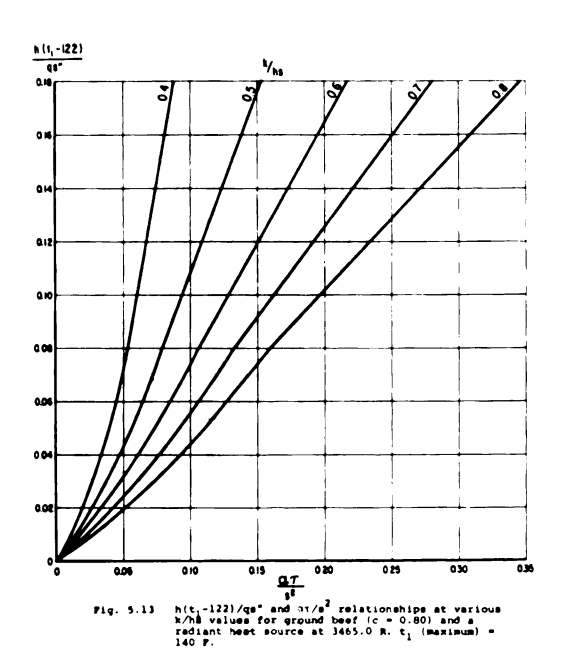


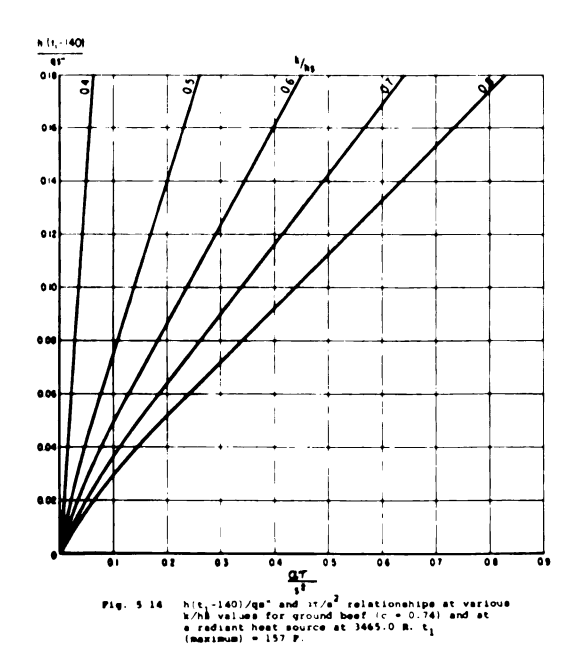


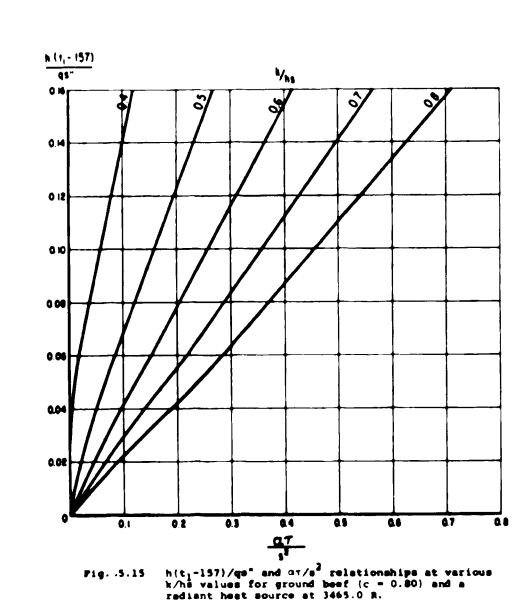


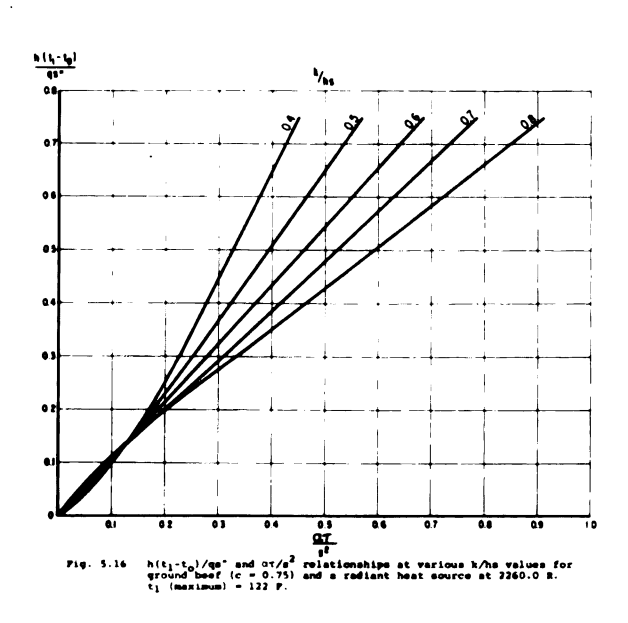


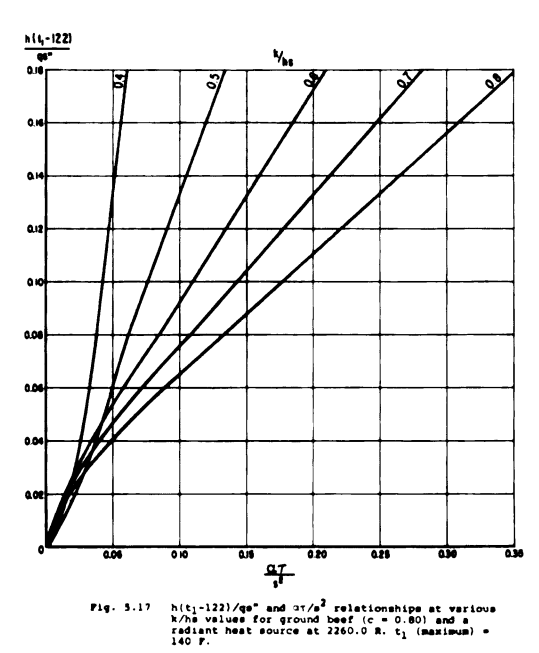


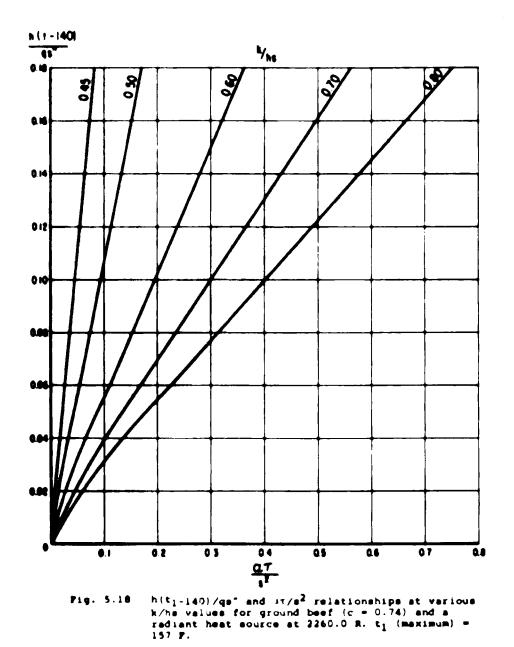


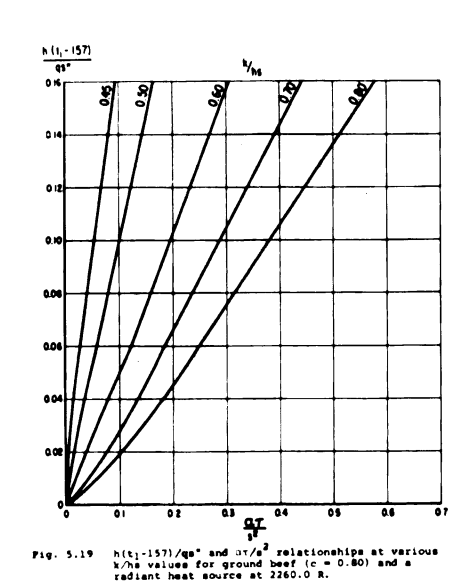


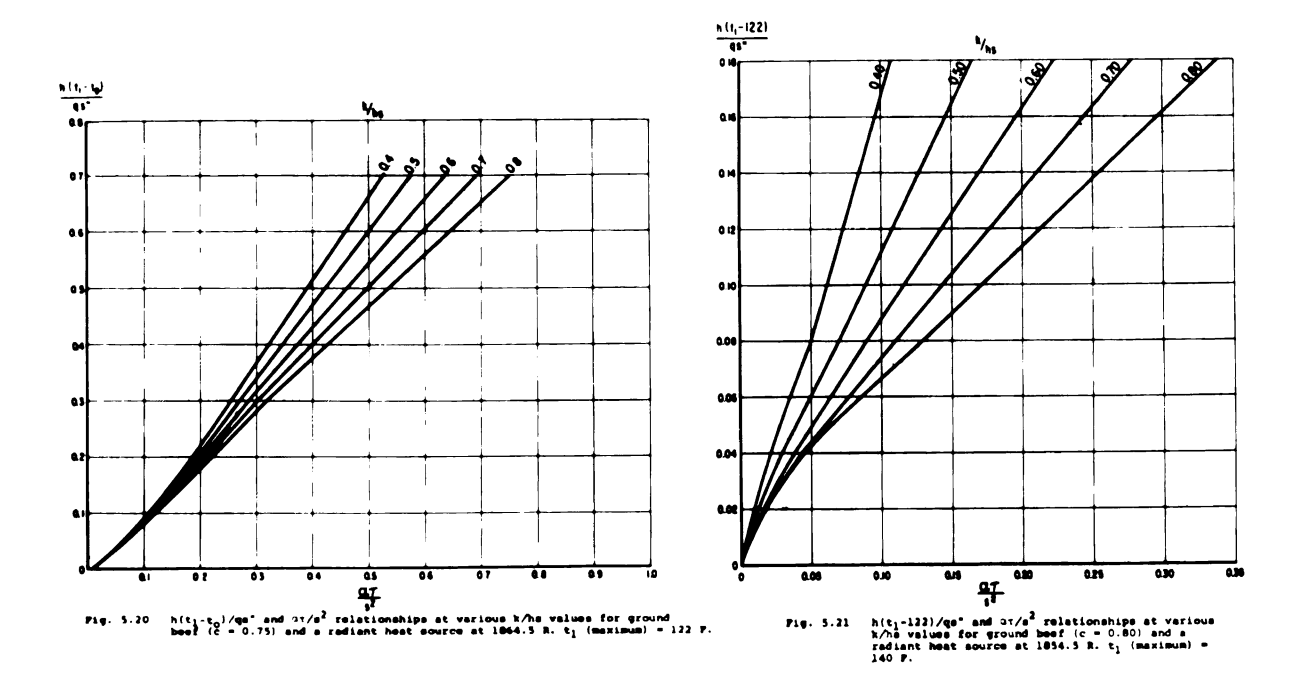


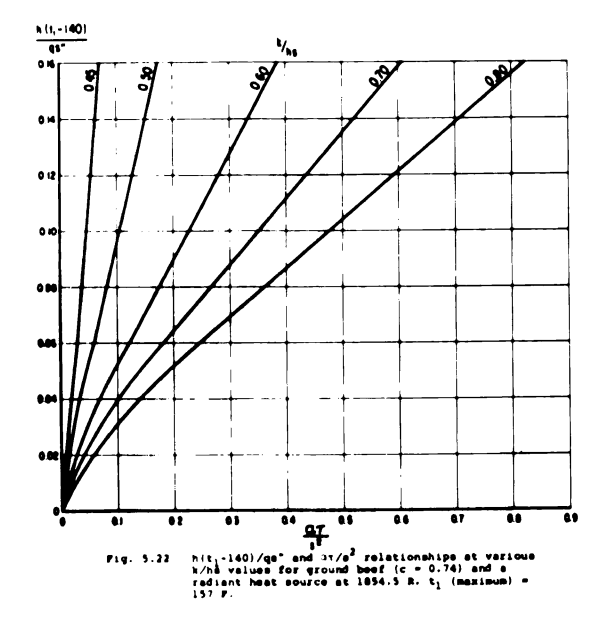












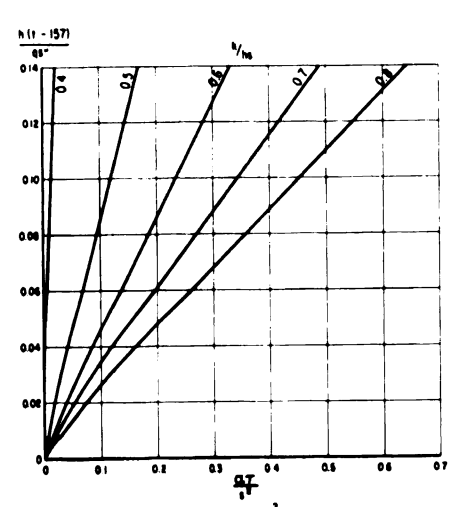
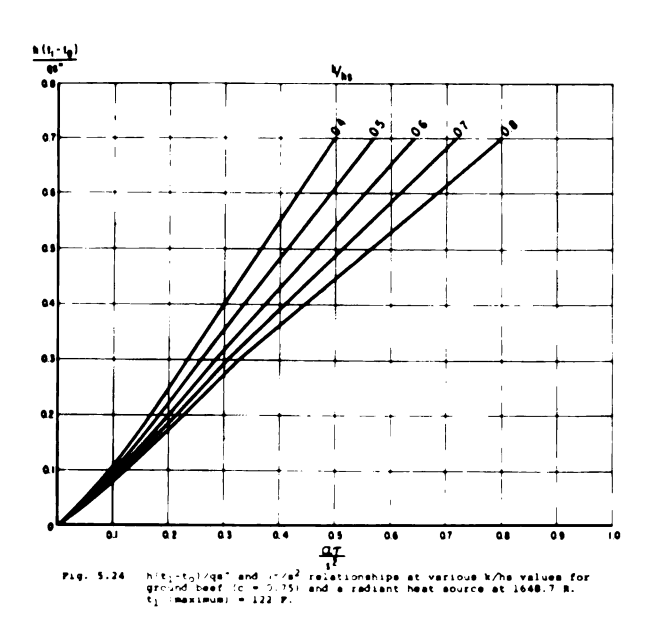


Fig. 5.23 $h(t_1-140)/qs^n$ and $3\pi/s^2$ relationships at various χ/hs values for ground beef (c = 0.80) and a radiant heat source at 1864.5 R.



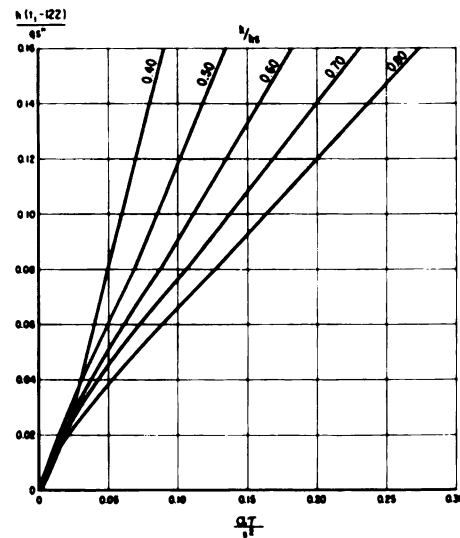
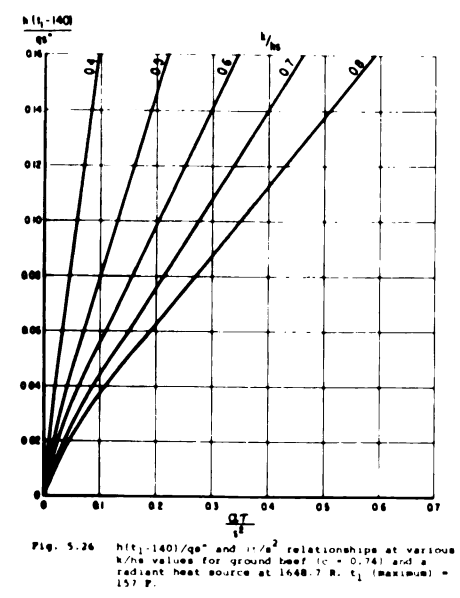
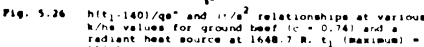
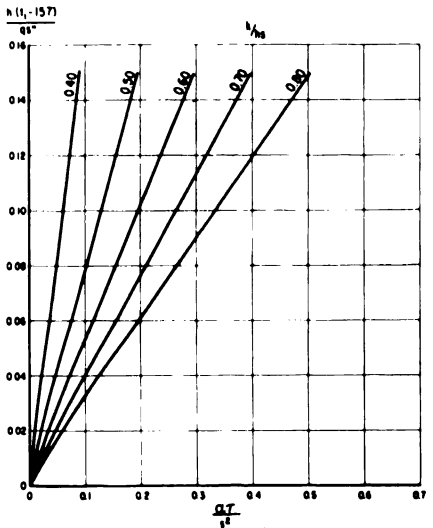


Fig. 5.25 $h(t_1-122)/q^2$ and ar/s^2 relationships at various h/hs values for ground beef (c=0.80) and a radiant heat source at 1648.7 R. t_1 (maximus) = 140 F.







0? 03 04 05 06 07 $\frac{GT}{4}$ h(t₁-157)/qs" and 2^{1} /s² relationships at various k/hs values for ground beef (c=0.80) and a radiant heat source at 1646.7 R.

5.9.16 The final step, if two or more of the Figs.
5.8 through 5.27 add together the determined times from each of the figures.

The solution for a product temperature at a specific depth would follow a similar pattern, but the final step would be eliminated, as the time would already be known.

Examples of the use of the above figures and steps are included in the appendix.

These results are similar to Heisler's, in that with increased surface heat fluxes the time to reach a particular temperature at a depth (s) is less, for a constant k/hs parameter. Also, as the surface heat flux increases the surface temperature increases which in turn affects the Arrhenius empirical equation, that is volatile losses increase, which generates a higher coefficient of heat transfer on the surface. But, a high surface temperature also causes an increased heat flow into the product and hence reduces the time to reach a specific temperature. This phenomenon is also indicated on the Heisler charts (26). Also if the surface heat flux could be held constant and different coefficients of heat transfer, say $h_2 > h_1$, both at the same heat flux, the time required to reach a specific temperature would be greater for the higher coefficient of heat transfer (greater surface heat loss) than for the lower coefficient, this is also shown by Heisler (26). The major difference between Fig. 5.8 through 5.27 and Heisler's plots is the linear relationships at specific k/hs

parameters. However, Heisler has even broken his graphical solutions in two parts, one solution for $\alpha\tau/s^2$ values equal to or greater than 0.2 and another solution for those values less than 0.2. The latter graphical solution has a linear region of $h(t_1 - t_0)/qs$ " vs $\alpha \tau/s^2$, and a high linear correlation exists in the other region for low values of $\alpha \pi/s^2$. The thermal diffusivity is the major factor that keeps the ατ/s² values low and in a highly correlated linear region. With moist food products the thermal conductivity is low, lower than water (36). The density is low, when compared to metals, and the specific heat is rather high, less than that of water. These factors contribute to a low thermal diffusivity and hence a low $\alpha \tau / s^2$ parameter. The product thickness is important, but generally it again tends to keep $\alpha \tau / s^2$ factor low, first by appearing as s^2 , so when the depth is increased at a fixed time, the $\alpha\tau/s^2$ parameter is reduced. It also appears in another parameter, k/hs, and as s is increased k/hs is reduced for fixed k/hs values and this again tends to reduce $\alpha \tau / s^2$ values.

The results of Lukianchuk's (38) dry heat and deep fat processing of beef also indicate four possible temperature ranges in processing. Within temperature regions she gave heat penetration data, minutes per degree centigrade rise. These results were checked with the latent heat of fusion temperature of the α - and β -forms of fat and the heat penetration data indicated a linear temperature rise within the various temperature ranges for both types of

processing. Similar results were also found in other data, unpublished, on heat penetration at the Department of Foods and Nutrition, Michigan State University, East Lansing, Michigan.

Lowe (2, 37) presents graphs of temperature vs time data for the processing of lean beef. Linear relationships exist for the above temperature ranges except for a temperature lag period at the beginning of heating and at temperatures above 80 C it is apparent that a logarithmic temperature-time relationship exists, because the product temperature is approaching the source temperature.

A consideration of the above factors, plus the rather low final product temperatures reached in processing support the linear relationships obtained in Figs. 5.8 through 5.27.

Utilizing known information about the product, the thermal properties, density and rate of moisture loss and comparing the results of the procedure given above to the Heisler graphical solution for a specific heat flux and a final product temperature, the Heisler charts always indicate a greater processing time than was actually required or as determined from above. Jakob (33) indicates that for transpiration cooling, that is when a liquid is moving through the void spaces in a product, an apparent conductivity of the mixture should be used. This apparent conductivity is lower than the conductivity of the liquid moving through and higher than the conductivity of the porous substance.

Again, at a fixed heat flux and fixed final temperature, this would result in lower processing times, hence reducing the differences between Heisler's charts and the above results. Another factor could influence the above difference, Jakob's apparent conductivity is based on the fact that the fluid was primarily moving in one direction, toward the transpirating surface. However, if this was not the case, the fluid could move with freedom to other parts of the product, convection could then take place within the product itself. This could then further increase the rate of heat transfer at a depth s, and again reduce the above differences between the results and Heisler's graphical solution.

It is apparent that the above or similar such considerations are included in the graphical presentation of the results. Until such a time when these effects are measured and correlated for moist food products, a difference will probably exist between Heisler charts and actual processing time-temperature distributions within a product.

Finally, Heisler assumed a boundary condition of qs"/h as the final temperature of the body above its initial temperature, which did not hold true in these experiments, for the entire processing range. This boundary condition would increase the time to reach a particular temperature at a particular heat flux, if the final product temperature or equilibrium temperature was greater than qs"/h, plus the initial product temperature.

Fig. 7.28 shows a comparison of the effect of heat source temperature, or λ 's, on a constant k/hs parameter for various values of $h(t_1-t_0)/qs$ " and $\alpha\tau/s^2$. This figure indicates that the higher λ 's or lower source temperatures, that is $\lambda > 1.505~\mu$ or a source temperature \langle 3465.0 R, are approximately equivalent in time-temperature relationships at the same heat fluxes. For shorter wave lengths or higher source temperatures greater times are required to reach a specific product temperature at a given heat flux. DeWerth (19) and Sayles (48) state that the absorption of electromagnetic energy by water is the critical factor and the critical wave length is about 1.5 μ . Water has a high reflectivity for wave lengths below 1.5 μ and a high absorptivity above 1.5 μ . This is also indicated in Fig. 5.28.

The percent volatile and dripping losses and the decrease of product volume are shown in Table 5.34. The decrease of volume, assumes a constant depth, which was not measureable, however Lowe (37) points out that the depth of the product increases, while there is a decrease in both length and width. Daniels and Alberty (18) state that coefficient of volumetric expansion or contraction is at a constant rate in the three dimensions. But the American Meat Institute Foundation (3) indicates the depth does increase because of the relative change in protein linkages, which appear to unfold. Lowe also indicates that the change in volume is always less than the sum of the volatile and dripping losses, as indicated in Table 5.34.

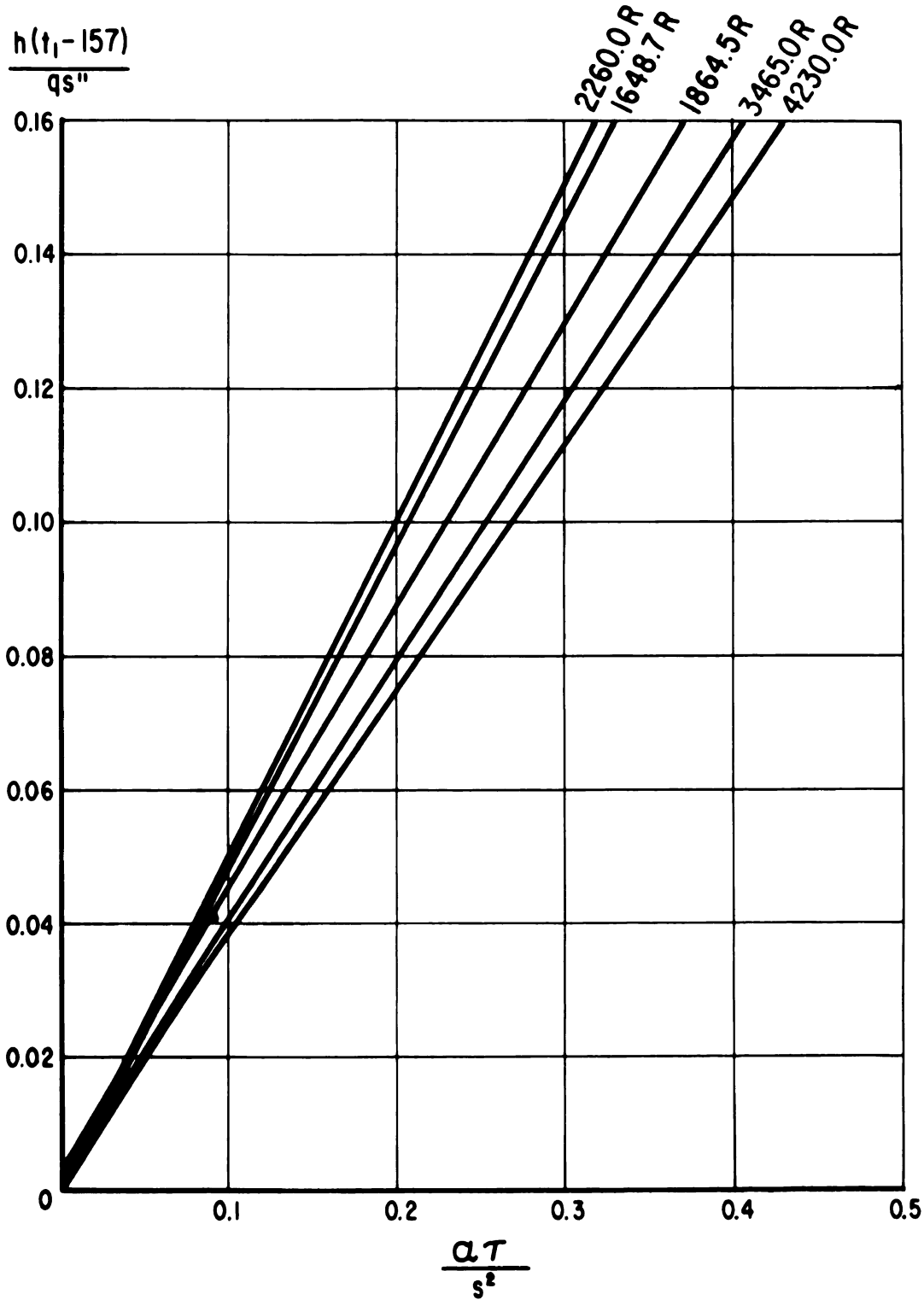


Fig. 5.28 $h(t_1-157)/qs$ " and $\alpha\tau/s^2$ relationships at k/hs = 0.6 for ground beef (c = 0.80) at different radiant heat source temperatures, R.

4 1 1
i
! !

Table 5.34. Percent volatile and dripping losses and volume change in length and width for ground beef processed to 170 F at various radiant heat source temperatures and at different heat fluxes.

		Losse	es, percent		***-1
Test	Heat flu x	Volatile	Dripping	Total	Volume reduction percent
(Source	temperature,	4230.0 R)			
35 34 33 32 1 2 3 4 5 6 7 8	1124.01 1077.69 1024.06 967.05 903.57 843.72 777.33 729.93 692.37 643.27 580.94 545.35	7.51 8.34 8.20 8.04 10.41 7.22 10.33 10.32 11.40 10.33 12.16 10.15	18.27 17.79 17.28 17.86 16.52 17.94 14.94 15.45 14.26 15.86 11.42 14.91	25.78 26.13 25.48 25.90 26.93 25.16 25.27 25.87 25.66 26.19 23.58 25.06	22.8 20.0 22.8 21.9 17.8 19.0 20.0 20.0 19.0 19.0
9	472.90	12.15	14.25	26.40	20.0
(Source	temperature,	3465.0 R)			
10 11 12 13 36 14 15 16 37 17 18 38	1163.87 1077.48 1009.85 934.40 899.23 868.11 797.34 716.54 671.65 637.57 562.60 507.88	11.05 9.37 9.37 8.83 7.17 9.35 8.92 9.33 9.09 9.69 9.89 10.04	13.66 14.84 15.12 16.64 18.30 16.68 17.18 15.15 16.15 16.28 15.08 17.47	24.71 24.21 24.59 25.47 25.47 26.03 26.10 24.48 25.25 25.97 24.97 25.51	21.0 21.9 21.9 19.0 22.0 21.9 20.0 21.0 21.0 21.0
(Source	temperature,	2260.0 R)			
59 63 57 58 69 60 62 66 61	1151.82 1081.34 1016.45 947.25 893.41 836.52 778.42 721.09 666.42	7.32 6.26 7.61 7.19 8.19 7.18 7.43 7.90 8.02	20.42 22.20 18.83 19.92 19.13 21.81 20.15 20.99 20.07	27.74 28.46 26.44 27.11 27.32 28.99 27.58 28.89 28.09	25.5 22.8 22.0 25.5 20.0 24.7 22.8 23.8 20.0

Table 5.34.--Continued.

		Volume			
Test	Heat flux	Volatile	Dripping	Total	reduction percent
68 65 67 64	624.24 576.10 528.96 484.86	7.80 8.46 8.41 8.92	20.36 20.10 21.81 21.57	28.16 28.56 30.22 30.49	22.8 21.0 22.0 23.8
(Source	temperatur	e, 1864.5 R)			
55 56 29 54 28 53 27 26 25 19 20 21 22 23 24 31 30	1029.76 955.46 916.62 913.90 862.77 860.29 813.66 761.61 712.07 650.08 601.10 561.91 510.22 489.10 426.28 387.42 348.24	8.71 8.44 7.43 8.00 8.14 7.93 8.76 8.79 8.29 8.93 10.86 10.85 11.31 10.31 9.57 12.12	17.17 16.97 20.67 17.57 18.53 18.32 15.24 17.20 18.95 17.70 17.03 16.22 14.31 15.75 20.69 16.00 14.86	25.88 25.41 28.10 25.57 26.67 26.25 24.00 25.99 27.24 26.63 27.89 27.07 25.62 26.06 30.26 28.12 27.31	23.8 22.8 25.3 22.8 22.8 23.0 20.0 21.0 20.0 21.0 20.0 21.9 20.0 20.0
(Source	temperature	e, 1648.7 R)			
39 52 47 46 45 42 44 40 41 43 49 51 50 48	1281.52 1203.40 1144.89 1063.17 988.37 931.20 857.93 792.69 718.77 655.43 595.28 544.16 487.96 436.25	9.69 9.73 8.37 7.77 8.07 7.65 7.48 8.83 8.23 9.77 8.01 8.58 8.37 9.84	14.85 15.87 17.45 17.65 18.02 18.90 18.83 16.58 17.82 18.67 19.16 19.24 18.62 18.56	24.54 25.60 25.82 25.42 26.09 26.55 26.31 25.41 26.05 28.44 27.17 27.82 26.99 28.40	26.3 22.8 25.5 24.7 25.5 23.8 24.7 21.9 22.8 21.9 22.8 20.0 21.0

Table 5.35. Analysis of variance of total processing losses for the different heat source temperatures.

Variance	Sum of squares	đf	Mean square	F ratio*
Means	72.21	4	18.0525	14.75
Within	78.33	64	1.2239	
Total	150.54	68		

*F.95 (4, 64) = 2.52

The total processing losses are not equal, as shown in Table 5.35. Therefore, the heat source temperature affects the total processing losses. This could be expected as the heat source temperatures covered the critical range of the water absorption spectrum. From the water absorption spectrum, it appears that the energy from lower heat source temperatures would be more readily absorbed and lead to higher product temperatures and hence, higher product losses, if the product losses are dependent on temperature. In order to isolate the source temperature or temperatures which lead to higher processing losses the means and deviations of total losses must be investigated. Table 5.36 is a table of contrasts, comparing the average losses and their variances for each of the heat source temperatures. The results in the table are "t" test results.

It is apparent from Table 5.36 that a heat source temperature of 2260.0 R leads to significantly higher total losses. This particular source temperature corresponds to a black body energy emission curve that has a maximum energy

Table 5.36. Summary of "t" tests for comparing the percent total losses for each of the heat source temperatures. (Column means are subtracted from row means.)

		Heat sou			
Heat source temperature, R	4230.0	3465.0	2260.0	1864.5	1648.7
4230.0		0.43	-1.97*	-0.67	-0.58
3465.0			-2.42*	-0.99	-0.97
2260.0				0.90	1.16
1864.5					0.14
1648.7	_				

^{*}These t's are significant at a 95% level of confidence.

level at 2.308 microns. This energy emission curve also exists in the critical water absorption area. See Fig. 2.2. The heat source temperatures lower than 2260.0 R have higher average total product losses than those temperatures above 2260.0 R, but the differences are not statistically different. It is also interesting to note that while a heat source temperature of 2260.0 R results in statistically different total losses with both the higher temperatures, it is not statistically different from the lower heat source temperatures. This might indicate that a maximum total loss heat source temperature exists between 3465.0 and 1864.5 R. Also, as the water absorption curve is rapidly changing in the area of two microns, this could suggest a transition region, similar to the transition region between laminar and turbulent boundary layers in convection heat transfer.

If this were the case, one specific heat source temperature could not be defined for maximum total product losses only a region. In the case of food processing this region would then be avoided, because it is desirable to have maximum product yields.

According to Lowe (37) the volume change in a product is a function of final product temperature. If this hypothesis is accepted, an analysis of the volume changes for products subjected to different heat source temperatures would not have any significant effect, because all products were processed to a final temperature of 170 F. However, the hypothesis of Lowe must be rejected as an analysis of variance of volume changes indicates that the percent volume change is a function of heat source temperature.

See Table 5.37.

Table 5.37. Analysis of variance of percent volume change for the different heat source temperatures.

Variance	Sum of squares	df	Mean squares	F ratio*
Means	92.26	4	23.065	7.859
Within	187.85	64	2.935	
Total	280.11	68		

^{*}F.95 (4,64) = 2.52

Lukianchuk (38) processed meat in an oven and in deep fat, the fat temperature was lower than the oven temperature, and she reported significantly higher percentage volume changes with the lower temperature of processing. She

did not explain the phenomenon. It should be possible to isolate the heat source temperature or temperatures causing the differences in Table 5.37. Table 5.38 is a table of contrasts, comparing the average volume changes and their variances for each of the heat source temperatures. The results in the table are "t" test results.

Table 5.38. Summary of "t" tests for comparing the percent volume change for each of the heat source temperatures. (Column means are subtracted from row means.)

Wash same		Heat sou	rce tempe:	rature, R	
Heat source temperature, R	4230.0	3465.0	2260.0	1864.5	1648.7
4230.0		-0.19	-1.17	-0.56	-1.74*
3465.0			-1.02	-0.39	-1.17
2260.0				+0.60	-0.14
1864.5					-0.70
1648.7					

*This "t" is significant at the 95% level of confidence.

Table 5.38 reveals only one significant difference, at the 95% level of confidence. This value is not significant at the 99% level of confidence. It could be stated that this is a chance difference and a hypothesis could not be formulated without further investigation. However, Table 5.37 indicates that there is a very significant effect of source temperature on percent volume change. As the source temperature is reduced, the wave length of the maximum energy

is increased. Planck (46) states this energy is not absorbed on the geometrical surface, but is destroyed in a depth below the surface. Hall (25) has stated that the absorptivity of non-conductor or insulators increase as the wave length of electromagnetic radiation in the infrared region is increased and most hygroscopic materials have high absorption beyond 3 microns. As the point of maximum energy emission is 3.164 microns for a 1648.7 R source, which according to Hall has a higher absorption than for higher source temperatures, the rate of heat absorption would be higher. This higher rate of heat absorption could then cause faster chemical reactions within the product, especially the contraction of the meat fibers and would then lead to greater volume changes. This effect is indicated in Tables 5.37 and 5.38.

6.0 SUMMARY AND CONCLUSIONS

The processing of ground beef by a radiant heat source is dependent on two major factors: (a) the temperature of the radiant source, and (b) the product surface heat flux as generated by the heat source. The latter factor also affects the volatile weight loss of ground beef.

Three different electric heat source units were used to investigate the effects of heat source temperature on processing times within similar product temperature ranges. Varying the electrical voltage on the heat source resulted in different heat source temperatures. Changing the distance between the heat source and the surface of the product resulted in different surface heat fluxes. The radiant heat sources were: fused quartz lamps; metal sheathed resistance elements, commonly known as calrods; and fused quartz tubes. The quartz lamp filament was operated at two temperatures, 4230.0 and 3465.0 R. The calrod was operated at metal sheathed temperatures of 1864.5 and 1648.7 R. The fused quartz tube was operated at a filament temperature of 2260.0 R. These temperatures correspond to a black body radiator, with a maximum energy emission of 1.233, 1.505, 2.797, 3.164 and 2.308 microns, respectively. The heat flux range varied from about 350 to 1290 Btu per sq ft-hr. All samples were of ground beef and were processed from about 45 F to a final temperature of 170 F.

6.1 Calculated and measured heat fluxes

The radiation and convection heat losses were calculated for three heat sources. The calculated radiation losses were then compared to the manufacturer's radiation rating of the units. In all cases the calculated radiant heat output was higher. The maximum percent difference at the actual operating voltage was 11.20%; this occurred with the calrod unit operated at 180 volts.

An accurate comparison could not be made between calculated and measured heat fluxes. The measured heat flux, as measured by an Eppley pyroheliometer, was a function of the distance between the heat source and instrument. The measured heat fluxes approached the calculated heat fluxes at greater distances between the source and the instrument.

6.2 The effect of environment wall reradiation on processing time.

Six samples of ground beef were processed at 946

Btu per sq ft-hr, which was generated by a source temperature of 4365 R. Three of the samples were processed in an open room. The remaining three samples were processed in an enclosed volume, which was interiorly painted blackboard black. All samples were processed from about the same initial temperature to 170 F. The following is a summary of the results:

6.2.1 A higher product yield was observed with the enclosed volume.

- 6.2.2 A high dripping loss occurred in the nonenclosed volume.
- 6.2.3 There was no significant difference in volatile loss.
- 6.2.4 There was no significant difference in total processing time.
- 6.2.5 There was no significant difference in the timetemperature relationships at a one inch sample depth.
- 6.3 The effects of heat source temperatures and surface heat fluxes on processing times and weight losses of ground beef

Five different heat source temperatures were selected, 4230.0, 3465.0, 2260.0, 1864.5 and 1648.7 R. A range of heat fluxes was selected for each of the heat source temperatures. The following data were obtained:

(a) product weight losses, volatile and dripping; (b) rate of volatile loss; (c) time-temperature relationship on the surface of the product; (d) time-temperature relationship, one inch below the surface of the product, this corresponded to the maximum depth of the product; (e) volume change of the product. The following is a summary of the results:

- 6.3.1 A linear relationship exists between surface heat flux and the average surface temperature of the product.
- 6.3.2 A linear relationship exists between volatile loss and time at a given surface heat flux, or

- at an average product surface temperature.
- 6.3.3 The volatile loss rate follows the empirical Arrhenius equation, for first order chemical reactions.
- 6.3.4 A linear relationship exists for values of h(t - t₁)/qs" vs cτ/s² for various parameter values of k/hs, within the following product temperature ranges: (a) above freezing to 122 F; (b) 122 to 140 F; 140 to 157 F; 157 F and above, to at least 170 F.
- 6.3.5 The linear relationships in 6.3.4 above, also depend on another parameter, heat source temperature.
- 6.3.6 A procedure is given to determine the total processing time to reach a specific product temperature. The procedure is summarized below.
 - 6.3.6.1 Given a surface heat flux, the average surface temperature can be found from Fig. 5.6.
 - 6.3.6.2 The percent volatile weight loss per hour can be found, if the surface temperature is known, Fig. 5.7.
 - 6.3.6.3 If the surface temperature and volatile

 weight loss per hour are known the radia
 tive, convective and apparent coefficients

 of heat transfer on the sample surface can

- be calculated, the sum of these three coefficients is then called the combined coefficient of heat transfer.
- 6.3.6.4 If the thermal properties of the product are known, the time to reach specific temperatures at a specific depth can be determined from Fig. 5.8 to 5.27, for various radiant heat source temperatures.
- 6.3.6.5 The final step consists of summing the increment times determined from step 6.3.6.4.
- 6.3.6.6 If a temperature is desired at a specific time, an iteration technique can be used by reversing the above five steps.
- 6.3.7 Some general remarks concerning the timetemperature relationships at various k/hs parameters are given below.
 - 6.3.7.1 The higher the heat flux, the shorter the time required to reach a specific temperature at a specific depth.
 - 6.3.7.2 The higher the heat flux, the higher the surface temperature, which results in higher surface coefficients of heat transfer.
 - 6.3.7.3 If two equal heat fluxes could be compared with different surface coefficients of heat transfer, a shorter processing time would be

- required for the lower surface coefficient.

 A high coefficient indicates a greater loss
 of heat from the surface to the environment.
- 6.3.7.4 The greater the product depth, the longer the required processing time to reach a specific temperature at the depth.
- 6.3.8 Decreasing the radiant heat source temperatures from 4230.0 to 2260.0 R results in decreased processing times at the same heat flux. Any further reduction of heat source temperatures to 1648.7 R does not essentially affect the processing time required at 2260.0 R.
- 6.3.9 The maximum total product losses occurred with a source temperature of 2260.0 R. The total losses at 4230.0, 3465.0, 1864.5 and 1648.7 R were not significantly different.
- 6.3.10 The percent volume changes were not significantly different except for a radiant heat source temperature reduction from 4230.0 to 1648.7 R.

 For the latter case, the volume reduction was significantly greater with a 1648.7 R heat source temperature.
- 6.4 In general the following recommendations could be made, concerning radiant heat processing. It appears that the 1864.5 R heat source temperature has the most desirable processing effects on ground beef. A higher

total product loss occurred with a heat source temperature of 2260.0 R and a larger volume reduction occurred with a heat source temperature of 1648.7 R. Also, processing times were longer at 4230.0 and 3465.0 R. And finally, a higher surface heat flux results in shorter processing times, at the heat source temperatures investigated.

7.0 APPENDIX

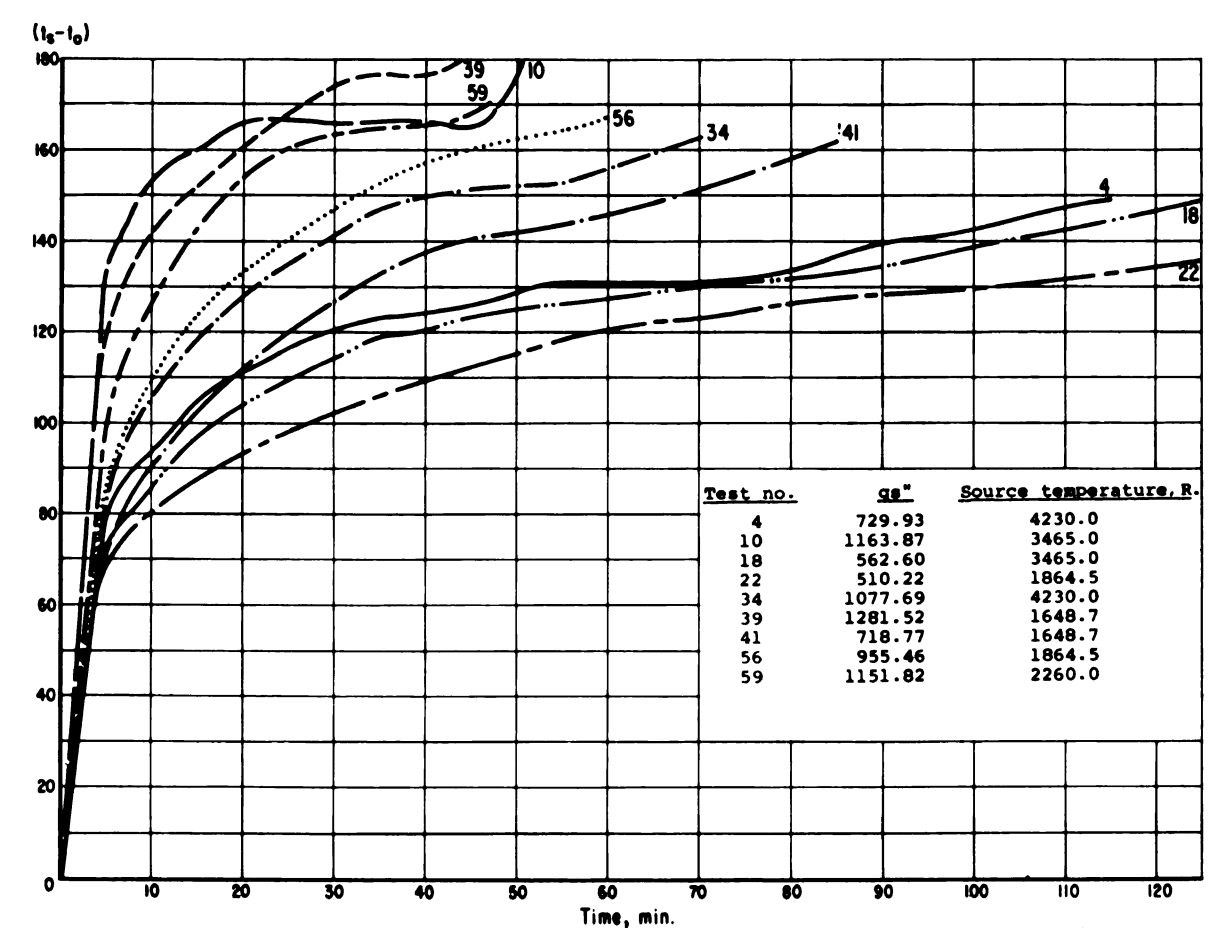
Processing results of ground beef, processed to 170 F. Table 7.1.

ion inches	Width	.37	\dashv	7		٦	\vdash	٦	Ч	Н	\vdash	13	7	13	\vdash	7	.375	\vdash	٦	7	\vdash	7	1
Dimension Changes, inches	Length W	5	68	5	689	0	2	ω	∞	∞	7	2	∞	∞	2	ω	689	2	\vdash	∞	∞	7	C
Time to	170 F, min.	65	72	80	85	82	93						164	222	53		09						
grams	Volatile	4.	7	9	9	3.	2	3.	4.	9	4.	œ	2.	39.3	9	6	30.3	φ.	3	0	œ	0	c
Losses,	Dripping	9		9	œ	2	9	œ	ä	5.	2.	9	φ.		4.	9	48.9	4.	0	3	5.	ထုံ	c
Initial	Weight grams	25.	24.	27.	2	17.	14.	25.	31.	21.	29.	17.	23.	23.	26.	12.	323.4	25.	27.	21.	21.	21.	c
Initial	Temperature, F				46									49			50						
Heat flux	Btu per sq ft-hr	124.0	77.6	024.0	967.05	03.5	43.7	77.3	29.9	92.3	43.2	80.9	45.3	72.9	163.8	077.4	1009.85	34.4	99.2	68.1	97.3	16.5	,
1	λ max. of Source, μ	.23	.23	.23	1.233	.23	.23	.23	.23	.23	.23	.23	.23	.23	.50	.50	1.505	.50	.50	.50	.50	.50	L
	Test Number			33		7	7	m	4	5	9	7	ω	6			12						

.375 .250 .313	. 375 . 313 . 313 . 375 . 375 . 313 . 313 . 375	ししくしししししししししし
.689 .625 .689	.940 .875 .815 .815 .689 .750 .750 .750	81 945 945 945 945 945 945 945 945 945 945
113 125 181	47 51 58 60 61 71 79 101 199 113	
31.6 31.8 32.6	23.8 20.3 24.3 25.6 25.6 25.7 27.5 29.0	00190000000000000000000000000000000000
53.1 48.5 56.7	66.4 72.0 61.6 64.6 62.1 65.1 65.3 70.8	556.0 557.0 560.3 560.3 57.7 57.7 58.2 58.2 58.2 58.2
326.1 321.6 324.6	325.2 324.4 324.1 324.7 324.7 325.4 325.7 325.7	
449 49	18 44 44 44 46 45 45 45 45	0.4446 0.4446 0.004444 0.004444 0.004444 0.004444 0.0044444 0.00444444 0.0044444444
637.57 562.60 507.88	1151.82 1081.34 1016.45 947.25 893.41 836.52 778.42 721.09 666.42 624.24 576.10 528.96	1029.76 955.46 916.62 913.90 862.77 860.29 813.66 761.61 712.07 650.08 601.10 561.91 5489.10 426.28 348.24
1.505 1.505 1.505	2.308 2.308 2.308 2.308 2.308 2.308 2.308 2.308	C
17 18 38	59 63 57 60 60 60 61 63 64	55 56 57 58 58 58 58 58 58 58 58 58 58 58 58 58

Changes, inches .438 .375 .375 .375 .375 .375 .375 .375 Width Dimension Length .875 .815 .815 .875 .750 .689 750 689 Time to 170 F, min. 46 48 55 54 60 62 68 84 84 1111 104 147 Volatile 31.6 27.1 27.1 225.1 226.0 226.0 226.1 31.6 31.6 31.6 grams Losses, Dripping 48.4 51.2 551.2 550.5 57.0 60.7 60.7 57.8 60.7 60.7 60.1 Weight Initial 323.8 323.0 326.0 322.6 322.4 324.4 322.4 322.7 324.3 323.6 325.7 322.8 322.7 323.3 grams Temperature, Initial Heat flux sq ft-hr Btu per 1203.40 1144.89 931.20 857.93 792.69 655.43 595.28 544.16 487.96 1063.17 988.37 718.77 1281.52 ュ λ max. of Source, 3.164 3.164 3.164 3.164 3.164 3.164 3.164 3.164 3.164 3.164 3.164 Number Test

Table 7.1. -- Continued.



Time, min.

Pig. 7.1 Product (t_s-t_o) and time, min., relationships at different surface heat fluxes.

Btu per sq. ft.-hr., and heat source temperatures, R. t_s, product surface temperature, F. t_o, initial product temperature, F.

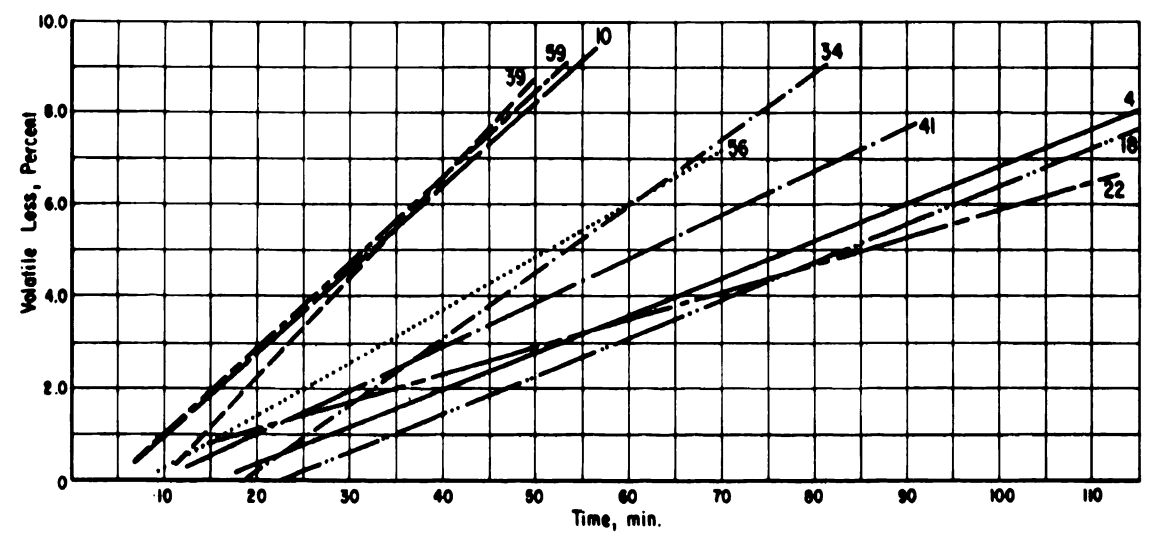


Fig. 7.2 Volatile loss, percent of initial product weight, and time, min., relationships at different surface heat fluxes, Btu per sq. ft.-hr., and heat source temperatures, R.

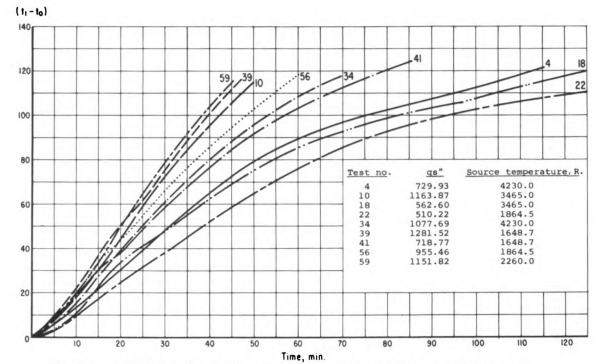


Fig. 7.3 Product (t₁-t₀) and time, min. relationships at different surface heat fluxes. Btu per sq. ft.-hr., and heat source temperatures. R. t₁, product temperature, one inch depth, F. t₀, initial product temperature. F.

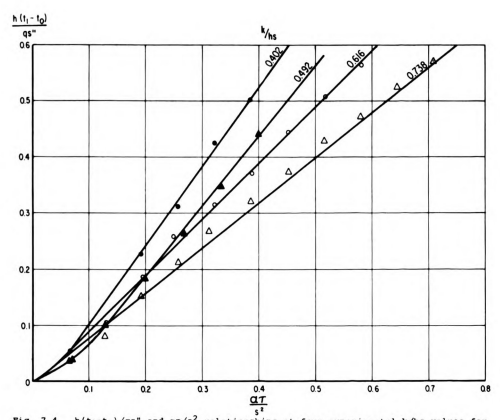


Fig. 7.4 $h(t_1-t_0)/qs^n$ and $\alpha\tau/s^2$ relationships at four experimental k/hs values for ground beef (c = 0.75) and a radiant source at 3465.0 R. t_1 (maximum) = 122 F.

8.0 EXAMPLE CALCULATIONS

Example Problem: Determine the processing times at surface heat fluxes of 1100 and 600 Btu per sq ft-hr at heat source temperatures of 4230.0 and 2260.0 R. Product is ground beef: K = 0.276 Btu ft per sq ft-hr F; S (depth) = 1/12 ft; initial temperature 50 F and final temperature at S is 170 F.

1. Surface temperature for ground beef (Fig. 5.6) for qs'' = 1100 , $t_s = 186$ F for qs'' = 600 , $t_s = 165$ F

2. Volatile product loss (Fig. 5.7) for $t_s = 186 \text{ F}$, loss = 7.74% per hr for $t_s = 165 \text{ F}$, loss = 4.77% per hr

3. Compute the coefficients of heat transfer:

qs" 1100 600 1.17 h 1.23 1.03 hr 1.00 h_{T.} 5.60 3.50 5.67 7.86 h therefore: k/hs 0.421 0.584

> 4. Processing times to attain specific temperatures (Fig. 5.8 to 5.28).

Product Temperature	Pro	es					
	qs"=	1100	qs"= 600				
	4230.0 R	2260.0 R	4230.0 R	2260.0 R			
122	37	27	57	46			
140	7	5	20	15			
157	2	3	32	22			
170	4	3	26	18			

5. Total processing times, minutes.

		qs"
	1100	600
Heat source temperature, F	₹	
4230.0	50	135
2260.0	38	101

9.0 REFERENCES

- 1. Advances in Food Research (1957)
 Advances in Food Research, Vol. 7. Academic Press,
 Inc., New York.
- 2. Aldrich, P. J. and B. Lowe (1954) U.S. Choice and Good grade beef rounds: Effect of extent of cooking on palatability and edible portion cost. J. Am. Dietet. Assoc. 30:39.
- 3. American Meat Institute Foundation (1960)

 The Science of Meat and Meat Products. W. H. Freeman and Company. San Francisco, Calif., pp. 438.
- 4. American Society of Refrigerating Engineers (1951)
 Refrigerating Data Book. Basic vol. 7th ed.
 American Society of Refrigerating Engineers, New
 York. 253-5.
- 5. American Society of Refrigerating Engineers (1955)
 Air Conditioning Refrigeration Data Book.
 Applications volume, 5th ed. American Society
 of Refrigerating Engineers, New York. 18-20.
- 6. Anonymous. (1951)
 Infrared rays in fish canning. Food Manuf., 26:137.
- 7. Anonymous. (1955)

 Quick-dries with infrared. Food Engr. 27:58.
- 8. Asselbergs, E. A., W. P. Mohr, and J. G. Kemp (1960)
 The studies on the applications of infrared in
 food processing. Food Technol., 14, (9):449.
- 9. Asselbergs, E. A., W. P. Mohr, J. G. Kemp, and A. R. Yates (1959) Blanching of cerely and apples by infrared shows flavor, texture, appearance gains. Quick Frozen Foods, 21:45.
- 10. Asselbergs, E. A., and W. P. Powrie (1956)

 The peeling of apples with infrared radiation.
 Food Technol., 10:297.
- 11. Awberry, J. H., and E. Griffiths (1933)

 Thermal properties of meat. Journal of Society of Chemical Industries, London. 52:326.

- 12. Barber, I. J. (1957)

 Volts vs. temperature and radiant heat output of electric infrared devices. Chart No. 57132, The Fostoria Pressed Steel Corporation, Fostoria, Ohio.
- 13. Carslaw, H. S. and J. C. Jaeger (1959)

 Conduction of Heat in Solids. Oxford University

 Press, London.
- 14. Chase, D. R. (1961)
 Some aspects of heat transfer in oven design.
 Proceedings of the Fifth Conference of the
 Society for the Advancement of Food Service
 Research, Chicago, Feb. 27-28. 32-48.
- 15. Chase, D. R. (1963)

 Equipment manufacturers and food processors.

 Proceedings of the Eighth Conference of the Society for the Advancement of Food Service Research, Chicago, May 23-24. 76-88.
- 16. Chatfield, C. and G. Admans (1940)

 Proximate composition of American food and materials.

 U.S. Department of Agriculture Circ. No. 549.
- 17. Cherneeva, L. I. (1956)
 Study of the thermal properties of foodstuffs
 (Report of VNIKHI) Gostorgisdat, Moscow, 16.
 Translated by C. P. Lentz.
- 18. Daniels, F. and R. A. Alberty (1961)

 Physical Chemistry. John Wiley and Sons, Inc.

 New York. pp. 744.
- 19. DeWerth, D. W. (1960)

 Literature review of infra-red energy produced with gas burners. Research Bull. 83, American Gass Association Laboratories, Cleveland, Ohio. pp. 49.
- 20. Egeler, C. E. (1948)
 Infrared energy in food processing. Food Packer,
 29, 50.
- 21. Evans, H. L. (1958)
 Studies in canning processes II: the effects of the variation with temperature of the thermal properties of foods. Food Technol. 17:276.
- 22. Ferguson, F. P. (1943)
 Food dehydration with infrared rays. Food in Canada. 3, (9):17.

- 23. Fourier, J. (1955)

 The Analytical Theory of Heat. Translated, with notes by A. Freeman. Dover Publications, Inc. New York, pp. 466.
- 24. Giedt, W. H. (1957)
 Principles of Engineering Heat Transfer. D. Van
 Nostrand Company, Inc. Princeton, New Jersey,
 pp. 372.
- 25. Hall, C. W. (1960)
 Theory of infrared drying of agricultural products.
 Paper No. 60-813 presented at the Winter Meeting,
 American Society of Agricultural Engineers, Memphis,
 Tennesee, Dec. 4-7.

7

- 26. Heisler, M. P. (1947)

 Temperature charts for induction and constant temperature heating. Trans. ASME, 69:227.
- 27. Hienton, T. E., D. E. Wiant and O. A. Brown (1958)

 Electricity in Agricultural Engineering. McGrawHill Book Co., New York.
- 28. Hottel, H. C. (1930)

 Radiant heat transmission between surfaces separated by non-absorbing media. Trans. ASME, 53:265.
- 29. Hurwicz, H. and R. G. Tischer. (1952)

 Heat processing of beef II: developments of isothermal and isochronal distribution during heat processing of beef. Food Research, 17:518.
- 30. Hurwicz, H. and R. G. Tischer. (1956)

 Heat processing of beef VI: thermal diffusivity and slopes of heating and cooking curves for the high temperature process. Food Research, 21:147.
- 31. Jackson, J. M. (1940)

 Mechanisms of heat transfer in canned foods during thermal processing. Proceedings of the Food Conference of the Institute of Food Technologists, Chicago, June 16-19.
- 32. Jakob, M. (1949)

 Heat Transfer. Vol. I. John Wiley and Sons, Inc.

 New York. pp. 758.
- 33. Jakob, M. (1957)

 Heat Transfer. Vol. II. John Wiley and Sons, Inc.

 New York, pp. 652.

- 34. Keating, R. T. (1960)

 Research into the utilization of forced air ovens.

 Proceedings of the Fourth Conference of the Society
 for the Advancement of Food Service Research,

 East Lansing, Michigan, Sept. 19-20. pp. 51-64.
- 35. Krupp, P. H. (1960)
 Infrared possibilities in food processing.
 Proceedings of the Fourth Conference of the Society
 for the Advancement of Food Service Research,
 East Lansing, Michigan, Sept. 19-20. pp. 24-28.
- 36. Lentz, C. P. (1961)

 Thermal conductivity of meats, fats, gelatin gels, and ice. Food Technol. 15 (5):243-7.
- 37. Lowe, B. (1955)

 Experimental Cookery from the Chemical and Physical Standpoint. John Wiley and Sons, Inc. New York. pp. 573.
- 38. Lukianchuk, F. J. (1960)

 Effect of two methods of dry heat cookery on palatability of cooking losses of semimembranosus muscle of beef round. Unpublished M.S. Thesis, Michigan State University, East Lansing, Michigan. pp. 102.
- 39. Mannhiem, H. C. (1955)

 Specific heat of foodstuffs. Food Technol.

 9 (11):556-559.
- 40. Marks, L. S. (1951)

 Mechanical Engineers' Hardbook. McGraw-Hill Book
 Company, Inc. New York. pp. 2236.
- 41. Marks, L. S. and H. N. Davis (1916)

 Tables and Diagrams of the Thermal Properties of
 Saturated and Superheated Steam. Longmans, Green
 and Co. New York. pp. 106.
- 42. McAdams, W. H. (1942)

 Heat Transmission. McGraw-Hill Book Co., New York.
- 43. McCance, R. A. and H. L. Shipp (1933)

 The chemistry of flesh foods and their losses on cooking. Med. Research Council (But), Special Report Ser. No. 187.
- 44. Meigs, E. B. (1909)

 Concerning the supposed connection between protein coagulation and the heat shortening of animal tissues. Am. J. Physiol. 24:178.

- 45. Olson, F. C. W. and O. T. Schultz (1942)

 Temperatures in solids during heating or cooling.

 Industrial and Engineering Chemistry, 34:874.
- 46. Planck, M. (1959)

 The theory of Heat Radiation. Translated by M.

 Masius. Dover Publications, Inc. New York. pp. 224.
- 47. Pollak, G. (1960)

 Comparative efficiencies of cooking meat by conventional oven, microwave oven, and infrared device. Proceedings of the Third Conference of the Society for the Advancement of Food Service Research, Bayonne, New Jersey, Feb. 28-29.

 pp. 42-49.
- 48. Sayles, C. I. (1963)

 Heat transfer to food. The Cornell Hotel and Restaurant Adm. Quart. 4 (2):25-32.
- 49. Schroeder, H. W. (1960)

 Drying rough rice with infra-red radiation.

 Paper No. 60-816 presented at the Winter Meeting,

 American Society of Agricultural Engineers, Memphis,

 Tennessee, Dec. 4-7.
- 50. Schweigert, B. S. and B. J. Payne (1956)

 A summary of the nutrient content of meat. American Meat Institute Foundation Bull. No. 30.
- 51. Sevcik, V. J. and J. E. Sunderland (1962)
 Emissivity of beef. Food Technol. 16 (9):124.
- 52. Siebel, E. (1892)

 Specific heats of various products. Ice and Refrig. 2:256.
- 53. Short, B. E., W. R. Woolrich and L. H. Bartlett (1942) Specific heats of foodstuffs. Refrig. Engr. 44:385.
- 54. Shuman, A. C. (1960)

 Experimentation versus theory in infrared drying of industrial products. Paper No. 60-814 presented at the Winter Meeting, American Society of Agricultural Engineers, Memphis, Tennessee, Dec. 4-7.
- 55. Shuman, C. A. and C. H. Staley (1950)

 Drying by infrared radiation. Food Technol. 4:481.
- 56. Snedecor, G. W. (1946)
 Statistical Methods. The Iowa State College Press,
 Ames, Iowa. pp. 485.

- 57. Tappel, A. L., A. Couroy, M. R. Emerson, L. W. Regier and G. F. Stewart (1955) Freeze dried meat I, Food Technol. 9:401.
- 58. Tiller, F. M., E. E. Lithenhous and W. Turbeville (1943) Infrared dehydration of meats and vegetables tested. Food Ins., 15:77.
- 59. Towson, A. M. (1940)
 Palatability studies of beef rib roasts, I. As affected by high versus low oven temperatures.
 M.S. Thesis, unpublished, Iowa State College Library, Ames, Iowa.
- 60. Tressler, D. K. and C. F. Evans (1957)

 The Freezing Preservation of Foods. Vol. I.

 The Avi Publishing Co., Westport, Connecticut.

agril EMGR. LIBA

PHY 1 8 '66